



UNIVERSITÀ DEGLI STUDI DI NAPOLI
“FEDERICO II”



Tesi di Dottorato

**“New insights in the etiopathogenesis of muscle
inflammation and aging in animals”**

Coordinatore

Ch.mo Prof.
Giuseppe Cringoli

Candidato

Dott.ssa
Teresa Bruna Pagano

Tutor

Ch.ma Prof.ssa
Serenella Papparella

Desidero ringraziare innanzitutto i miei genitori Livia e Nicola e mia sorella Arianna per tutto l'amore, il supporto e la fiducia che mi hanno dato in questi anni;

La prof.ssa Serenella Papparella e il prof. Orlando Paciello per le conoscenze e l'onestà intellettuale trasmesse, nonché per l'opera di guida lungo il percorso di dottorato e non solo.

I prof. del settore di anatomia patologica del Dipartimento di Medicina Veterinaria di Napoli: Brunella Restucci, Paola Maiolino, Manuela Martano, Pippo Borzacchiello, Valeria Russo, Franco Peppino Roperto ed il tecnico di laboratorio Raffaele Ilami, da ognuno dei quali ho potuto imparare qualcosa.

Tutti i colleghi e colleghe del settore di anatomia patologica con cui ho condiviso gioie e dolori della vita in laboratorio: Francesca Trapani, Alessandro Costagliola, Davide De Biase, Valentina Iovane, Davide Ciccarelli, Karen Power, Giuseppe Piegari, Francesco Prisco, Chiara Urraro, Dora Ceccarelli e Roberta Lucà.

Tutti i colleghi del XXX ciclo di dottorato per il supporto reciproco, le catene di messaggi whatsapp nei momenti di crisi e le soddisfazioni condivise.

La prof. Paola Roccabianca e tutti i fantastici colleghi conosciuti a Milano: Valeria Bertani, Luca Pazzini, Laura Nordio, Sara Turchetto, Marco Tecilla, Marian Tulescu, Valeria Baldassarre, Luisa Muscatello e Silvia Benali per avermi accolto in un clima di amicizia e aiuto reciproco in quell'oasi felice, nonché circolo culturale dall'inestimabile valore che da sempre è il TPL.

I prof. Anna Oevermann e Torsten Seuberlich e la dott.ssa Fabienne Serra per l'interessante esperienza formativa e di ricerca che ho svolto con loro presso il NeuroCenter di Berna durante il mio periodo all'estero.

I prof. Mariapia Pasolini, Raffaelina Mercogliano e Vincenzo Veneziano e i colleghi Giovanni della Valle, Michele Greco e Luigi Auletta per le proficue collaborazioni scientifiche avute in questi anni. Il dott. Gianluigi Zullo per l'aiuto fondamentale offertomi in "terra belga".

Le mie amiche "storiche" Angela Spagnuolo, Claudia Smeraglia, Giovanna Sodano e Francesca Coscia per essermi state vicine durante questo percorso anche nonostante la lontananza.

Index

List of abbreviations:	12
List of figures:	13
General Background:	21
Skeletal muscle pathology: comparative aspects and personal experiences at the Laboratory of Comparative Neuromuscular Pathology of Naples:	21
<i>I. Neurogenic atrophies</i>	25
<i>II. Muscular Dystrophies</i>	26
<i>III. Inflammatory myopathies</i>	28
<i>IV: Infectious Myopathies:</i>	32
<i>V. Ischemia</i> ³³	
<i>VI. Metabolic Myopathies</i>	34
<i>VII. Endocrine Myopathies</i>	35
<i>VIII. Necrotizing myopathies causing myoglobinuria</i>	35
<i>IX. Nutritional myopathies</i>	36
<i>X. Other congenital Myopathies</i>	36
<i>XI. Diseases of Neuromuscular Transmission</i>	39
<i>XII. Muscle aging.</i>	40
References:	44
Chapter 1	47

Inflammatory myopathy in horses with chronic piroplasmosis	47
1.1 Introduction:	48
1.2 Materials and methods	50
1.2.1 Animals:	50
<i>1.2.2 Hematology and Serum Biochemistry</i>	51
<i>1.2.3 Parasitological Diagnosis</i>	51
<i>1.2.4 Histopathology and Immunohistochemistry</i>	53
<i>1.2.5 Indirect Immunofluorescence</i>	55
<i>1.2.6 Reverse Transcription Quantitative Polymerase Chain Reaction</i>	56
<i>1.2.7 Reverse Transcription Quantitative PCR for T. equi and B. caballi DNA</i>	57
<i>1.2.8 Statistical Analysis</i>	59
1.3 Results:59	
1.3.1 <i>Parasitological Diagnosis, Hematology, and Serum Biochemistry</i>	59
1.3.2 <i>Histopathology and Immunohistochemistry</i>	62
1.3.3 <i>Indirect Immunofluorescence</i>	68
1.3.4 <i>Molecular Findings</i>	70
1.4 Discussion:	71
References:	78
Chapter 2 Lymphoplasmacytic myositis and expression of Major Histocompatibility Complex class I in ovine muscular sarcocystosis	84

Table of Contents

2.1 Introduction	85
2.2 Materials and methods	93
2.2.1 Animals:	93
2.2.2 Sarcocyst species identification:	94
2.2.3 Histology and immunohistochemistry	95
2.2.4 Immunofluorescence	97
2.2.5 Statistical analysis.	98
2.3 Results:98	
2.3.1 <i>Sarcocystis</i> species identification:	98
2.3.2 Histology and Immunohistochemistry	99
2.3.3 Immunofluorescence	103
2.3.4 Statistical analysis	103
2.4 Discussion	108
References:114	
3.1 Introduction	121
3.2: Materials and methods	123
3.2.1 Animals and tissue samples	123
3.2.2 Histological examination	125
3.2.3 Immunohistochemical examination	126
3.2.4 Western blotting	127
3.2.5 Statistical methods	128
3.3 Results128	

Table of Contents

3.3.1 Histochemical analysis	128
3.3.2 Immunohistochemistry	132
3.3.3 Western blotting analysis	132
3.4 Discussion	137
3.5 Conclusions	140
References	142
4.1 Introduction	147
4.1.1 Cellular prion protein in somatic tissues:	148
4.1.2: Functions of Cellular Prion Protein in nervous system	150
4.1.3: Function and localization of Cellular Prion Protein in skeletal muscle	150
4.1.4 The cellular prion protein in muscle diseases	152
4.1.5 The pathological prion protein (PrP ^{Sc}) in muscle tissue	153
4.1.6: Prion protein and aging. (from Gasperini 2014)	154
4.2 Aim of the project:	155
4.3 Materials and Methods	157
4.3.1: Animals:	157
4.3.2: Histology and histochemistry	159
4.3.3: Immunohistochemistry and immunofluorescence:	159
4.3.4 Statistical analysis of histological data:	162
4.3.5 Sample preparation and western blotting:	164
4.3.6 Velocity sedimentation in sucrose step gradient	166

Table of Contents

4.3.7 Separation of detergent-soluble and -insoluble PrP by one-step ultracentrifugation	166
4.4 Results:167	
4.4.1 Histopathology:	167
4.4.2: Immunohistochemistry:	168
4.4.3 Immunofluorescence:	173
4.4.4 <i>Statistical analysis of histopathological findings</i>	174
4.4.5 Quantitative western blot	176
4.4.6 Glycoprofile and epitope mapping	177
4.4.7 Proteinase K titration, sucrose gradient, soluble/insoluble fraction:	178
4.5 Discussion:	182
References:187	
List of Abbreviations	12
List of Figures and tables	13
Abstract	16

List of Abbreviations

List of abbreviations:

APC= antigen presenting cell

ATP = Adenosin Triphosphate

BEC 1=beclin 1

COX= Cytochrome oxidase

DYS1= Dystrophyn rod domain

EP= equine piroplasmosis

ER=endoplasmic reticulum

HE=hematoxylin and Eosin

HRP=horseradish peroxidase

IBM=inclusion body myositis

IFN=Interferon

IL= Interleukin

LC3= Microtubule-associated proteins light chain 3

MHC I and II= Major Histocompatibility Complex class I and II

NADH= Nicotinamide Adenine Dinucleotide

PCR= Polymerase Chain Reaction

PM= Polimyositis

PrP= prion protein

PV=parasitophorous vacuole

SDH= Succynate Dehydrogenase

TNF α = Tumor necrosis factor alpha

List of figures:

General background:

Fig. 1.1: Main histochemical techniques used in the study of muscle tissue in specialized laboratories (from Paciello, 2009).

Fig. 1.2: From Paciello, 2009. Expression of MHC class I also faraway from inflammatory cells.

Fig. 1.3: Agents of infectious myopathies

Fig. 1.4: Comparative table of glycogenoses in humans and domestic animals (modified from Jubb, Kennedy and Palmer's).

Chapter 1:

Fig. 1.1 IFAT results.

Figure 1.2. Myositis associated with chronic piroplasmosis, horse, histology

Figures 1.3. Myositis associated with chronic piroplasmosis, immunohistochemistry, horse.

Figure 1.4. Indirect immunofluorescence.

Figure 15. Normal canine, feline and sheep muscle cryosections stained with serum from horse

Figure 1.6. Analysis of (a) tumor necrosis factor (TNF)- α , (b) interleukin (IL)-10, (c) IL-12, and (d) interferon- γ (IFN- γ) gene expression based on rPCR.

Chapter 2:

Fig. 2.1 Sarcocystis spp. lifecycle (modified from Bruxton et al., 1998)

Fig 2.2: Transmission electron micrograph of a transversally sectioned sarcocyst

Fig. 2.3: Sarcocystis species identification.

Fig. 2.4 Histopathology.

Fig. 2.5: Immunohistochemistry.

Fig. 2.6 Immunohistochemistry and Immunofluorescence.

Fig. 2.7: Immunofluorescence.

Chapter 3:

Fig. 3.1: Representative histological sections of biceps femoris muscle from geriatric dogs.

Fig. 3.2: Immunohistochemical staining for Beclin-1 in biceps femoris muscle.

Fig. 3.3: Immunohistochemical staining for LC3 in biceps femoris muscle

Chapter 4:

Fig. 4.1: Expression of PrPC in bovine tissues. From Peralta et al. 2009.

Fig. 4.2: Macroscopical pictures of aged cows at the slaughterhouse.

Fig. 4.3: Cryosections of skeletal muscle from old animals

Fig. 4.4: Normal immunohistochemical findings.

Fig.4.5: Normal findings.

Fig. 4.6: Rigen/degen fibers show increased sarcolemmal positivity to PrP .

Fig. 4.7: Pathological findings.

Fig. 4.8: Immunohistochemistry (and immunofluorescence

Fig. 4.9: Quantitative western blot.

Fig. 4.10: Western blotting of crude de-glycosylated and crude muscle and brain homogenate.

Fig. 4.11: Epitope mapping.

Fig. 4.1.: PK titration.

Fig. 4.12: Sucrose gradient.

Fig. 4.13: Soluble-insoluble fractions.

List of tables

Chapter 1:

Table 1: Signalment, muscle enzymes and IFAT titre.

Table 1.2 Histological findings.

Chapter 2:

Table 2.1: Sarcocystis in domestic species.

Table 2.2: Summary of histopathological findings.

Chapter 3:

Table 3.1 Study population.

Table 3.2 Summary of histopathology and immunohistochemistry results.

Chapter 4:

List of Figures and tables

Table 4.1: samples collected, signalment and auricular marks of the animals

Table 4.2: antibodies and relative techniques used in the study

Table 4.3: histological scores

Table 4.4: Histopathology and immunohistochemistry results.

Muscle pathology has unique relevance in many different fields of veterinary research, ranging from the diagnostics, to the comparative medicine involving animal models of human diseases, to the animal based food safety. The Laboratory of Comparative of Neuromuscular Disorders was established decades ago at the Department Veterinary Medicine of Naples in order to contribute to the knowledge of muscle pathology in domestic animals using modern techniques and undertaking international scientific collaborations. In this context, the project of this doctoral thesis had the main purpose to produce new scientific data in at least two interest area: the etiopathogenesis of inflammatory myopathies and skeletal muscle aging. Thus, the experimental results of four research project conducted in four different species are presented, including: 1) Inflammatory myopathy in horses affected by chronic piroplasmosis; 2) Lymphoplasmacytic myositis and expression of Major Histocompatibility Complex class I and II in ovine muscular sarcocystosis; 3) Age related skeletal muscle atrophy and upregulation of autophagy in dogs; 4) Expression and biochemical properties of cellular Prion protein in skeletal muscle of aged cows.

In the first and second chapters of the thesis, two inflammatory myopathies associated with parasites having or not having a specific tropism for skeletal muscle (*Sarcocystis tenella* and *Theileria equi* -*Babesia caballi*, respectively) are explored.

In the first study, an inflammatory myopathy characterized by a mainly CD8-CD4+ lymphocytic population and fiber degeneration is described in 16 horses serologically positive for equine piroplasms with clinical signs and serum biochemical evidence of a myopathy. To test the hypothesis of

circulating autoantibodies directed against an unknown muscular antigen, the serum from affected horses was tested by indirect immunofluorescence to sections of normal equine muscle. In all cases, distinct sarcolemmal staining was detected in sections incubated with serum from affected horses, in contrast to sections incubated with phosphate-buffered saline or equine control sera. Furthermore, a significant increase of interferon- γ , interleukin-12, and tumor necrosis factor- α gene expression by compared to healthy controls was revealed by Reverse transcription polymerase chain reaction (RT-PCR). Thus, we concluded that inflammatory myopathy associated with equine piroplasmosis may involve an autoimmune pathogenesis with upregulation of inflammatory cytokines that may cause myofiber atrophy and degeneration.

The aim of the second chapter, leading with muscle inflammation in ovine muscular sarcosytosis, was to investigate if parasitized muscle fibers could play a role in immune-stimulation, as sporadically described in accidental muscular sarcocystosis in definitive hosts.

Skeletal muscle samples from 78 sheep presenting muscular sarcocysts revealed inflammatory changes in 69% of cases, consisting of an endomysial lymphoplasmacellular infiltrate, with attendant myofiber degeneration and necrosis. The predominant T cell populations were CD3+, CD8+ with lesser numbers of CD4+ and CD79 α + cells. Eosinophils were constantly absent. Notably, moderate to strong sarcolemmal labeling to Major histocompatibility complex (MHC) I and II was found both in biopsies with evident inflammatory infiltrate and in cases without inflammation. The wall of the cysts resulted strongly positive to MHC I

and II, and occasionally co-localized with the membrane associated protein Dystrophin. Our data suggest that muscle fibers respond to the presence of cysts by expression of MHC I and II that can play a role in stimulating and maintaining the lymphoplasmacellular inflammation. The possible role of MHC I on the cyst wall is discussed, but basically more research is needed in order to evaluate its possible involvement in inflammation. Moreover we speculated about the possibility that the abnormal expression of MHC I and II on muscle fibers is not only typical of myopathies having an immune-mediated pathogenesis but also of myositis associated with muscular parasites.

The last two chapters of the thesis are dedicated to muscle aging, and in particular to the role of autophagy in canine sarcopenia and of cellular prion protein in bovine muscle aging. Sarcopenia, the age related loss of muscle mass and strength, is a multifactorial condition that occurs in a variety of species and represents a major healthcare concern in human medicine. We evaluated the expression of three markers of autophagy, Beclin 1, LC3 and p62, in muscle wasting of 25 geriatric dogs, to establish whether the levels of autophagy change with increasing age. Our results indicated a marked intracytoplasmic staining for Beclin 1 and LC3 in 80% of the muscle samples from the older dogs and a significantly greater expression of LC3 II and Beclin 1, by Western blotting. The results of the study suggest that enhanced autophagy might be one of the factors underlying muscle atrophy in canine age related muscle wasting.

Finally, we explored the expression and biochemical properties of cellular prion protein (PrPC) in skeletal muscle of cows as well as their

possible changes in geriatric animals. PrPC over expression has been described in many different human neuromuscular disorders but little is known about PrPC in health and disease in bovine muscle tissue. Skeletal muscle and brain samples of 12 aged and 8 young Podolica cows were collected and compared by histomorphological techniques as well as several experiments involving immunoblot and specifically analyzing the amount of PrPC, its glycosylation profile, proteinase resistance, solubility levels and tendency to aggregate. Histologically, muscle biopsies of aged cows showed typical myopathic features already described in bovine sarcopenia. Immunohistochemistry for PrP revealed a distinct granular positivity in intramuscular nerve branches and muscle spindles in all cases. Membrane immunopositivity was more prominent on angular atrophic fibers. Increased levels of positivity were found in degenerated fibers (desmin depleted) with a positive labeling of rimmed vacuoles. Prion protein positivity levels was also significantly increased in cases displaying inflammatory changes. No differences between muscles and brains of young and old animals were detected by quantitative immunoblot and Proteinase K titration. The glycoform profile and the molecular mass of PrPC in muscle samples appeared slightly different compared to the brain. Sucrose gradient velocity sedimentation gave variable results, with a generally lower amount of PrP in high density sucrose fractions in the muscle compared to the brain. After high speed centrifugation the majority of muscle PrPC was found in the soluble fraction, without significant differences between young and old animals. Our preliminary data suggest that: 1) the amount and the main biochemical properties of prion protein do

not change with age, 2) PrPC is overexpressed in degenerated, vacuolated and angular muscle fibers; 3) The glycoform profile of PrPC differs between brain and muscle tissue.

In conclusion, the main innovative aspects of this thesis are:

- 1) The first description in the literature of a likely immune-mediated myositis occurring in chronic equine piroplasmosis
- 2) The demonstration of high prevalence of lymphoplasmacellular myositis in ovine muscular sarcocystosis implying the overexpression of MHC I on muscle fibers as well as on the cyst wall.
- 3) The report of enhanced autophagy in age-related muscle atrophy in dogs.
- 4) The first detailed description of PrPC localization and biochemical properties in bovine muscle tissue and its possible involvement in neurogenic atrophy, muscle degeneration and chronic inflammation.

Collectively, these results enhance the relevance of morphological studies as starting point to investigate the pathogenesis of muscle diseases in veterinary and comparative pathology.

General Background:

Skeletal muscle pathology: comparative aspects and personal experiences at the Laboratory of Comparative Neuromuscular Pathology of Naples:

Skeletal muscle is an unique and highly specialized tissue expressing a wide variety of lesions. The study of muscle diseases in veterinary medicine offers the irreplaceable opportunity to compare different species, interchanging concepts and scientific approaches from human to veterinary medicine and vice-versa. In recent years, veterinary skeletal muscle pathology is progressively gaining importance due to its interdisciplinary relevance in many fields, ranging from the diagnostics, to the comparative medicine involving animal models of human diseases, to the animal based food safety. The Laboratory of Comparative Neuromuscular Disorders (LCND) was established decades ago at the Department of Veterinary Medicine and animal production of Naples in order to provide its own contribution to the knowledge about muscle pathology in domestic animals using modern techniques and undertaking international scientific collaborations.

Microscopic analysis is essential for the study of muscle pathology in human as well as in veterinary medicine. The study of most neuromuscular diseases is based on clinical issues, ancillary tests such as electromyography, microscopic evaluation of muscle morphology, and, if required, molecular and genetic studies. Muscle biopsy, associated to histochemical and immunohistological techniques, plays a key role in diagnosis of many neuromuscular disorders, likely more than in other

tissues (Paciello, 2009). Histochemical techniques (Fig. I.1) are essential for the study of muscle tissue for four main reasons. First, they can demonstrate selective involvement of different fiber types in certain disease processes. Second, they may show an absence of a particular enzyme. Third, an excess of a particular substrate can be demonstrated. Fourth, they may show structural changes in the muscle which would not be apparent with routine histological stains, such as mitochondrial abnormalities (Paciello, 2009). While immunohistochemistry is very useful in identifying abnormal expression of primary protein abnormalities in recessive conditions, it is less helpful in detecting primary defects in dominantly inherited disorders. Abnormal immunohistochemical expression patterns can be confirmed by Western blot analysis which may also be informative in dominant disorders, although its role has yet to be established. Besides identification of specific protein defects, immunohistochemistry is also helpful in the differentiation of inflammatory myopathies by subtyping cellular infiltrates and demonstrating up-regulation of subtle immunological parameters. The pattern of fiber types can be studied accurately only by subjecting cryostat-sectioned unfixed, frozen muscle to myofibrillar adenosine triphosphatase (ATP) reactions at pHs 4.3, 4.6 and 9.4.

Some of the most used histochemical techniques are reported in table 1. Reference can be made to the book on muscle biopsy of Dubowitz and Sewry (2007).

Specific importance have special histoenzimatic stains such as Oil Red O (ORO), PAS (Periodic acid Schiff) and Congo Red in the diagnostics of muscle diseases characterized by cytoplasmic accumulations of abnormal

material; using these techniques, the basic distinction between lipid (ORO positive), glycidic (PAS) or amyloid (Cong Red) deposits can be made in a very quick and reliable way on muscle cryosections.

STAIN	MAJOR USE
Haematoxylin & eosin	General structure: fiber size and contours, position of nuclei, fibrosis, inflammation, nerves, blood vessels
Engel Trichrome	Mitochondria red, nemaline rod red, membranous whorls of rimmed vacuoles red
Periodic Acid-Schiff	Checkerboard pattern of fibre types; fibers with excess glycogen heavily stained; fibers with loss of glycogen white
Reduced nicotinamide adenine dinucleotide-tetrazolium reductase (NADH-TR)	Fiber type pattern; distribution of mitochondria; myofibrillar disruption
Succinic dehydrogenase (SDH)	Fiber type pattern; fibers with abnormal mitochondria
Cytochrome oxidase (COX)	Fiber type pattern; fibers devoid of activity
ATPase or myosin isoforms (different PH)	Distribution and involvement of fiber types and their subtypes
Phosphorylase	Absent in type V glycogenosis (McArdle's diseases)
Phosphofructokinase	Absent in type VII glycogenosis
Adenylate deaminase	Absent/deficient in exertional myalgia
Acid phosphatase	High in lysosomal storage disorders and vacuolar myopathies
Alkaline phosphatase	High in blood vessels in some inflammatory myopathies
Menadione-linked α -glycerophosphate dehydrogenase	Stains reducing bodies
Congo red	Shows presence of β -amyloid

Fig. 1. 1 Main histochemical techniques used in the study of muscle tissue in specialized laboratories (from Paciello et al., 2009).

Immunohistochemistry, since its introduction in the 1960s, had a significant positive impact in the study of neuromuscular disorders as well as in the diagnostics field. Overall, it is important to mention that, as for enzyme histochemical preparations, muscle specimen preservation by freezing is a prerequisite for accurate immunohistochemical and for immunoblot analysis as there are only a limited number of antibodies that work on paraffin sections. Immunohistochemistry consist in the localization of antigens in tissue sections by the use of antibodies as specific reagents through antigen antibody interactions. Similar to

immunohistochemistry, immunofluorescence can be used to detect the location and relative quantity of an antigen on muscle fibers. The technique use a fluorescent dye that is covalently attached to the primary or secondary antibody. When a light illuminates the fluorescent dye, the light is absorbed and the dye emits a different color light which is visible under the microscope. Direct immunofluorescence requires only one single-step incubation with directly conjugated antibodies, while indirect immunofluorescence uses unconjugated primary antibodies which are labeled by fluorescently conjugated secondary antibodies in a second-step (Paciello, 2009).

Western blots are used to detect the proteins in homogenized skeletal muscle samples by using specific antibodies. It gives information about the presence and the relative amount of those proteins, compared with a control. The proteins of the sample are electrophoresed into a gel and separated based upon molecular weight and charge. In the blotting process, they are transferred on a membrane made of nitrocellulose or PVDF by applying a current. To detect the antigen blotted on the membrane, a primary antibody is incubated with the membrane and then labeled by a secondary enzyme conjugated antibody. Finally, the enzyme substrate is added which will precipitate upon reaction with the conjugate so that the position of the membrane-bound primary antibody will become visible. Size approximations can be done by comparing the stained band with that of a prestained protein size marker.

Muscle diseases may be subdivided into six broad categories on the basis of sets of fairly distinctive clinicopathologic characteristics: atrophies, dystrophies, inflammatory myopathies, metabolic myopathies, "congenital"

myopathies, and disorders of neuromuscular transmission (De Girolami, 1982).

An extensive review of neuromuscular disorders in humans and animals is not the purpose of this section; basic concepts and classifications are presented with special attention about personal scientific experiences in the LCND of Naples and comparative aspects between different species.

I. Neurogenic atrophies

Neuropathic or neurogenic muscular disease refers to those conditions in which fiber atrophy is secondary to an interruption of innervations resulting from an abnormality of the anterior horn cell, its axonal processes, or the neuromuscular junction. The histopathological character of denervated muscle fibers is usually pathognomonic: fiber becomes smaller and assumes a characteristic angular, sharply contoured configuration. The pyknotic nuclei tend to cluster in clumps. With progression of the disease, the atrophic, angulated fiber clusters in small groups—a process often referred to as group atrophy. Utilizing histochemical techniques, one can see that both major fiber types are involved. Through the process of collateral sprouting, previously denervated muscle fibers may then become reinnervated. The reinnervated muscle fiber, however, will assume the fiber type of its new innervations resulting in a loss of normal mosaic pattern at the ATPase stains. Such a histochemical change is termed fiber-type grouping. Type II fiber atrophy is, in contrast, a relatively nonspecific form of muscle atrophy that may occur in a wide variety of conditions, including disuse, cachexia, chronic

disease, upper motor neuron lesions, and steroid administration (De Girolami, 1982).

In veterinary medicine, the most popular neurogenic muscle disorders are probably the neurogenic masticatory muscle atrophy in dogs secondary to diseases of trigeminal nerve (i.e, inflammation or neoplasia) the laryngeal hemiplegia of the horse and the Equine Motor Neuron Disease (EMND), a condition depending on the progressive motor neuron degeneration in the spinal cord (Cummings, 1990). Similar conditions have been reported in some canine breeds as well.

II. Muscular Dystrophies

The muscular dystrophies are a heterogeneous group of inherited disorders depending on specific defects of one or more structural protein which may lead to muscle fiber necrosis and apoptosis with subsequent muscle fiber loss and fibrosis. Since identification of the dystrophin gene mutation and protein defect responsible for progressive muscular dystrophy types Duchenne and Becker in 1987 (Hoffman, 1988), many other protein defects have been identified allowing further classification and accurate diagnosis of muscular dystrophies (Sewry, 2000). These gene mutations and protein defects are subtyped in sarcolemmopathies with sarcolemmal protein deficiencies and in non-sarcolemmal muscular dystrophies with defects of nuclear, i.e. emerin, and sarcomeric proteins, i.e. myotilin and telethonin, as well as enzymes, i.e. calpain 3, and can be documented by immunohistochemistry and by immunoblot analysis.

The characteristic morphological abnormalities of the most known muscle Dystrophy, Duchenne Dystrophy, include: 1) variability in fiber size with a

greater than normal size range in the cross-sectional fiber; 2) internalization of subsarcolemmal nuclei); 3) degeneration, necrosis, and phagocytosis of muscle fibers; 4) regeneration of muscle fibers; and 5) proliferation of endomysial connective tissue.

When a mutation disrupts the reading frame of amino acids (an out-of-frame mutation), the defect in dystrophin results in a severe phenotype of Duchenne Muscle Dystrophy. A mutation, which maintains the reading frame (an in-frame mutation) results, less frequently, in the production of truncated and only partly functional dystrophin. This mutation leads to the more benign phenotype (Monaco et al., 1988) known as Becker muscular dystrophy (BMD).

In 2014 we described one of the rare cases of Becker-like muscular dystrophy in a 3-year-old, male Labrador retriever dog. Immunoblotting revealed a truncated dystrophin protein of approximately 135 kDa. (Baroncelli, 2014).

Several spontaneous and genetically engineered animal models have been demonstrated extremely useful in the study of muscle dystrophies (for specific review see Vainzof, 2008). These models generally display similar alteration to the human counterpart and are considered extremely important tools for genetic, clinic, and histopathological studies. The MDX mouse is the most widely used animal model for Duchenne muscular dystrophy, even though it is not useful for clinical trials because of its mild disease phenotype due to protective utrophin upregulation. The canine golden retriever MD model represents a more clinically similar model of DMD due to its larger size and significant muscle weakness. Autosomal recessive limb-girdle MD forms models include the SJL/J mice, which develop a

spontaneous myopathy resulting from a mutation in the Dysferlin gene, being a model for LGMD2B. For the human sarcoglycanopathies (SG), the BIO14.6 hamster is the spontaneous animal model for δ -SG deficiency, whereas some canine models with deficiency of SG proteins have also been identified. All sarcoglycan-null animals display a progressive muscular dystrophy of variable severity and share the property of a significant secondary reduction in the expression of the other members of the sarcoglycan subcomplex and other components of the Dystrophin-glycoprotein complex. Mouse models for congenital MD include the dy/dy (dystrophia-muscularis) mouse and the allelic mutant dy2J/dy2J mouse, both presenting significant reduction of α 2-laminin in the muscle and a severe phenotype (Vainzof, 2008).

Feline X-linked muscular dystrophy affected cats develop marked muscle hypertrophy (cervical and proximal forelimb muscles). Thickening of tongue muscle may result in difficulties prehending food and in drooling. A muscular dystrophy associated with α -dystroglycan deficiency occurs in Sphynx and Devon Rex cats (Martin, 2008).

III. Inflammatory myopathies

In human medicine inflammatory myopathies (IM) constitute a heterogeneous group of subacute, chronic or sometimes acute acquired muscle diseases, which have in common the infiltration of inflammatory cells in muscle tissue and the presence of a variable degree of clinically evident muscle weakness. The most common IM are: polymyositis (PM), dermatomyositis (DM), necrotizing autoimmune myositis (NAM) and sporadic inclusion body myositis (sIBM). The disorders have primarily an

autoimmune pathogenesis, mediated either by cytotoxic T cells, as in PM and sIBM, by a complement-mediated microangiopathy as in DM, or by macrophages and possibly autoantibodies as in NAM (Dalakas, 2011). In veterinary medicine inflammatory myopathies are best studied in dogs and horses. In dogs, the main classes of IMs in dog are masticatory muscle myositis (MMM), polymyositis (PM), and generalized myositis related with infectious causes. Extraocular myositis (EOM) is a less commonly occurring immune-mediated myositis. Dermatomyositis (DM) occurs in certain breeds and is associated with characteristic dermal and muscular lesions imputable to an autoimmune reaction directed against vascular antigens (Shelton, 2007). Necrotizing myopathies have been described in dogs and may be a result of many diverse causes, including inherited metabolic diseases and muscular dystrophies, or may be an isolated event following exposure to drugs, toxins and infectious agents, or hyperthermic episodes including malignant hyperthermia syndromes (Shelton, 2007). Equine inflammatory myopathies have been reviewed by Aleman in 2008 are a result of immune-mediated and infectious causes (Alemann 2008).

A unique tool in the histomorphological study of inflammatory myopathies in humans and animals is the immunohistochemical detection of Major Histocompatibility complex class I and II MHC class I proteins are essential for immune surveillance. MHC class I molecules bind CD8+ T lymphocytes while MHC II molecules binds CD4+ T cells. In particular MHC I molecules are expressed on nearly all cells, with few exceptions, including skeletal muscle fibers. Muscle fibers normally do not express detectable amounts of MHC class I or II antigens. MHC class I molecules are usually extensively up-regulated in inflammatory myopathies,

displaying an abnormal sarcolemmal as well as sarcoplasmic expression. From a diagnostic point of view they are extremely useful in detecting muscle inflammation because sarcolemmal immunolabeling can be observed even in areas of muscle sections remote from inflammatory infiltrate (Fig. I, 2). Because the MHC-I is induced in vitro by cytokines and chemokines such as IFN- γ or TNF- α , and several of these cytokines are increased in PM and sIBM muscle, it is likely that the upregulation of MHC-I is related to continuous overexpression of cytokines. Moreover, the muscle, in vivo and in vitro, has the potential to secrete pro-inflammatory cytokines upon cytokine stimulation in an auto-amplificatory mechanism that may facilitate the recruitment of activated T cells to the muscle contributing to the self-sustaining nature of endomysial inflammation and disease chronicity.

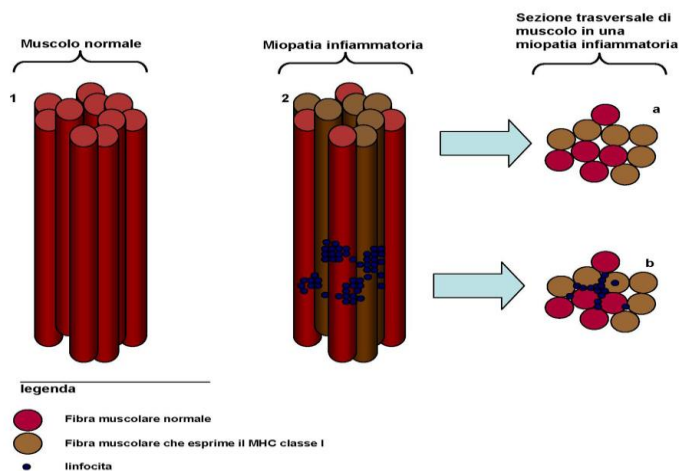


Fig. I, 2: From Paciello et al, 2009. Expression of MHC class I on muscle fibers in transversal sections that are faraway from inflammatory cells.

In PM and sIBM there is evidence of an antigen-directed cytotoxicity mediated by CD8+ T cells invading MHC-I antigen expressing muscle fibers. Specific components include:

1) activated, cytotoxic CD8+ T cells. The T cells invading muscle fibers are activated expressing MHC-I, and other adhesion molecules on their surface.

2) the CD8+ cells surround healthy, but MHC-I-class expressing, non-necrotic muscle fibers that eventually invade. The CD8/MHC-I complex is characteristic of sIBM and PM because it does not occur in inflammatory dystrophies or non-immune myopathies (Dalakas, 2001).

3) The CD8+ T cells contain perforin and granzyme granules, which are vectorially directed towards the surface of the muscle fiber inducing necrosis upon release; further, the perforin-positive CD8+ T cells are autoinvasive and express costimulatory molecules.

4) The muscle fibers can present antigenic peptides to CD8+ cells via the MHC-I molecule, thereby serving as antigen-presenting cells.

5) Other immune cells support the autoimmune process in PM and sIBM myeloid dendritic cells, potent cells in antigen presentation, which are abundantly found within the endomysial infiltrates of all IM. These cells may present local antigens to T and B cells and contribute to muscle fiber injury.

The very first event triggering the immunological activation of muscle fibers and inflammatory cells in IIM is still largely unknown, but a possible link with infectious disease has been proposed, with several viruses possibly involved in chronic and acute myositis. The best evidence of a viral connection is with the retroviruses. Monkeys infected with the

simian immunodeficiency virus and humans infected with HIV and human T-cell lymphotropic virus develop PM or sIBM (Dalakas, 2011). Even if viral antigens are not detected within the muscle it is likely that virtually several chronic infections triggers an situ persistent inflammatory response with specifically activated T cells that change the local milieu leading finally to IIM such as sIBM.

With reference to this concept, a Leishmania associated inflammatory myopathy and cardiomyopathy with suspect autoimmune pathogenesis has been described by the local scientific group (Paciello, 2009, Costagliola, 2016). This condition affects mainly the appendicular musculature and is often subclinical, with only a few clinical cases having been reported so far. Histologically, myopathic features are characterized by necrosis, regeneration, fibrosis and infiltration of mononuclear inflammatory cells. Lymphocytes, plasma cells and macrophages infiltrate muscle with an endomysial and perimysial distribution. The predominant leukocyte populations in both skeletal muscle and myocardium are CD3+, CD8+ and CD45RA+ with lesser numbers of CD4+ cells. Furthermore, only a few cells CD18+ were found mainly in the perivascular areas. Many muscle fibers have MHC class I and II expression at the sarcolemma. CD8+ T lymphocytes may invade histologically healthy muscle fibers expressing MHC class I antigens. No leishmanial DNA was amplified from the sarcoplasm of isolated muscle fibers.

IV: Infectious Myopathies:

Pyogenic (bacterial) and Clostridial myositis are uncommon condition in humans, while in animals many myositis sustained by toxins

of Clostridial bacteria are well known. These are usually the result of complicated mechanical trauma or postoperative wound infection. Pathologically, the affected muscle initially shows acute interstitial edema, which is followed by a pleomorphic inflammatory infiltrate consisting first of neutrophils and then lymphocytes. A variety of parasitic infections may involve muscle. The most common is trichinosis, which results from ingesting the larvae of the nematode *Trichinella spiralis*.

In domestic animals a variety of parasites infects specifically muscle masses and are able to induce variable muscle damages (Fig. I.3).

Agent	Type	Species affected
<i>Sarcosystis</i> spp.	Protozoan	Horses, ruminants, pigs, camelids
<i>Trichinella spiralis</i>	Nematode	Pigs
<i>Neospora caninum</i>	Protozoan	Dogs, cattle (fetal)
<i>Trypanosoma cruzi</i>	Protozoan	Dogs
<i>Cysticercus</i> spp.	Cestode (larval form)	Ruminants, pigs
Nematode larval migrans	Nematode	Dogs
<i>Hepatozoon americanum</i>	Protozoan	Dogs

Fig. I,3: agents of infectious myopathies

V. Ischemia

Muscle is relatively resistant to ischemia due to its blood supply. Varying degrees of ischemic damage, however, may occur in human patients in condition such as thromboembolism, arteriosclerosis or polyarteritis nodosa. The histologic changes seen in skeletal muscle

subjected to ischemia are not specific. The most famous ischemic myopathy in domestic animals is likely the so-called “deep pectoral myopathy” of turkey and poultry. In this disease the lesions, consisting of strictly focal ischemic necrosis, were confined entirely to the supra-coracoid (deep pectoral) muscles (Siller, 1989).

VI. Metabolic Myopathies

These are a group of diseases affecting skeletal muscle in which a congenital or acquired metabolic abnormality plays a predominant role in the pathogenesis of the lesions. In humans those conditions are classified into 4 categories: carbohydrate metabolic disorders, disorders of the lipid metabolism, disorders of the mitochondrial metabolism, and disorders of adenine nucleotide metabolism. In veterinary medicine the most important diseases are those depending on defects of glycogen metabolism, and have been described in several breeds and species (Fig. 1.4). These conditions have the unifying feature that an abnormal accumulation of glycid-rich material in muscle tissue and possibly other organs cause a progressive dysfunction leading to different pathologic phenotypes. Equine polysaccharide storage myopathy (Valentine, 2003) is a presumed hereditary autosomal dominant myopathy due to a defect of GSY 1 gene. It is characterized by abnormal accumulations of glycogen, glucose-6-phosphate, and abnormal polysaccharide within type II fibers. Two types are described: Type 1 is associated with GYS1, while Type 2 is not associated with such a defect and is still diagnosed only by histological examination of muscle biopsies. The disease is most common in draft

(prevalence of >50%), warm-blood, and Quarter-Horse-related breeds. Ponies and miniature horses are also affected.

disease	defect	organ affected	Species/breed
GSD I Von Gierke	G6P-phosphatase	Liver	Humans
GSD II Pompe	A-4-Glucosidase (acid maltase)	Liver, muscle, heart	Humans Cow (Brahman, Shorthorn) Sheep (Corriedale) Dog (Lapland)
GSD III	De-branching enzyme	Liver, muscle	Humans Dog (German sheperd) Cats
GSD IV	Branching enzyme	Liver, muscle (severe phenothype)	Humans Horse (quarter horse, paint) Cats (norwegian)
GSD V Mc Ardle	Myo-phosphorylase	Muscle (mild phenotype)	Humans, Cattle (Charollais)
GSD VI Herse	Phosphoryl-kinase	Liver	Humans
GSD VII Tarui	phosphofruktokinase	Muscle	Humans, dog (springer spaniel)
GSD VIII	phosphorylase	Liver	Humans

Fig. 1, 4. Comparative table of glycogenoses in human and domestic animals.

VII. Endocrine Myopathies

Secondary muscle damage may result from hypothyroidism (less frequently in hyperthyroidism), hyperadrenocorticism and, in both human and animals. In this condition the main histological change is the selective type II fiber atrophy.

VIII. Necrotizing myopathies causing myoglobinuria

This group of diseases is characterized by injury of muscle and excretion of myoglobin in the urine which may lead to death. A number of these conditions occur sporadically and include massive trauma (crush injury, severe burns), toxins (alcohol, barbiturates), ischemia, excessive heat, exercise, electrolyte imbalance, infections, polymyositis, and dermatomyositis. Several hereditary disorders may also be associated with myoglobinuria. In malignant hyperthermia, certain genetically predisposed individuals may suffer, during induction of anesthesia (usually halothane or succinylcholine), a syndrome characterized by muscular rigidity, myoglobinuria, rapidly rising body temperature, metabolic acidosis, and circulatory collapse, which leads to death.

IX. Nutritional myopathies

Nutritional myopathies are principally diseases of calves, lambs, swine and foals and goats. The most common cause is deficiency of selenium. Nutritional myopathy resulting from vitamin E deficiency in the absence of selenium deficiency is uncommon in mammals, but may be more common in birds and reptiles.

X. Other congenital Myopathies

In human and domestic animals the major congenital myopathies include:

1) central core disease. It is an autosomal dominant trait and is characterized clinically by infantile hypotonia and mild, nonprogressive weakness involving the proximal muscles. It is characterized by pathognomonic microscopical findings, revealing the presence of a

rounded, centrally placed "core" of myofibrillar disorganization within muscle fibers. Professor Paciello and colleagues described a similar condition in a 10-month-old, male, pony foal displaying marked contractures of the distal portion of the limbs (Paciello, 2006).

2) centronuclear (myotubular) myopathy. In contrast to the other congenital myopathies, patients with this disorder show prominent involvement of extraocular and facial muscles in addition to infantile hypotonia and slowly progressive limb muscle weakness. Pathologically, the muscle shows a centrally placed nucleus in almost every fiber. This defect has been described in Labrador retrievers as an autosomal recessive defect (Blot, 2002).

3) nemaline (rod body) myopathy. Nemaline myopathy is a nonprogressive illness characterized by mild weakness involving particularly the facial and proximal limb muscles. The pathologic hallmark of this disorder is the nemaline or rod body. They are dark-staining ovoid or elongated structures that tend to accumulate in the subsarcolemmal region of the muscle fiber. They are difficult to see with the H&E stain but are readily identified with the modified Gomori trichrome method. By electron microscopy, the rod bodies are seen as moderately electron-dense lattice-like structures with periodic lines oriented parallel and perpendicular to their long axis. They may be derived from disarranged Z band material. A similar myopathy has been described in cats (Kube, 2006).

4) congenital fiber type disproportion. Clinically, patients with this disease present as floppy infants, and about half will have skeletal abnormalities, including congenital hip dislocation, joint contractures, foot deformities, a high-arched palate, and kyphoscoliosis. In general, weakness improves

with age. The muscle biopsy characteristically shows uniformly small Type I fibers, relatively large Type II fibers, and Type I fiber predominance. Fiber type disproportion has been observed sporadically in puppies affected by the “swimming puppy syndrome” (Paciello, unpublished).

5) mitochondrial myopathies. A number of cases of congenital myopathy have been described in which the principal abnormality on muscle biopsy consisted in the presence of abnormal mitochondria. The specific diagnosis of mitochondrial myopathy should ideally be based on the combination of the clinical, morphologic, and biochemical information in a given case. These conditions are poorly documented in veterinary medicine.

6) Malignant hyperthermia (MH) is a condition that results in a sudden increase in myoplasmic calcium concentration leading to prolonged myofiber contraction and muscle rigidity, hyper-metabolism, tachycardia, dyspnea, metabolic acidosis, and life-threatening hyperthermia.

Episodes are triggered by a variety of circumstances, including stress and pharmacologic agents such as halothane anesthesia. MH is an inherited disorder in humans, pigs, horses, and some dogs. The defect is in the ryanodine receptor (RYR1), a calcium-release channel of the sarcoplasmic reticulum that serves a critical role in triggering release of calcium from the sarcoplasmic reticulum during excitation-contraction coupling.

Our group directly contributed to the studies about animal models mimicking hereditary human muscle disorders in 2012 (Iovane, 2012, unpublished data). In this work the authors described a spontaneous x-linked myopathy in a strain of C57/BL6 mice sharing many features of

X-linked myopathy with excessive autophagy (XMEA). XMEA is caused by VMA21 gene hypomorphic alleles resulting in an impaired lysosomal acidification and progressive skeletal muscle degeneration. Affected mice displayed increase in fiber size variation, and massive presence of large intracellular vacuoles containing basophilic material which was reddish at Engel's trichrome stain. Some vacuoles were positive for the LAMP-2 lysosomal membrane, for autophagic markers LC3, Beclin1 and P62, for complement membrane attack complex (C5b9). At the ultrastructural investigation two types of vacuoles were found, corresponding to pre-autophagosomes and autophagolysosomes accumulations. Q-RT-PCR analysis revealed a significant decrease of VMA21 mRNA rate and confirmed this mouse strain a possible new spontaneous model for XMEA (Iovane, 2012, unpublished data).

XI. Diseases of Neuromuscular Transmission

Myasthenia gravis is a disorder characterized by abnormal weakness and rapid fatigue of voluntary muscles. Electromyography shows characteristic decremental action potentials following repetitive stimulation of motor nerves. It is also possible to detect anti-acetylcholine receptor antibodies in the majority of patients with myasthenia gravis. Pathologic examination of the skeletal muscle in this disorder is generally not rewarding. The occurrence of thymic abnormalities in a high proportion of patients, plus the recent identification of "myoid" cells in the thymus, has led to the suggestion that anti-muscle antibodies might be formed in the thymus that may cross-react with myoneural junctions. Myasthenia gravis is

well known in dogs and other domestic animals in concomitance or not with thymoma.

XII. Muscle aging.

Sarcopenia, from the greek “poverty of flesh”, is the term used for the first time by Irwin Rosenberg to define the loss of muscle mass and strength occurring with aging (Evans, 1995). Typically, sarcopenia is a multifactorial condition that occurs in a variety of species and represents a major healthcare concern for older adults in human medicine. A lack of a well defined etiology is a critical barrier to developing treatments. Generally speaking, its pathogenesis depends on a balance between positive and negative regulators of muscle growth (Woo, 2017).

The age-related alterations in skeletal muscle are attributed to several factors, including neuromuscular junction, muscle structure (architecture and fiber composition), and metabolism (Ryall et al., 2008; Sakuma et al., 2012). The loss of muscle mass and strength results from the progressive atrophy and loss of single muscle fibers, along with loss of both types of motor units (slow and fast). The pathogenesis of these alterations is associated with specific biological processes, such as oxidative stress (Sullivan-Gunn et al., 2013). Oxidative metabolism generates reactive oxygen species (ROS), which accumulate over time and are responsible for damaging and altering cell components, particularly mitochondria and DNA sequences. Several studies have demonstrated that the age-related reduction in the synthesis of specific muscle proteins with a concurrent increase in proteolysis may result in the decline of muscle protein content and, subsequently, of muscle mass (Proctor et al., 1998; Nair, 2005;

Augustin and Partridge, 2009). Skeletal muscle has four main proteolytic systems, namely, lysosomal, caspase, calpain and ubiquitin–proteasome, all of which could potentially contribute to age-related muscular atrophy.

Animal models represent convenient and clinically relevant tools in the research on many human diseases. They are essential for three main reasons: explore the underlying pathology and molecular mechanisms of disorders; evaluate the potential efficacy of therapeutic interventions; and provide an initial estimate of the safety margin and human dosing parameters of a drug candidate. Rodents (mostly mouse and rat) are the most commonly used animal models among the vertebrate species because of their ease of management and handling, fast reproduction, and low maintenance cost. However, the use of rodents in research has some limitations due mostly to the challenge associated with attempting to model complex and still poorly understood human disorders in a lower species (McGonigle, 2014). Thus, it has been suggested that larger mammals may also be a valuable tool because their more complex anatomy and physiology make them more directly comparable to humans in some respects. Sarcopenia has been described in several animal species, from nematodes, flies, rodents, domestic and wild animals, and nonhuman primates to humans. Podolica breed, which is a dual-purpose bovine breed very common in the south of Italy that it is usually raised free outdoors in the mountains with a lifespan of about 15 years.

Recently our group described the age-related changes of skeletal muscle in Podolica cows to highlight a new model of sarcopenia for comparative studies (Costagliola, 2016).

The most relevant results indicated a statistically significant positive association between (1) age and increasing percentage of COX-negative fibers,(2) age and increasing percentage of angular atrophic fibers and fiber-type grouping, (3) increase of sarcoplasmic deposits of b-amyloid/AbPP and presence of lymphocytic inflammation, and (4) age and lymphocytic inflammation associated with MHC I sarcolemmal expression.

Of special interest was the detection inflammatory changes: lymphocytic infiltrates were observed in 40% of samples from aged animals and MHC I-positive fibers in 60%. Furthermore, there was a statistically significant positive association between age and presence of MHC I-immunopositive fibers. What triggers T-cell activation in age-related bovine myositis still remains unclear. In human polymyositis and sIBM, there is evidence of an antigen-directed and MHC I-restricted cytotoxicity mediated by CD8+ T cells, as supported by the following: the cytotoxicity of endomysial T cells to autologous myotubes, the clonal expansion of autoinvasive T cells and the restricted usage of T-cell receptor gene families, the upregulation of costimulatory molecules, and the release of perforin granules by autoinvasive CD8 cells to lyse muscle fibers (Dalakas, 2004). Upregulated cytokines, chemokines, and adhesion molecules enhance the transmigration of T cells from the circulation to the muscle. In this work the use of immunohistochemical detection of MHC I in bovine myositis demonstrated to be an useful tool even in this species. Skeletal muscle atrophy was also statistically correlated with age in old animals versus young controls. This is a typical histologic finding of sarcopenia in all species. Muscle atrophy reflects a condition of unbalanced protein

metabolism that, in sarcopenia, has been associated with a chronic low-grade systemic inflammation (called inflammaging) (Franceschi, 2007), increased levels of muscle-impairing inflammatory cytokines such as TNF- α , age-related hormonal changes, and an imbalanced protein synthesis/degradation (Ryall, 2008, Sakuma, 2012).

References:

Aleman M A review of equine muscle disorders. *Neuromuscul Disord.* 2008 Apr;18(4):277-87.

Augustin, H., Partridge, L., 2009. Invertebrate models of age-related muscle degeneration. *Biochimica et Biophysica Acta* 1790, 1084–1094.

Bach, J. F. Infections and autoimmune diseases. *J. Autoimmun.* 25, 74–80 (2005).

Baroncelli AB, Abellonio F, Pagano TB, Esposito I, Peirone B, Papparella S, Paciello O. Muscular dystrophy in a dog resembling human becker muscular dystrophy. *J Comp Pathol.* 2014 May;150(4):429-33.

Blot S, Tiret L, Devillaire AC, Fardeau M, Dreyfus PA. Phenotypic description of a canine centronuclear myopathy. *J Neurol Sci* 2002, 199: S9.

Buford TW, Anton SD, Judge AR. Models of accelerated sarcopenia: critical pieces for solving the puzzle of age-related muscle atrophy. *Ageing Res Rev.* 2010;9(4):369–383.

Costagliola A, Piegari G, Otrocka-Domagala I, Ciccarelli D, Iovane V, Oliva G, Russo V, Rinaldi L, Papparella S, Paciello O. Immunopathological Features of Canine Myocarditis Associated with *Leishmania infantum* Infection. *Biomed Res Int.* 2016; 2016: 8016186.

Cummings JF, de Lahunta A, George C, Fuhrer L, Valentine BA, Cooper BJ, Summers BA, Huxtable CR, Mohammed HO. Equine motor neuron disease; preliminary report. *Cornell Vet.* 1990 Oct;80(4):357-79.

Dalakas MC. Inflammatory disorders of muscle: progress in polymyositis, dermatomyositis and inclusion body myositis. *Curr Opin Neurol.* 2004;17(5): 561–567

De Girolami U., Smith TW., *Pathology of Skeletal Muscle Diseases TEACHING MONOGRAPH.* The American Journal of Pathology, 1982.

Evans WJ. What is sarcopenia? *J Gerontol A BiolSci Med Sci.* 1995;50:5–8

Franceschi C, Capri M, Monti D, et al. Inflammaging and anti-inflammaging: a systemic perspective on aging and longevity emerged from studies in humans. *Mech Ageing Dev.* 2007;128:92–105

Hoffman EP, Kennedy KH, Brown RH et al. Characterization of dystrophin in muscle biopsy specimens from patients with Duchenne muscular dystrophy. *N. Engl. J. Med.* 1988; 318:1363-1368

Iovane V, Paciello O, Papparella S- A spontaneous mouse model of x-linked myopathy with excessive autophagy. Doctoral thesis, 2012<http://hdl.handle.net/11588/486366>

Jubb KVF, Kennedy PC, Palmer N. Chapter 3. Muscle and Tendons. In: Grant Maxie M, ed. *Pathology of Domestic Animals*. 6th ed. Vol 1. St. Louis, Missouri. USA: Saunders Elsevier;

Kube SA, Vernau KM, LeCouteur RA, Mizisin AP, Shelton GD. Congenital myopathy with abundant nemaline rods in a cat. *Neuromuscul Disord.* 2006 Mar;16(3):188-91.

Martin PT, Shelton GD, Dickinson PJ, Sturges BK, Xu R, LeCouteur RA, Guo LT, Grahn RA, Lo HP, North KN, Malik R, Engvall E, Lyons LA. Muscular dystrophy associated with alpha-dystroglycan deficiency in Sphynx and Devon Rex cats. *Neuromuscul Disord.* 2008 Dec;18(12):942-52

McGonigle P. Animal models of CNS disorders. *Biochem Pharmacol.* 2014 Jan 1;87(1):140-9.

Melmed, C., Shelton, G. D., Bergman, R. & Barton, C. Masticatory muscle myositis: pathogenesis, diagnosis, and treatment. *Compend. Contin. Educ. Pract. Vet. Am.* Ed. 26, 590–605 (2004).

Monaco AP, Bertelson CJ, Liechti-Gallati S, Moser H, Kunkel LM. An explanation for the phenotypic differences between patients bearing partial deletions of the DMD locus. *Genomics*, 1988 2, 90e95.

Nair, K.S., 2005. Aging muscle. *The American Journal of Clinical Nutrition* 81, 953– 963.

Paciello O, Oliva G, Gradoni L, Manna L, Foglia Manzillo V, Wojcik S, Trapani F, Papparella S. Canine inflammatory myopathy associated with *Leishmania Infantum* infection. *Neuromuscul Disord.* 2009 Feb;19(2):124-30.

Paciello O, Papparella S. Histochemical and immunohistological approach to comparative neuromuscular diseases. *Folia Histochem Cytobiol.* 2009;47(2):143-52.

Paciello O., Pasolini MP, Navas L, Russo V, Papparella S. Myopathy with Central Cores in a Foal. *Vet Pathol* Vol 43, Issue 4, 2006

Paciello, O., Shelton, G. D. & Papparella, S. Expression of major histocompatibility complex class I and class II antigens in canine masticatory muscle myositis. *Neuromuscul. Disord.* 17, 313–320 (2007).

Podell, M., Chen, E. & Shelton, G. D. Feline immunodeficiency virus associated myopathy in the adult cat. *Muscle Nerve* 21, 1680–5 (1998).

Proctor DN, Balagopal P, Nair KS. Age-related sarcopenia in humans is associated with reduced synthetic rates of specific muscle proteins. *J Nutr.* 1998;128(2):351S–355S.

Ryall JG, Schertzer JD, Lynch GS. Cellular and molecular mechanisms underlying age-related skeletal muscle wasting and weakness. *Biogerontology.* 2008;9(4):213–228.

Sakuma K, Yamaguchi A. Molecular and cellular mechanism of muscle regeneration. In: Cseri J, ed. *Skeletal Muscle: From Myogenesis to Clinical Relations.* Rijeka, Croatia: InTech; 2012: 3–18.

Sewry CA. Immunocytochemical analysis of human muscular dystrophy. *Microsc. Res. Techn.* 2000; 48:142-154.

Shelton, G. D. From dog to man: The broad spectrum of inflammatory myopathies. *Neuromuscul. Disord.* 17, 663–670 (2007).

Woo J. Sarcopenia. *Clin Geriatr Med.* 2017 Aug;33(3):305-314.

Chapter 1

Inflammatory myopathy in horses with chronic piroplasmosis

Published as: Pasolini MP, Pagano TB, Costagliola A, De Biase D, Lamagna B, Auletta L, Fatone G, Greco M, Coluccia P, Veneziano V, Pirozzi C, Raso GM, Santoro P, Manna G, Papparella S, Paciello O. Inflammatory Myopathy in Horses With Chronic Piroplasmosis. Vet Pathol. 2017.

1.1 Introduction:

Equine piroplasmosis is a tick-borne protozoal disease of horses, donkeys, mules, and zebra (DeWaal, 2004; Phipps 1996; Ribeiro 1999).

The etiological agents are two apicomplexan hemoprotozoa, *Theileria equi* (Mehlhorn, 1998) and *Babesia caballi* (Nuttall 1910), that are mainly transmitted by ixodid ticks. Equine piroplasmosis (EP) occurs in tropical, subtropical, and temperate regions, and it is maintained within equine populations as long as competent arthropod vectors are present (Boldbataar, 2005; Camacho, 2005; Gummow 1996, Ribeiro 1999, Xu, 2003). In Italy, especially in the central-southern regions, EP can be considered endemic, and high rates of seropositive animals are reported (Bartolomè, 2016, Grandi, 2011, Laus, 2013, Moretti, 2010).

Clinically, piroplasmosis can cause acute to chronic forms in adult equids (de Waal, 1987, Phipps, 1996, Ribeiro 1999), as well as neonatal syndromes and abortion in mares (de Waal, 2004; van Heerden 1996). With acute *T. equi* infection, clinical signs are usually related to marked hemolysis and varying degrees of thrombocytopenia, hypophosphatemia, anemia, and hyperbilirubinemia that coincide with high levels of parasitemia (de Waal, 2004, de Waal 2004).

Chronic *T. equi* or *B. caballi* infection can present with nonspecific signs, including lethargy, anorexia, weight loss, and poor performance (Wise, 2013). Anemia may be minimal or absent in equids with chronic or persistent infection; these animals are termed inapparent carriers, have no appreciable signs of disease, and are reservoirs for tick and iatrogenic transmission (Rothschild, 2007). Among racehorses, seropositive animals

can show decreased performance compared with seronegative horses and may be at risk for developing overt clinical disease or even sudden death (Hailat, 1997, Rothshild, 2007).

The response of the equine immune system to piroplasms infection is considered complex and multifaceted (Wise, 2013). No crossprotection between *T. equi* and *B. caballi* is documented, as horses can be infected with both parasites simultaneously. A humoral response is induced and correlates with control of parasitemia (Cunha, 2006). The function of cell-mediated immunity in piroplasmosis has yet to be fully determined (Banerjee, 1997; Wise, 2013), although it is considered essential as in other hemoprotozoan infections such as *Babesia bovis*; it is generally accepted that CD4+ T lymphocytes play an important role in immune defense against apicomplexan parasites, including *Plasmodium*, *Toxoplasma*, and *Babesia* (Frolich, 2012). Development of antierythrocyte antibodies has been implied in the pathogenesis of anemia in human, murine, canine, and bovine piroplasmosis (Adachi, 1998; Gdes, 2007).

Causes of inflammatory myopathy in horses include bacterial (*Actinobacillus equuli*, *Clostridium* spp., *Streptococcus equi* infections) and parasitic (*Sarcocystis fayeri*) infections and immune-mediated (purpura hemorrhagica, idiopathic immune-mediated myositis) conditions (Alemann, 2008; Durward-Akhust 2016; Lewis, 2007).

In the present study, we describe for the first time an inflammatory myopathy in horses affected by chronic piroplasmosis and provide insight into the pathogenesis.

1.2 Materials and methods

1.2.1 Animals:

The study included 16 horses, 10 females and 6 males, aged from 3 to 28 years, referring with mild to severe clinical signs of myopathy and that were serologically positive by indirect fluorescent antibody test (IFAT) for one or both agents of piroplasmosis (cutoff of 1:80). More information about the animals' signalment and clinical signs are reported in Table 1. Clinical signs included mild to severe muscle atrophy (Figs. 1, 2), poor performance, fatigue, and weight loss. None of the studied animals showed hematologic or serum biochemical alterations consistent with acute piroplasmosis or clinical signs such as fever, anemia, or hemoglobinuria. Horses seropositive for equine herpes virus type 1 or 4 or with a clinical history of strangles were excluded from the study. Normal control specimens of equine muscle (taken from semitendinosus muscle) for immunohistochemical and molecular studies were selected from the archive of the Laboratory of Neuromuscular Pathology of the Department of Veterinary Medicine and Animal Production of Naples, from horses serologically negative for both agents of piroplasmosis and without histological evidence of myopathy.

All sampling procedures from animals were performed for diagnostic purposes; thus, the study did not require consent or ethical approval according to European Directive 2010/63/EU.

Animal sampling, including muscle biopsies, was performed by a veterinary surgeon (M.P.P.) after receiving the consent of the owner. Each

owner approved the use of tissues for research purposes, according to the internal rules of Diagnostic Service of the Department of Pathology and Animal Health of the University of Naples Federico II.

1.2.2 Hematology and Serum Biochemistry

Blood samples were collected from the jugular veins into vacuum tubes (Vacutainers; Becton Dickinson, Franklin Lakes, NJ), one with EDTA for complete blood count (CBC) and the other one without anticoagulant for serum biochemistry. Samples were sent to the laboratory on ice packs within 2 hours from collection, immediately centrifuged, and processed. CBC was performed using a cell counter analyzer (Cell Dyn 3700; Abbott, Chicago, IL), and a complete biochemical profile (sodium, potassium, chloride, iron, ionized calcium, urea, creatinine, bilirubin, aspartate aminotransferase [AST], alanine aminotransferase [ALT], lactate dehydrogenase [LDH], creatine kinase [CK], g-glutamyltranspeptidase [GGT], total proteins, albumin, albumin-globulin ratio, globulin) was performed on samples of parasitized animals using an ADVIA 1650 Chemistry System (Siemens Healthcare, Tarrytown, NY). Serum from 2 healthy horses that were serologically negative to both agents of EP protozoa were also collected.

1.2.3 Parasitological Diagnosis

Sera were screened at a dilution of 1:80 for antibodies against *B. caballi* and *T. equi* using an IFAT, according to the manufacturer's instructions (Laboratory Dr. Bose GmbH, Harsum, Germany). Each sample was run in duplicate. Ten microliters of diluted serum was placed

in wells on masked slides, which contained fixed horse erythrocytes infected with *B. caballi* and *T. equi*. Positive and negative controls were supplied from the manufacturer. The slides were incubated in a humid chamber at 37°C for 30 minutes, successively rinsed, and soaked in buffer for 10 minutes. Ten micro liters of fluorescein-conjugated rabbit anti-horse IgG (Sigma Chemical, St Louis, MO) was applied to each well, and then incubation and rinse-soak steps were repeated.

Finally, the slides were dried and mounted with 50% glycerol and 50% carbonate-bicarbonate buffer (pH 9). The slides were observed under an epifluorescent microscope (DM2500; Leica, Wetzlar, Germany) using a xenon light source. A positive reaction appeared as peripheral clusters of distinct apple-green inclusion bodies within the infected erythrocytes (see Fig. 1.1).

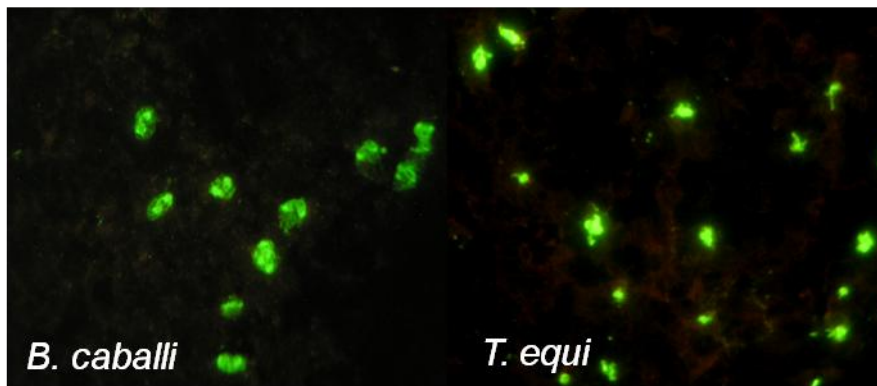


Fig. 1.1 IFAT results.

1.2.4 Histopathology and Immunohistochemistry

Muscle biopsies from the semitendinosus muscle were collected and snap frozen in isopentane precooled in liquid nitrogen.

Muscle samples from the same muscle of 5 healthy horses were used as control for immunohistochemical and molecular analysis. Specimens from both affected and control animals were frozen within 2 hours after sampling. Frozen sections (10 mm thick) were subjected to a standard panel of histochemical stains (Paciello, 2009) including hematoxylin and eosin (HE), Engel's trichrome (ET), NADH-tetrazolium reductase (NADH-TR), succinate dehydrogenase (SDH), Cytochrome oxidase (COX), ATPase at pH 9.4 and 4.3, and periodic acid–Schiff (PAS) reaction. A scoring system was designed to assess the degree of fiber atrophy as follows based on assessment of 100 fibers at 200X magnification: mild (score 1), <10% atrophic fibers; moderate (score 2), 10% to 50% atrophic fibers; and severe (score 3), >50% of atrophic fibers. A scoring system was also defined for perivascular and/or endomysial lymphocytic inflammation based on light microscopy: no inflammation (score 0); mild inflammation (score 1), 5 to 25 lymphocytes/plasma cells per high-power field (HPF) (400X); and moderate inflammation (score 2), 26 to 50 lymphocytes/ plasma cells per HPF. At least 10 fields at 400X magnification were evaluated for each section by 2 independent pathologists (T.B.P. and O.P.) under an optical microscope (Nikon E600; Nikon, Tokyo, Japan), with a concordance rate of 95%. For immunohistochemistry (IHC), frozen sections (8 mm thick) were

processed with the MACH1 Universal HPR Polymer Detection Kit (Biocare Medical LLC, Concord, CA). Briefly, the sections were dried for 1 hour at room temperature and fixed in acetone at 4C for 3 minutes; peroxide block was applied for 15 minutes at room temperature, and then the sections were incubated for 30 minutes with background sniper (Biocare Medical LLC). The primary antibodies were diluted in phosphate-buffered saline (PBS) and incubated overnight at 4C. MACH1 mouse probe was applied for 20 minutes at room temperature. Horseradish peroxidase (HRP)–polymer was added for 30 minutes at room temperature. After every step of the procedure, the sections were washed in 0.01 M PBS (pH 7.2–7.4). The reaction was revealed by using 3,30- diaminobenzidine (DAB) chromogen diluted in DAB substrate buffer. Finally, sections were counterstained in Carazzi's hematoxylin. Primary antibodies were directed against major histocompatibility complex I (H58A, mouse monoclonal antibody, dilution 1:200; VMRD, Pullman, WA), major histocompatibility complex II (H42A, mouse monoclonal antibody, 1:200; VMRD), CD3 (IS503, rabbit polyclonal antibody, 1:50; Dako, Milan, Italy), CD79a (HM57, mouse monoclonal antibody, 1:50; Dako), CD4 (HB61A, mouse monoclonal antibody, 1:50; VMRD), and CD8 (HT14A, mouse monoclonal antibody, 1:50; VMRD). The percentage of muscle fibers with sarcolemmal positivity to major histocompatibility complex I and II (MHC I and II) was scored as follows: absent/none (score 0), 0%; mild (score 1), 1% to 25%; and moderate (score 2), 26% to 50%. For evaluation of MHC I and II, fibers directly adjacent to the inflammatory infiltrate were avoided, since positive endomysial inflammatory cells can make evaluation of

sarcolemmal positivity difficult. The positive staining for MHC I and II varied from a continuous staining throughout the sarcolemma to a discontinuous sarcolemmal pattern. Endomysial blood vessels, which are normally positive for MHC I and II, were used as positive internal controls for immunohistochemistry with anti-MHC I and MHC II antibodies. Frozen section of normal horse lymph nodes was used as positive controls for immunohistochemistry with anti-CD3, CD79a, CD4, and CD8. The total inflammation score (IS) was obtained by summing the scores for lymphoplasmacytic inflammation, MHC I, and MHC II.

1.2.5 Indirect Immunofluorescence

To determine if IgG, IgM, or IgA autoantibodies directed against an unknown muscle antigen may be present in the bloodstream, we analyzed the serum from affected horses by using indirect immunofluorescence on sections of normal equine muscle (the same samples used as controls for histology and immunohistochemistry) as previously described in canine polymyositis (Hankel, 2006). Frozen sections (8 mm thick) were dried for 1 hour at room temperature and fixed in acetone at 4° C for 3 minutes. Protein block was performed using rabbit normal serum diluted 1:50 for 30 minutes at room temperature. Then, the sera from selected affected animals (horse Nos. 8, 10, 13, 14, and 15) were serially diluted in PBS (undiluted, 1:100, 1:300, 1:1000, 1:3000) and applied as primary antibody overnight at 4C.

Slides were then washed 3 times in PBS and incubated with a fluorescein isothiocyanate (FITC)–conjugated rabbit anti horse secondary antibody

(equine IgG/IgM/IgA [FITC], SA 136092; Thermo Fisher Scientific, Rockford, IL) diluted 1:100 in PBS for 2 hours at room temperature. Slides were rinsed with PBS and mounted with a solution of 1 part glycerol/ 1 part PBS. For scanning and photography, a laser scanning microscope (LSM 510; Zeiss, Goettingen, Germany) was used with illumination at 488 nm and read using a 505- to 560- nm band pass filter.

As a negative control, serial sections of muscle were incubated with PBS or with serum from 2 healthy horses that were serologically negative for piroplasms, rather than serum from affected horses.

To determine if the presumed autoantibodies were specific for equine muscle, the same sera were tested on sections of normal muscle from dog, cat, and sheep.

1.2.6 Reverse Transcription Quantitative Polymerase Chain Reaction

Total RNA, isolated from skeletal muscle tissue from 10 affected animals (horse Nos. 1–3, 6–10, 12, and 15) and 3 controls, was extracted using TRIzol Reagent (Invitrogen Biotechnologies, Carlsbad, CA), according to the manufacturer's instructions. Cases were selected based on the availability of frozen material for molecular analysis. Complementary DNA (cDNA) was synthesized using a reverse transcription kit (Maxima First Strand cDNA Synthesized Kit; Fermentas, Ontario, Canada) from 2 mg total RNA. Polymerase chain reactions (PCRs) were performed with a Bio-Rad CFX96 Connect Real-time PCR System instrument and software (Bio-Rad Laboratories, Hercules, CA). Primer and probe sequences used

were as follows: tumor necrosis factor (TNF)- α (F: TTACCGAATGCCTTCCAGTC, R: GGGCTACAGGCTTGTCACCTT), interferon- γ (IFN γ) (F: TGGACACCATCAAGG AGGAC, R: GGACCTTCAGATCATTTACCG), interleukin (IL)-10 (F: GTCATCGATTTCTGCCCTGT, R: GCTTCGT TCCCTAGGATGC), IL-12 (F: GACGCTGTGCCTTAGC, R: TCTGCCTCTGAGGATCTATCAACA), IL-4 (F: CAAAA CGCTGAACAACCTCA, R: CTGTTGAAGCACCTTTGCAG), and IL-6 (F: AGCAAGTGTGAAAACAGAAG, R: CAT CAGGCAGGTCTCCTGAT) as previously described (Ruimnaki, 2008; Sanchez-Matamoros, 2013). The PCR conditions were 10 minutes at 95° C followed by 40 cycles of 2-step PCR denaturation at 95° C for 15 seconds and annealing extension at 60C for 60 seconds. Each sample contained 1 to 100 ng cDNA in 2 Power SYBRGreen PCR Master Mix (Applied Biosystems, Foster City, CA) and 200 nmol/l of each primer (Eurofins MWG Operon, Huntsville, AL) in a final volume of 25 ml. The relative amount of messenger RNA (mRNA) for each cytokine was normalized to GAPDH as a housekeeping gene, and the data were analyzed according to the 2- $\Delta\Delta$ CT method.

1.2.7 Reverse Transcription Quantitative PCR for *T. equi* and *B. caballi* DNA

Reverse transcription quantitative PCR (RT-qPCR) for *T. equi* 18S and *B. caballi* was performed on 11 of 16 frozen samples of affected horses (horse Nos. 1-4, 6-10, 12, and 15). Cases were selected based on the

availability of frozen material for molecular analysis. Remaining 5 cases could not be evaluated due to lack of sufficient muscle tissue. Muscle tissue (100 mg) was disrupted in 1 ml PBS using FastPrep1 FP120 Cell Disrupter Instrument (Qbiogene, Montreal, Quebec) in Lysing Matrix D tubes (MP Biomedicals, Santa Ana, CA). DNA was extracted from 200 µl of the homogenized tissue (QIAcube; Qiagen, Hilden, Germany) using the QIAampcador Pathogen Mini Kit according to the manufacturer's instructions. Each sample was extracted in duplicate, and the average nucleic acid concentration was measured using a NanoDrop 1000 Spectrophotometer (Thermo Fisher Scientific, Wilmington, DE). RT-qPCR for *T. equi* primers (F: Be18SF; R: Be18SR) and TaqMan probe (VIC-TAMRA, Be 18SP) were those previously reported (Kim, 2008) and amplified an 81-bp fragment outside the V4 hypervariable region of the 18S ribosomal RNA (rRNA) gene. For *B. caballi*, primers (F: Bc-18SF402; R: Bc-18SR496) and TaqMan MGB™ probe (FAM-MGB, Bc-18SP) were those reported (Bhoora, 2010) and amplified a 95-bp fragment in the V4 hypervariable region of the 18S rRNA gene of *B. caballi*. TaqMan Universal PCR Master Mix Kit (Applied Biosystems) was used, and the reactions were carried out using the ABI PRISM 7900 HT Sequence Detection System (Applied Biosystems). Internal positive controls were RT-qPCR products of *B. caballi* and *T. equi*, obtained from EDTA blood samples of seropositive symptomatic horses, certified by the Office International des Epizooties (OIE) Reference Laboratory for Babesiosis of the Istituto Zooprofilattico Sperimentale della Sicilia and

cloned in the plasmid vector PCRII-TOPO (Invitrogen). The negative control was RNAase-free water.

1.2.8 Statistical Analysis

All data were imported into a program for statistical analysis (JMP 8.0; SAS Institute, Cary, NC). The level of significance was set at $P = .05$. Data of cytokine mRNA levels are presented as mean+standard error of the mean (SEM), whose statistical analysis was performed by analysis of variance test for multiple comparisons followed by Bonferroni's test, using GraphPad Prism (GraphPad Software, San Diego, CA). Statistical significance was set at $P < .05$. For each animal, an inflammation score was obtained summing the scores of lymphocytic inflammation, MHC I, and MHC II. Data were checked for normality of distribution with a Shapiro-Wilk's W test. The relationship between IS, histological score, and fiber atrophy was evaluated by a Spearman rank correlation test (r_s).

1.3 Results:

1.3.1 Parasitological Diagnosis, Hematology, and Serum Biochemistry

Signalment, clinical signs, selected serum biochemical findings, and serologic titers are provided in Table 1. By IFAT, 10 of 16 horses were positive for serum antibodies against both parasites, 3 of 16 were positive for *B. caballi*, and 3 of 16 were positive for *T. equi* (see Table 1).

Hematocrit was lower than 0.3 in 5 of 16 horses. The mean corpuscular volume (MCV) was lower than 45 fl in 2 of 16 horses. White blood cell

Inflammatory myopathy in horses with chronic piroplasmosis

(WBC) count was higher than $9.5 \times 10^9/L$ in 2 of 16 horses, and in 11 of 16, platelets were lower than $1.6 \times 10^{11}/L$. In 11 of 16 horses, β_1 -globulins were above the normal range (30–110 g/l), and albumin was reduced (<45 g/L) in 2 of 16 horses. In 3 of 16 horses, raised levels of serum bilirubin (>50 mmol/l) were observed. In 2 of 16 horses, hemoglobin (Hb) was lower than normal range (<68.3 mmol/L).

case number	breed	sex	age (years)	Clinical Signs	CK (U/l)	LDH (U/l)	AST (U/L)	<i>T. equi</i>	<i>B. caballi</i>
#1	Italian Saddle Horse	F	18	muscle atrophy, poor performance, weight loss	414	1072	696	-	1:80
#2	Sardinian Anglo-arab	NM	21	mild muscle atrophy, poor performance, weight loss, muscle fatigue	314	448	417	-	1:80
#3	Italian Trotter	F	6	moderate muscle atrophy, weight loss	183	495	249	1:80	1:80
#4	Appaloosa	F	12	moderate muscle atrophy, poor performance, muscle fatigue	96	339	226	1:320	1:640
#5	Italian Trotter	F	25	moderate muscle atrophy, weight loss	185	713	306	1:1280	-
#6	Italian Trotter	F	3	severe muscle atrophy, poor performance, weight loss, muscle fatigue	76	313	264	-	1:80
#7	Italian Trotter	M	3	moderate muscle atrophy, poor performance, weight loss, muscle fatigue	62	309	215	1:320	1:640
#8	Italian Trotter	M	20	moderate muscle atrophy, muscle fatigue, weight loss	180	610	210	1:2560	1:320

Inflammatory myopathy in horses with chronic piroplasmosis

case number	breed	sex	age (years)	Clinical Signs	CK (U/l)	LDH (U/l)	AST (U/L)	<i>T. equi</i>	<i>B. caballi</i>
#9	Italian Saddle Horse	F	21	moderate muscle atrophy, weight loss	148	773	313	1:1280	-
#10	Mixed Quarter Horse	F	15	moderate muscle atrophy, poor performance	198	630	381	1:1280	1:80
#11	Quarter Horse	F	5	moderate muscle atrophy, poor performance,	159	588	213	80	1:160
#12	Appaloosa	NM	12	mild muscle atrophy	112	439	230	2560	1:80
#13	Pony	F	24	mild muscle atrophy, poor performance, weight loss	*	*	*	1:1280	1:80
#14	Mixed Quarter Horse	NM	21	mild muscle atrophy, poor performance	130	347	206	1:2560	1:80
#15	Italian Trotter	M	28	moderate muscle atrophy, poor performance, weight loss	140	441	220	1:80	1:160
#16	Italian Trotter	F	14	moderate muscle atrophy, weight loss	238	578	239	1:320	-

Table .11: Signalment, muscle enzymes and IFAT titre.

Hematocrit was lower than 0.3 in 5 of 16 horses. The mean corpuscular volume (MCV) was lower than 45 fl in 2 of 16 horses. White blood cell (WBC) count was higher than 9.5 10⁹/L in 2 of 16 horses, and in 11 of 16, platelets were lower than 1.6 10¹¹/L. In 11 of 16 horses, b1-globulins were above the normal range (30–110 g/l), and albumin was reduced (<45 g/L) in 2 of 16 horses. In 3 of 16 horses, raised levels of serum bilirubin (>50 mmol/l) were observed. In 2 of 16 horses, hemoglobin (Hb) was lower than

normal range (<68.3 mmol/L). Serum activity of CK was mildly elevated in 10 of 16 horses, AST in 5 of 16, and LDH in 8 of 16 (Table 1), and SDH and g-glutamyltransferase (g-GT) were both elevated (>4 IU and 35 IU, respectively) in 1 of 16. Those minor serum biochemical abnormalities were consistent with a chronic form of equine piroplasmosis.

1.3.2 Histopathology and Immunohistochemistry

Pathological changes in muscle from all affected horses were similar, although they varied in severity (Table 1.2).

Case number	Atrophy score	Lymphocytic inflammation	distribution of inflammation	CD	CD	CD	CD79	MH	MH	IS
				3	4	8	α	C I	C II	*
#1	3	1	perivascular	2	1	1	0	2	1	4
#2	1	0	-	0	0	0	0	0	0	0
#3	2	0	-	0	0	0	0	1	1	3
#4	2	1	perivascular	1	0	2	1	1	1	5
#5	2	2	perivascular	2	2	1	1	1	1	5
#6	2	1	perivascular	1	1	1	1	1	1	5
#7	2	1	perivascular and endomysial	1	1	1	1	1	1	4
#8	2	2	perivascular	2	2	2	1	1	1	5
#9	2	1	perivascular	1	1	1	1	1	1	3
#10	2	1	perivascular	1	1	2	1	1	1	3
#11	2	1	perivascular	1	1	1	0	1	1	3
#12	1	1	perivascular	1	2	1	1	1	1	3
#13	1	1	perivascular and endomysial	1	1	1	1	1	1	3
#14	1	0	-	0	0	0	0	1	1	3
#15	2	1	endomysial	1	1	0	0	1	2	4
#16	2	1	perivascular	1	1	1	0	1	1	4

Table 1.2 Histological findings.

In 11 of 16 cases (94%), the muscle contained small lymphocytes with fewer macrophages, plasma cells, and rare eosinophils (Figs. 1.2, C).

In 12 of 16 cases, lymphocytic infiltrate formed cuffs around perimysial and endomysial blood vessels (perivascularitis; Fig. 1.2, C) with small numbers of lymphocytes scattered in the endomysium; 3 of 16 cases had mild lesions only in the endomysium. Only in 1 case with evident inflammation perivascular cuffing was not observed. In addition to lymphocytes, macrophages were also present in 5 of 16 cases (31%) (Fig. 1.2 E). Various degrees of nonangular fiber atrophy was observed (Table 1.2), scored as mild in 4 of 16 cases (25%), moderate in 11 of 16 cases (69%), and severe in 1 case (6%). No fiber type selectivity was detected by ATPase staining at pH 9.4 and 4.3 (Fig. 1.2, E). Furthermore, mitochondrial abnormalities were identified using histoenzymatic stains in 13 of 16 cases (82%), including ragged blue fibers with SDH (Fig. 1.2, G) and fibers with a moth-eaten appearance with COX (Fig. 1.2, H) and NADH stains. Importantly, mitochondrial alterations were more prominent in muscle fibers adjacent to inflammatory infiltrates (Fig. 1.2, H). Additional morphological findings were as follows: necrotic fibers associated with sarcoclastosis (phagocytes invading necrotic fibers) in 11 of 16 cases (69%); hypereosinophilic, round, and swollen degenerated fibers in 12 of 16 cases (75%) (Fig. 1.2, D); and mild perimysial fibrosis in 5 of 16 cases (31%). No parasites or PAS-positive accumulations related to polysaccharide storage myopathy were found. The control biopsies did not contain histologic lesions or abnormalities in serum CK, LDH, or AST.

The immunophenotype of inflammatory cells in skeletal muscle was identified by immunohistochemistry. All cases contained CD3+ T-cell populations with CD4+ and CD8+ equally represented in 7 of 16 cases (43.7%; Fig. 1.3 B, C). Only in 2 cases (horse Nos. 5 and 12) were CD4+ lymphocytes more abundant than CD8+. Scattered CD79a+ cells were present in 9 of 16 cases (56%), especially where the degree of inflammatory change was more severe. Lymphocytic infiltrate was graded as follows (Table 1.2): mild (score 1) in 11 of 16 (69%), severe (score 2) in 2 cases (13%), and absent (score 0) in 3 cases (19%). Furthermore, we evaluated the expression of MHC I and II antigens in myocytes. As expected, endothelial cells were positive in sections both from control and affected animals (Fig. 1.3 E- H) as well as many inflammatory cells (not shown). The majority of biopsies from affected animals (11/16 cases; 94%) showed a mild (score 1, 14/16 cases; 88%) to moderate (score 2, 2/16 cases; 13%) immunoreactivity to MHC I and II (Fig. 1.3 E, F). The staining pattern was localized to the sarcolemma or the cytoplasm (sarcoplasm) in both the atrophic and normal sized fibers. The staining pattern varied from a distinct, continuous sarcolemmal positivity, to discontinuous sarcolemmal positivity, to sarcoplasmic positive spots. Positive muscle fibers were even found distant from the inflammatory infiltrate. In control cases, MHC I and II expression was restricted to endothelial cells (Fig. 1.3, G, H). The histopathologic data were analyzed, and a statistically significant correlation between inflammation and atrophy scores was found ($r_s = 0.6$; $P = .02$, Spearman rank correlation test). The atrophy and MHC I scores were also correlated ($r_s = 0.6$; $P = .008$). No

correlation was found between inflammation score and serum levels of muscular enzymes (CK, $P = .24$; LDH, $P = .8$; AST, $P = .53$) or between inflammation score and serum titers to etiological agents (*T. equi*, $P = .09$; *B. caballi*, $P = .86$; *T. equi* and *B. caballi*, $P = .22$).

Inflammatory myopathy in horses with chronic piroplasmosis

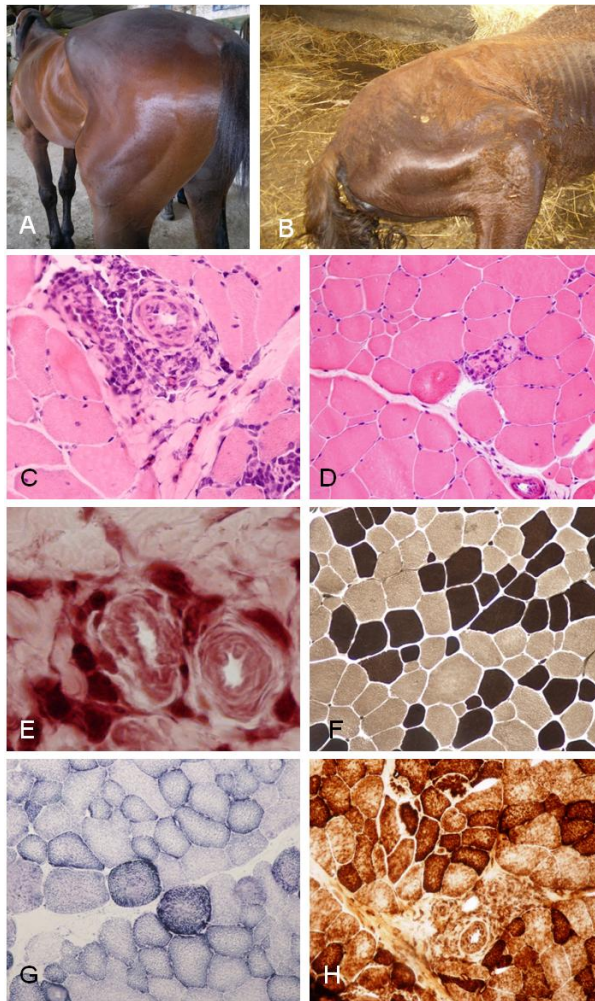
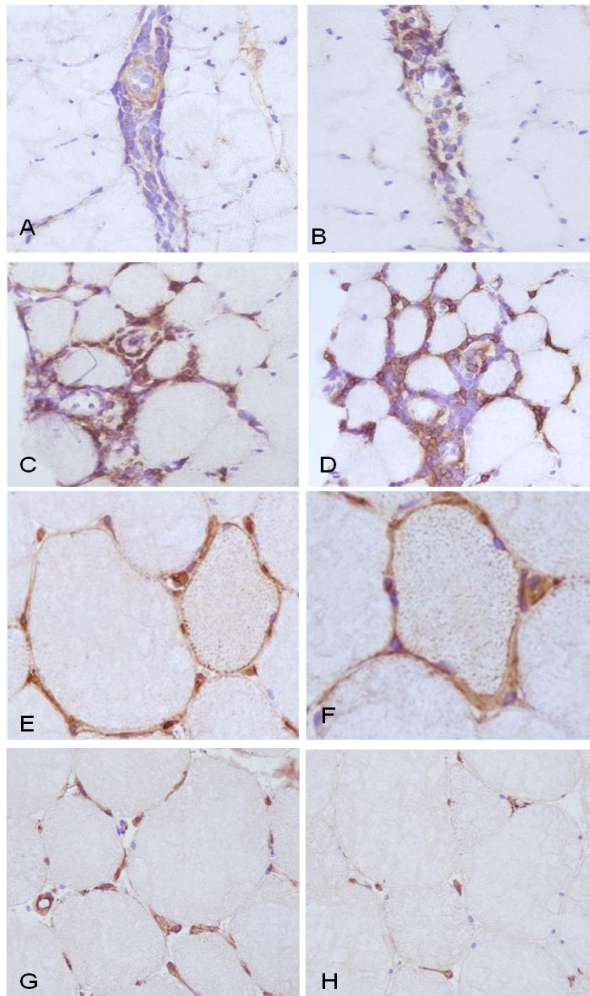


Figure 1.2. Myositis associated with chronic piroplasmosis, histology results, horse. **A** Horse No. 7. Moderate atrophy of hindlimb muscles. **B** Horse No. 1. Severe atrophy of hindlimb muscles. **C** Horse No. 5. Perivascular, perimysial, and endomysial accumulation of lymphocytes and plasma cells. Hematoxylin and eosin (HE). **D** Horse No. 8. Moderate variability in fiber size with mainly nonangular atrophic fibers, a swollen hyper eosinophilic degenerated fiber, and a necrotic fiber invaded by phagocytes (sarcoclastosis). HE. **E** Horse No. 5. Perivascular aggregates of esterase-positive macrophages. Nonspecific esterase stain. **F** Horse No. 7. Atrophic muscle fibers of both fiber type. ATPase stain pH 9.4. Type II fibers are dark; type I are light. **G**. Horse No. 10. Ragged blue fibers. Succinic dehydrogenase stain. **H**. Horse No. 6. Several moth-eaten fibers, especially near the perivascular inflammatory infiltrate (asterisk). Cytochrome oxidase stain.



Figures 1.3. Myositis associated with chronic piroplasmosis, immunohistochemistry, horse. **A.** Horse No. 4. Perivascular lymphocytes are mainly (B) CD3+ T cells with fewer (A) CD79+ B cells. Immunoperoxidase, 3,30-diaminobenzidine chromogen. **B.** Horse No. 5. Equal proportions of (a) CD4+ and (b) CD8+ T lymphocytes. Immunoperoxidase, 3,30-diaminobenzidine chromogen. **C.** Horse No. 1. Abnormal sarcolemmal staining for major histocompatibility complex (MHC) class I (arrow) scored as 2. Immunoperoxidase, 3,30-diaminobenzidine chromogen. **D.** Horse No. 15. Abnormal sarcolemmal staining for MHC II scored as 2. Immunoperoxidase, 3,30-diaminobenzidine chromogen. **E, F** Skeletal muscle, horse, normal control. Absence of staining for MHC I (G) and MHC II (H). Only endomysial blood vessels are positive. Immunoperoxidase, 3,30-diaminobenzidine chromogen.

1.3.3 *Indirect Immunofluorescence*

To detect muscle-specific antibodies in serum of affected horses, serum was applied to sections of muscle and then probed with antibody against equine IgG, IgM, and IgA. Distinct sarcolemmal labeling was detected in all sections subjected to serum from 4 affected animals even at high dilution (1:3000) of the conjugate (Fig. 1.4, A). Sections incubated with serially diluted serum from normal control horses did not show the same dilution-dependent fluorescence pattern (Fig. 1.4, B). Weak sarcolemmal staining was detected in sections incubated with serum from normal control horses and interpreted as nonspecific background, because its intensity did not vary significantly at different dilutions, whereas the labeling was dilution dependent for sections incubated with serum from affected horses. No staining was observed in sections incubated with PBS rather than equine serum (Fig. 1.4, A,B) or sections treated with PBS rather than FITC-conjugated secondary antibody (not shown).

To investigate species specificity of the target antigens, equine serum was applied to sections of skeletal muscle from dog, cat, and sheep and detected as above. Using serum from affected horses, antibodies bound to dog, cat, and sheep skeletal muscle cryosections, with similar staining intensity (Fig. 15, A). In contrast, normal control horse serum showed no immunolabeling of muscle from these species (Fig. 15, B).

Inflammatory myopathy in horses with chronic piroplasmosis

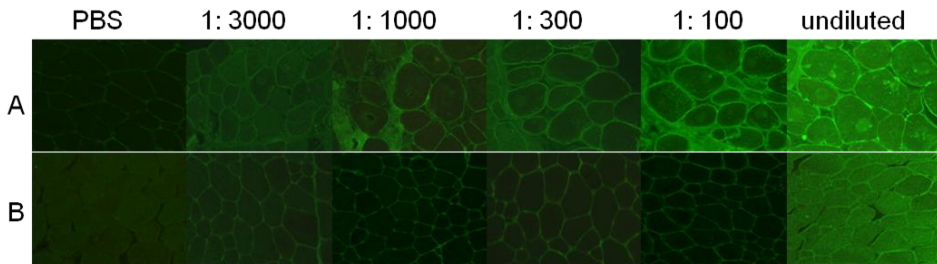


Figure 1.4. Control equine muscle cryosections stained with undiluted and serially diluted serum from horse No.14 (A) and serum from a normal healthy horse (B). Strong, dilution dependent, sarcolemmal positivity is evident only on sections treated with serum from affected horse (A); sections treated with PBS rather than serum are also negative (A and B). Indirect immunofluorescence, FITC-conjugated rabbit anti-horse IgG.

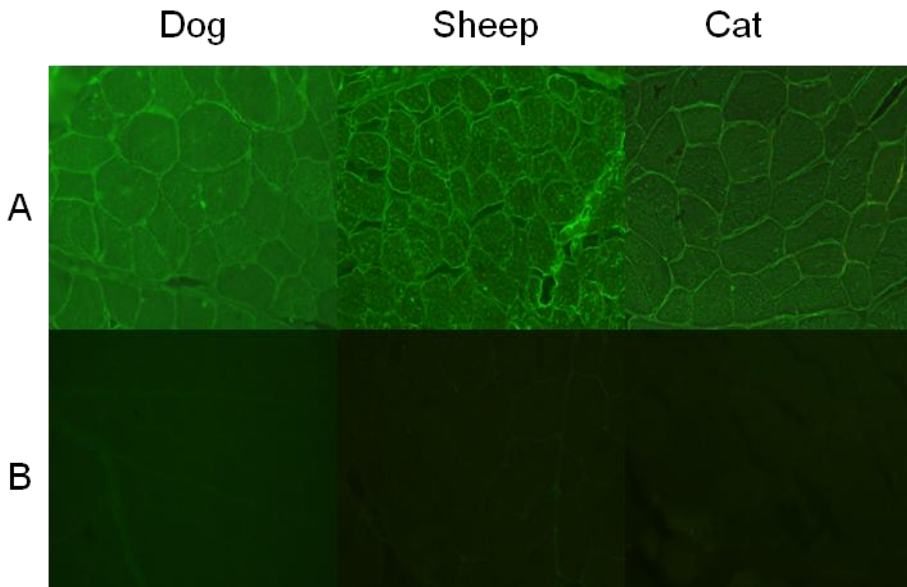


Figure 1.5. Normal canine, feline and sheep muscle cryosections stained with serum from horse No.14 diluted 1:300 (A) and serum from a normal healthy horse (B) and a FITC-conjugated rabbit anti-horse IgG, IgM, IGA. Strong sarcolemmal positivity is evident only on sections treated with serum from affected horse (A); sections treated with control serum are negative (B). Indirect immunofluorescence.

1.3.4 Molecular Findings

Using RT-qPCR, significantly increased mRNA levels of IL- 12, TNF- α , and IFN- γ were found in muscle samples from affected animals compared to controls, while IL-10 mRNA levels were not different between affected and control animals (Fig. 1.6). No amplification of IL-4 and IL-6 was found either in specimens from affected animals or controls. *T. equi* and *B. caballi* DNA was not detected by RT-qPCR in any of the 11 muscle samples tested from horses with chronic piroplasmosis.

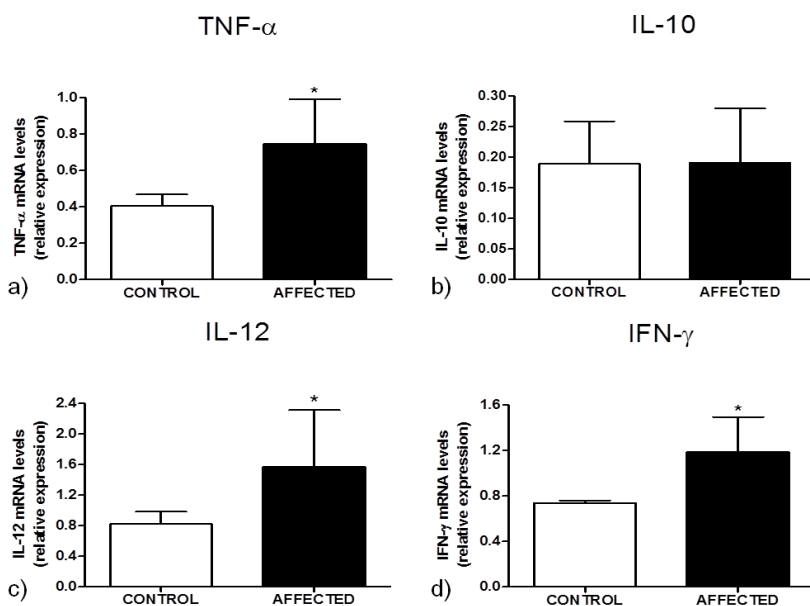


Figure 1.6. Analysis of (a) tumor necrosis factor (TNF)- α , (b) interleukin (IL)-10, (c) IL-12, and (d) interferon-g (IFN- γ) gene expression based on reverse transcription quantitative polymerase chain reaction, from skeletal muscle of horses with myositis associated with chronic piroplasmosis compared to healthy controls. Data are mean + SD of 5 samples per group. * $P < .05$ vs control. mRNA, messenger RNA.

1.4 Discussion:

Although clinical evidence of muscle impairment has been reported in chronic equine piroplasmosis (Wise, 2013) the histopathological and immunological features have not been documented to date. This study provides the first evidence of muscle pathology in horses chronically affected by piroplasmosis and with a clinical history of muscle atrophy and poor performance. Our results suggest that in chronic equine piroplasmosis, functionally important muscle damage may depend on an immune-mediated muscle damage involving circulating autoantibodies, and local cytokine expression may contribute to impaired muscle function. If so, this common protozoal disease should be included in the differential diagnosis of polymyositis and poor performance in horses as well as one of the possible causes underlying equine immune-mediated myopathy. Our work highlights the importance of the histopathological evaluation of muscle biopsies as a starting point for a more precise understanding of the pathogenesis of clinical signs of muscle impairment.

To date, histopathological features and pathogenetic aspects of idiopathic inflammatory myopathies have been extensively studied, especially in humans and dogs (Dalakas, 1996; Dalakas, 2011, Evans, 2004, Ghiraredello, 2013; Grundtmann, 2007; Lundberg, 1995; Pumarola, 2004; Vattemi, 2014). In humans, the main idiopathic inflammatory myopathies are polymyositis (PM), dermatomyositis (DM), immune-mediated necrotizing myopathy (NM), and sporadic inclusion body myositis (sIBM) (Dalakas, 2011). The disorders have primarily an autoimmune

pathogenesis, mediated either by cytotoxic T cells, as in polymyositis and inclusion body myositis; by a complement mediated microangiopathy, as in DM (dermatomyositis); or by macrophages and possibly autoantibodies, as in NM (necrotizing myopathy) (Dalakas, 2011). In dogs, the best-known immune-mediated myopathies are masticatory muscle myositis (Wu, 2007), polymyositis, dermatomyositis, extraocular muscles myositis (Jubb, 2015) and inflammatory myopathy associated with *Leishmania infantum* infection (Paciello, 2009). Masticatory muscle myositis and extraocular muscle myositis involve an immune response directed against unique antigens of this muscle group, while polymyositis and dermatomyositis share many pathogenetic aspects with their human counterparts (Evans, 2004; Pumarola, 2004). Systemic infectious diseases have been proposed as triggering factors of inflammatory myopathies and cardiomyopathies in humans, dogs, and hamsters (Costagliola, 2016, Dalakas, 2011; Evans, 2004, Iwai, 2005; Paciello, 2010). At least 3 main mechanisms have been proposed to explain the role of infectious factors as a trigger for autoimmune disease involving skeletal muscles: (1) polyclonal B- or T-cell activation, (2) molecular mimicry, or (3) immunogenicity of muscle autoantigens secondary to infection-mediated inflammation (Bach, 1998; Fujinami, 1989; Sakkar, 2008).

Based on anamnestic and histopathological data, we described an equine inflammatory myopathy that seems to involve an immune-mediated pathogenesis. A similar pattern of cellular infiltration has been described in equine immunemediated myositis, (Dirward-Akurst, 2016; Lewis, 2007) with the only exception that CD4+ cells were the predominant lymphocyte

in immune-mediated myositis but were rare in the myopathy associated with chronic piroplasmosis (only 2 of 16 cases). Given the perivascular pattern of the mixed T-lymphocytic infiltrate (CD4+ and CD8+ cells), we cannot exclude an immune reaction against blood vessels as the primary target as in human and canine dermatomyositis (Bach, 1998; Fujinami, 1989). However, the absence of a true vasculitis (ie, inflammatory cells invading and causing damage to vessel walls) and binding of serum antibodies to myocytes identified by indirect immunofluorescence are findings that argue against an immune reaction against blood vessels. A more likely explanation for the inflammatory myopathy caused by piroplasmosis seems to be an immune reaction to a protozoal antigen priming molecular mimicry, with subsequent development of autoantibodies against muscle antigens that result in damage to myocytes.

Recently, in another project from our group, the same hypothesis has been tested in canine polymyositis associated to *Leishmania infantum* (Prisco et al., unpublished data 2017). In particular, indirect immunofluorescence using sera from leishmania infected dogs has been performed, and gave similar results from the present study (dose dependent sarcolemmal positivity on muscle sections from normal skeletal muscle of dog, sheep and mouse). As further experiment, the author performed immunoblot analysis using the same sera and normal muscle proteins extract to check the molecular weight of the unknown antigen(s). A band to about 120 kDa was identified in all immunoblot experiments using the sera positive to immunofluorescence. This 120 kDa protein (p120) was not detected in muscle extracts using the sera of normal dogs.

The sarcolemmal upregulation of MHC I, the presence of cytotoxic CD8+ T lymphocytes that are the histological hallmark of human and canine PM (polimyositis) (Dalakas, 2011, Das, 2013; Evans, 2004), and the presence of sarcolemmal staining following incubation with infected horse sera all support this hypothesis. Moreover, the similar findings when serum of infected horses was incubated with muscle tissue from 3 other species (dog, cat, and sheep) make it likely that such autoantibodies are not species specific, resembling autoantibodies in canine PM (Hankel, 2006). In this study, we did not examine binding of serum antibodies to other normal tissues to determine if equine piroplasmosis autoantibodies are muscle specific.

Regarding the immunohistochemical detection of sarcolemmal MHC I and II, it is noteworthy that MHC upregulation has been found in immune-mediated idiopathic myositis. The diagnostic value of detection of sarcolemmal MHC I and II in human and canine inflammatory myopathies (Paciello, 2009; Paciello, 2007; van der Pas, 2004); has been recently confirmed in equine immune-mediated myositis (Durward-Akhurst, 2016). Upregulation of MHC I and II has been correlated to the active role of muscle fibers in antigen presentation and in initiating and maintaining pathological events in myositis independently of inflammatory infiltrates (Englund, 2001; Paciello, 2007) it is conceivable to speculate that during chronic piroplasmosis, an unknown stimulus could activate a series of inflammatory pathways resulting in sarcolemmal overexpression of MHC I and II, which in turn would attract T lymphocytes that exacerbate and perpetuate the inflammatory myopathy.

RT-qPCR for direct identification of piroplasmal DNA in skeletal muscle gave negative results in our study. Like in other immune-mediated myopathies (Dalakas, 2011), chronic infections do not cause muscle damage through a direct replication of the agent in the muscle but instead trigger a persistent inflammatory response with activated T cells. Indeed, in humans and monkeys infected with human immunodeficiency virus that develop PM or sIBM (sporadic Inclusion Body Myositis), sensitive PCR studies have repeatedly failed to confirm the presence of the virus in muscle (Dalakas, 1986a, Dalakas, 1986b; Leon-Monzon, 1993). Further studies are needed to definitely establish a direct link between chronic piroplasmosis and immunemediated myositis, such as the identification of clonally activated T lymphocytes stimulated by piroplasm antigens. For the inflammatory cytokines IL-12, TNF- α , and IFN- γ , the levels of gene expression within muscle were increased in affected compared to control animals. IL-12 is a proinflammatory cytokine produced by both immune and nonimmune cells (Mosaad, 2003; Temblay, 2007) that play a key role in autoimmune diseases and food allergies (Temblat, 2007). Indeed, it stimulates the production of IFN- γ and TNF- α from Th1 cells and natural killer (NK) cells, respectively. TNF- α (also named cachectin) is involved in the pathogenesis of muscle wasting in human sarcopenia and cachexia (Hall, 2011) TNF- α effects are mediated by the transcription factor nuclear factor (NF)- κ B, which upregulates the ubiquitin-proteasome pathway and increases the expression of inducible nitric oxide synthase (iNOS), leading to oxidative stress (Hall, 2011, Li, 2000) and decreased protein content in muscle fibers. In horses, TNF- α was demonstrated to stimulate granulocyte

diapedesis and their adherence to the endothelium (Bailey, 2001). Notably, TNF- α is able to antagonize the biological effects of insulinlike growth factor 1 (Frost, 2003), thus contributing to the development of muscle atrophy. TNF- α has a synergistic role with IFN- γ in inducing muscle atrophy in human muscle cell culture and animal models of cachexia (Kalovidouris, 1995; Matthys, 1991) TNF- α and IFN- γ are also considered strong inducers of MHC I antigens on muscle. Furthermore, previous studies demonstrate that cytokine stimulation induces muscle fibers to also secrete proinflammatory cytokines, such as IFN- γ , in an autoamplificatory mechanism that may facilitate the recruitment of activated T cells contributing to the self-sustaining nature of myositis and disease chronicity (Figarella-Branger, 2003; Lundberg, 1995) TNF- α , IFN- γ , and IL-12 are indicative of a typical Th1-mediated response (Kumar, 2009), and their involvement in the immune response in equine piroplasmosis (Hanafusa, 1998) could explain the prominent muscle atrophy in our cases considering their aforementioned biological function. Furthermore, a statistically significant correlation between inflammation score and muscle atrophy was found, suggesting a common pathogenic mechanism related to the chronic release of cytokines such as TNF- α or IFN- γ . Cytokines have been demonstrated to be a promising immunotherapeutic target (De Paepe, 2015; Ohsugi, 2007).

Mitochondrial abnormalities are frequently associated with muscle inflammation, as reported in several human inflammatory myopathies where they are generally associated with damage to the mitochondrial DNA (Oldfors, 2006; Varadhachari, 2010). In 82% of muscle biopsies

from affected horses, prominent mitochondrial histochemical alterations were found, possibly contributing to clinical muscle impairment. In conclusion, we described a clinically significant inflammatory myopathy associated with chronic equine piroplasmosis. The condition is characterized by infiltration of CD4⁺ and CD8⁺ T lymphocytes, evidence of binding of serum antibodies to muscle antigens, and increased gene expression of inflammatory cytokines, suggesting a likely immune-mediated pathogenesis.

References:

- Adachi K, et al. Anti-erythrocyte membrane antibodies detected in sera of dogs naturally infected with *Babesia gibsoni*. *J Vet Med Sci*. 1992;54(6):1081–1084. 2.
- Aleman M. A review of equine muscle disorders. *Neuromuscul Disord*. 2008; 18(4):277–287. 3.
- Bach JF, et al. Are there unique autoantigens triggering autoimmune diseases? *Immunol Rev*. 1998;164:139–155. 4.
- Bailey SR, Cunningham FM. Inflammatory mediators induce endotheliumdependent adherence of equine eosinophils to cultured endothelial cells. *J Vet Pharmacol Ther*. 2001;24(3):209–214. 5.
- Banerjee DP, et al. Cell-mediated immune response in equine babesiosis. *Trop Anim Health Prod*. 1977;9(3):153–158. 6.
- Bartolome', et al. *Babesia caballi* and *Theileria equi* infections in horses in central-southern Italy: sero-molecular survey and associated risk factors. *Ticks Tick Borne Dis*. 2016;7(3):462–469. 7.
- Bhoora R, et al. Development and evaluation of real-time PCR assays for the quantitative detection of *Babesia caballi* and *Theileria equi* infections in horses from South Africa. *Vet Parasitol*. 2010;168(3–4):201–211. 8.
- Boldbaatar D, et al. Epidemiological study of equine piroplasmosis in Mongolia. *Vet Parasitol*. 2005;127(1):29–32. 9.
- Bo'se R, Daemen K. Demonstration of the humoral immune response of horses to *Babesia caballi* by Western blotting. *Int J Parasitol*. 1992;22(5):627–630. 10.
- Camacho AT, et al. *Theileria (Babesia) equi* and *Babesia caballi* infections in horses in Galicia, Spain. *Trop Anim Health Prod*. 2005; 37(4):293–302. 11.
- Costagliola A, et al. Immunopathological features of canine myocarditis associated with *Leishmania infantum* infection. *Biomed Res Int*. 2016;2016:8016186. 12.
- Cunha CW, et al. Development of specific immunoglobulin G_a (IgG_a) and IgG_b antibodies correlates with control of parasitemia in *Babesia equi* infection. *Clin Vaccine Immunol*. 2006;13(2):297–300. 13.

- Dalakas MC, et al. Polymyositis in an immunodeficiency disease in monkeys induced by a type D retrovirus. *Neurology*. 1986; 36(4):569–572. 14.
- Dalakas MC, et al. Polymyositis associated with AIDS retrovirus. *JAMA*. 1986;256(17):2381–2383. 15. Dalakas MC. Review: an update on inflammatory and autoimmune myopathies. *Neuropathol Appl Neurobiol*. 2011;37(3):226–242. 16.
- Das L, et al. Major histocompatibility complex class I and II expression in idiopathic inflammatory myopathy. *Appl Immunohistochem Mol Morphol*. 2013;21(6):539–542. 17.
- De Paepe B, Zschuñtzsch J. Scanning for therapeutic targets within the cytokine network of idiopathic inflammatory myopathies. *Int J Mol Sci*. 2015;16(8): 18683–18713. 18.
- de Waal DT, van Heerden J, et al. An investigation into the clinical pathological changes and serological response in horses experimentally infected with *Babesia equi* and *Babesia caballi*. *Onderstepoort J Vet Res*. 1987;54(4): 561–568. 19.
- de Waal DT, Van Heerden J. In: Coetzer JAW, ed. *Equine Babesiosis in Infectious Diseases of Livestock*. 2nd ed. Cape Town, South Africa: Oxford University Press; 2004. 20.
- Durward-Akhurst SA, et al. Major histocompatibility complex I and II expression and lymphocytic subtypes in muscle of horses with immune-mediated myositis. *J Vet Intern Med*. 2016;30(4):1313–1321. 21.
- Englund P, et al. Skeletal muscle fibers express major histocompatibility complex class II antigens independently of inflammatory infiltrates in inflammatory myopathies. *Am J Pathol*. 2001;159(4): 1263–1273. 22.
- Evans J, et al. Canine inflammatory myopathies: a clinicopathologic review of 200 cases. *J Vet Intern Med*. 2004;18(5):679–691. 23.
- Figarella-Branger D, et al. Cytokines, chemokines, and cell adhesion molecules in inflammatory myopathies. *Muscle Nerve*. 2003; 28(6):659–682. 24.
- Frolich S, et al. Comparison of protective immune responses to apicomplexan parasites. *J Parasitol Res*. 2012;2012:852591. 25.

- Frost RA, et al. Tumor necrosis factor- α decreases insulin-like growth factor-I messenger ribonucleic acid expression in C2C12 myoblasts via a Jun N-terminal kinase pathway. *Endocrinology*. 2003;144(5): 1770–1779. 26.
- Fujinami RS, Oldstone MB. Molecular mimicry as a mechanism for virus-induced autoimmunity. *Immunol Res*. 1989;8(1):3–15. 27.
- Ghirardello A, et al. Autoantibodies in polymyositis and dermatomyositis. *Curr Rheumatol Rep*. 2013;15(6):335. 28.
- Go'és TS, et al. Bovine babesiosis: anti-erythrocyte antibodies purification from the sera of naturally infected cattle. *Vet Immunol Immunopathol*. 2007;116(3–4):215–218. 29.
- Grandi G, et al. Prevalence of *Theileria equi* and *Babesia caballi* infection in horses from northern Italy. *Vector Borne Zoonotic Dis*. 2011;11(7):955–956. 10 *Veterinary Pathology* XX(X) 30.
- Grundtman C, et al. Immune mechanisms in the pathogenesis of idiopathic inflammatory myopathies. *Arthritis Res Ther*. 2007;9(2):208. 31.
- Gummow B, et al. A sero-epidemiological survey of equine piroplasmosis in the northern and eastern Cape Provinces of South Africa. *J S Afr Vet Assoc*. 1996;67(4):204–208. 32.
- Hailat NQ, et al. Equine babesiosis associated with strenuous exercise: clinical and pathological studies in Jordan. *Vet Parasitol*. 1997;69(1–2):1–8. 33.
- Hall DT, et al. Inducible nitric oxide synthase (iNOS) in muscle wasting syndrome, sarcopenia, and cachexia. *Aging (Albany NY)*. 2011; 3(8):702–715. 34.
- Hanafusa Y, et al. Pathogenesis of *Babesia caballi* infection in experimental horses. *J Vet Med Sci*. 1998;60(10):1127–1132. 35.
- Hankel S, et al. Sarcolemma-specific autoantibodies in canine inflammatory myopathy. *Vet Immunol Immunopathol*. 2006;113(1–2):1–10. 36.
- Iwai LK, et al. T-cell molecular mimicry in Chagas disease: identification and partial structural analysis of multiple cross-reactive epitopes between *Trypanosoma cruzi* B13 and cardiac myosin heavy chain. *J Autoimmun*. 2005;24(2):111–117. 37.

- Jubb KVF, Kennedy PC, Palmer N. Chapter 3. Muscle and Tendons. In: Grant Maxie M, ed. *Pathology of Domestic Animals*. 6th ed. Vol 1. St. Louis, Missouri, USA: Saunders Elsevier; 2015:225–228, 229. 38.
- Kalovidouris AE, Plotkin Z. Synergistic cytotoxic effect of interferon-gamma and tumor necrosis factor-alpha on cultured human muscle cells. *J Rheumatol*. 1995;22(9):1698–1703. 39.
- Kim CM, et al. Diagnostic real-time PCR assay for the quantitative detection of *Theileria equi* from equine blood samples. *Vet Parasitol*. 2008;151(2–4):158–163. 40.
- Kumar V, Abbas AK, Aster JK. *Robbins and Cotran Pathologic Basis of Disease Professional Edition*. 9th ed. Amsterdam, the Netherlands: Elsevier Health; 2009. 41.
- Laus F, et al. Prevalence of tick borne pathogens in horses from Italy. *J Vet Med Sci*. 2013;75(6):715–720. 42.
- Leon-Monzon M, et al. Search for HIV proviral DNA and amplified sequences in the muscle biopsies of patients with HIV polymyositis. *Muscle Nerve*. 1993;16(4):408–413. 43.
- Lewis SS, et al. Suspected immune-mediated myositis in horses. *Vet Intern Med*. 2007;21(3):495–503. 44. Li YP, Reid MB. NF- κ B mediates the protein loss induced by TNF-alpha in differentiated skeletal muscle myotubes. *Am J Physiol Regul Integr Comp Physiol*. 2000;279(4):R1165–R1170. 45.
- Lundberg I, et al. Analysis of cytokine expression in muscle in inflammatory myopathies, Duchenne dystrophy, and non-weak controls. *J Neuroimmunol*. 1995;63(1):9–16. 46.
- Matthys P, et al. Severe cachexia in mice inoculated with interferon-gamma-producing tumor cells. *Int J Cancer*. 1991;49(1):77–82. 47.
- Mehlhorn H, Schein E. Redescription of *Babesia equi* Laveran, 1901 as *Theileria equi*. *Parasitol Res*. 1998;84(6):467–475. 48.
- Moretti A, et al. Prevalence and diagnosis of *Babesia* and *Theileria* infections in horses in Italy: a preliminary study. *Vet J*. 2010; 184(3):346–350. 49.
- Mosaad YM, et al. Proinflammatory cytokines (IL-12 and IL-18) in immune rheumatic diseases: relation with disease activity and autoantibodies production. *Egypt J Immunol*. 2003;10(2):19–26. 50.

- Nuttall GHF, Strickland C. Die Parasiten des Pferdepiroplasmose resp. der "Biliary fever." *Centralblatt für Bakteriologie Parasitenkunde Infektionskrankheiten Abteilung.* 1910;56(1):524–525. 51.
- Ohsugi Y. Recent advances in immunopathophysiology of interleukin-6: an innovative therapeutic drug, tocilizumab (recombinant humanized antihuman interleukin-6 receptor antibody), unveils the mysterious etiology of immune-mediated inflammatory diseases. *Biol Pharm Bull.* 2007;30(11): 2001–2006. 52.
- Oldfors A, et al. Mitochondrial abnormalities in inclusion-body myositis. *Neurology.* 2006;66(2)(suppl 1):S49–S55. 53.
- Paciello O, et al. Canine inflammatory myopathy associated with *Leishmania infantum* infection. *Neuromuscul Disord.* 2009;19(2): 124–130. 54.
- Paciello O, Papparella S. Histochemical and immunohistological approach to comparative neuromuscular diseases. *Folia Histochem Cytobiol.* 2009;47(2): 143–152. 55.
- Paciello O, et al. Expression of major histocompatibility complex class I and class II antigens in canine masticatory muscle myositis. *Neuromuscul Disord.* 2007;17(4):313–320. 56.
- Paciello O, et al. Syrian hamster infected with *Leishmania infantum*: a new experimental model for inflammatory myopathies. *Muscle Nerve.* 2010;41(3):355–361. 57.
- Phipps LP. Equine piroplasmosis. *Equine Vet Educ.* 1996;8(1):33–36. 58.
- Prisco F, Paciello O. Anti-skeletal muscle antibodies in sera of dogs with leishmaniasis. Degree thesis in Veterinary Medicine, 2017.
- Pumarola M, et al. Canine inflammatory myopathy: analysis of cellular infiltrates. *Muscle Nerve.* 2004;29(6):782–789. 59.
- Ribeiro MF, et al. Epidemiological aspects of *Babesia equi* in horses in Minas Gerais, Brazil. *Vet Res Commun.* 1999;23(6): 385–390. 60.
- Riihimäki M, et al. Epithelial expression of mRNA and protein for IL-6, IL-10 and TNF- α in endobronchial biopsies in horses with recurrent airway obstruction. *BMC Vet Res.* 2008;4:8. 61.
- Rothschild C, Knowles D. Equine piroplasmosis. In: Sellon DC, Long MT, eds. *Equine Infectious Diseases.* St Louis, MO: Saunders, Elsevier; 2007: 465–473. 62.

- Sakkas L, et al. Immunological features of visceral leishmaniasis may mimic systemic lupus erythematosus. *Clin Biochem.* 2008; 41(1–2):65–68. 63.
- Sa´nchez-Matamoros A, et al. Development and evaluation of a SYBR Green real-time RT-PCR assay for evaluation of cytokine gene expression in horse. *Cytokine.* 2013;61(1):50–53. 64.
- Temblay JN, et al. Production of IL-12 by Peyer patch– dendritic cells is critical for the resistance to food allergy. *J Allergy Clin Immunol.* 2007;120(3):659–665. 65.
- van der Pas J, et al. Diagnostic value of MHC class I staining in idiopathic inflammatory myopathies. *J Neurol Neurosurg Psychiatry.* 2004;75(1):136–139. 66.
- van Heerden J. Equine babesiosis in South Africa: a report of two cases. *Equine Vet Educ.* 1996;8(1):3–5. 67.
- Varadhachary AS, et al. Mitochondrial pathology in immune and inflammatory myopathies. *Curr Opin Rheumatol.* 2010;22(6):651–657. 68.
- Vattemi G, et al. Muscle biopsy features of idiopathic inflammatory myopathies and differential diagnosis. *Auto Immun Highlights.* 2014;5(3):77–785. 69.
- Wise LN, et al. Review of equine piroplasmosis. *J Vet Intern Med.* 2013;27(6):1334–1346. 70.
- Wu X, et al. Autoantibodies in canine masticatory muscle myositis recognize a novel myosin binding protein-C family member. *J Immunol.* 2007;179(7):4939–4944. 71.
- Xu Y, et al. Seroepidemiologic studies on *Babesia equi* and *Babesia caballi* infections in horses in Jilin province of China. *J Vet Med Sci.* 2003;65(9):1015–1017.

Chapter 2

**Lymphoplasmacytic myositis and expression of
Major Histocompatibility Complex class I in ovine
muscular sarcocystosis**

Based on: Lymphoplasmacytic myositis and sarcolemmal expression of Major Histocompatibility Complex class I and II associated with muscular sarcocystosis in sheep. Pagano TB, Costagliola A, De Biase D, Rinaldi L, Cringoli G, Bosco A, Papparella S, Paciello O. XII Convegno AIPVet Perugia, 15-17 Giugno 2015.

2.1 Introduction

Sarcocystosis (syn. Sarcosporidiosis) is a protozoal disease affecting a wide range of animals, including mammals, reptile and birds. The etiological agents are more than 130 species of *Sarcocystis*, an intracellular protozoan parasite classified in the phylum *Apicomplexa* (class *Conoidasida*, order *Eucoccidiorida*, family *Sarcocystidae*, genus *Sarcocystis* (from the old Greek: sarx = flesh and kystis = bladder (Levine, 1986).

Miescher in 1843 first reported white threadlike cysts in striated muscles of a house mouse, that's why, for the following 20 years, the parasite was simply referred to as "Meischer's tubules". In the following decades similar structures were found in other species, and the parasite was then re-named *Sarcocystis meischeriana* (Dubey, 1989). Scientists debated for a long time whether *Sarcocystis* species were protozoa or fungi, but it was not until 1967, after several studies at electron microscopy, that *Sarcocystis* was included in other apicomplexan protozoa such as *Toxoplasma* and *Eimeria* (Senaud, 1967).

In 1979 Rommel and colleagues reported that *Sarcocystis* underwent a coccidian-like indirect lifecycle cycle with each species having an obligatory two-host predator-prey lifecycle (Rommel et al., 1979): the definitive host(s) is usually a carnivore and the intermediate host(s) is usually an herbivore or an omnivore (Fig. 2.1). Infections are recognized to occur in all parts of the world and farm animals are intermediate hosts for a wide number of species.

Intermediate hosts become infected following ingestion of sporocysts released by the definitive host. Following excystation in the intestinal lumen, sporozoites penetrate the gut wall and multiply asexually by two schizogonous cycles in endothelial cells of blood vessels (first and second generation merogony), with an associated parasitaemia. The merozoites released after second generation merogony penetrate muscle cells and form characteristic sarcocysts filled with bradyzoites, although they may also invade the central nervous system (Rommel, 1985). Ingestion of infected muscle by the definitive host triggers a sexual life cycle in the intestine lining with the formation of macro- and microgamonts leading to the development of oocysts and then sporocysts which are excreted in the faeces (Bruxton, 1998, Fayer, 2004).

Sheep are the intermediate host for four species, two microcyst species (*S. tenella* [syn. *S. ovicanis*] and *S. arieticanis*) and two macrocyst species (*S. gigantea* [syn. *S. ovifelis*] and *S. medusiformis*) (Bruxton, 1998). The prevalence of muscular sarcocystosis in sheep and other ruminants is worldwide extremely high and virtually close to 100% (O'Donoghue, 1986, Meistro et al., 2015, Vangeel et al., 2007, Chiesa et al., 2013).

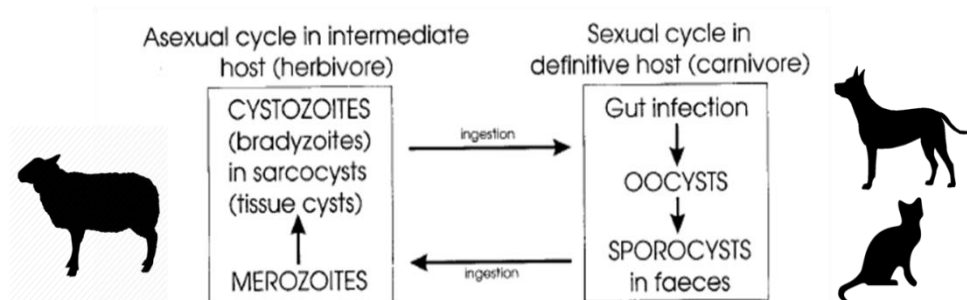


Fig. 2.1 *Sarcocystis* spp. lifecycle (modified from Bruxton et al., 1998)

However, a great geographical variation in the prevalence of infection has been reported, with highest percentages in Asia compared, for instance, to North America.

The definitive hosts are carnivores, including dogs, cats, mammalian wildlife, birds, reptiles and humans. The specific host varies with the species of *Sarcocystis*. In Table 2.1, the more known species of *Sarcocystis* in domestic animals with relative definitive and intermediate hosts are presented.

Intermediate host	Species	Definitive host
Cattle	<i>S. cruzi</i>	Dog, Wolves, coyotes, raccoons, foxes and hyenas
	<i>S. hirsuta</i>	Cat
	<i>S. hominis</i>	Human, Non human primates
(buffalo)	<i>S. fusiformis</i>	Cat
Horse	<i>S. fayeri</i>	Dog
	<i>S. bertrami</i>	Dog
Sheep	<i>S. gigantea</i>	Cat
	<i>S. medusififormis</i>	Cat
	<i>S. tenella</i>	Dog
	<i>S. arieticans</i>	Dog
Goat	<i>S. capricanis</i>	Dog
	<i>S. hericanis</i>	Dog
	<i>S. moulei</i>	Dog
Swine	<i>S. porcihominis</i>	Human , Non human Primates
	<i>S.porcifelis</i>	Cat
	<i>S. meisheriana</i>	Dog

Table 2.1: *Sarcocystis* in domestic species.

Sarcocystis spp. are genetically programmed to complete their life cycles in specific intermediate hosts or within closely related host species. For example, sporocysts of *S. hominis* infect cattle but not pigs whereas those of *S. suihominis* infect pigs but not cattle (Fayer, 2004).

Within the muscle fiber, mature banana-shaped bradyzoites reside within a specialized structure called parasitophorous vacuole (PV). The structure of the sarcocyst wall is the most important feature used in species identification. Based on examinations by transmission electron microscopy (TEM) Dubey identified 24 basic types (Dubey et al., 1989).

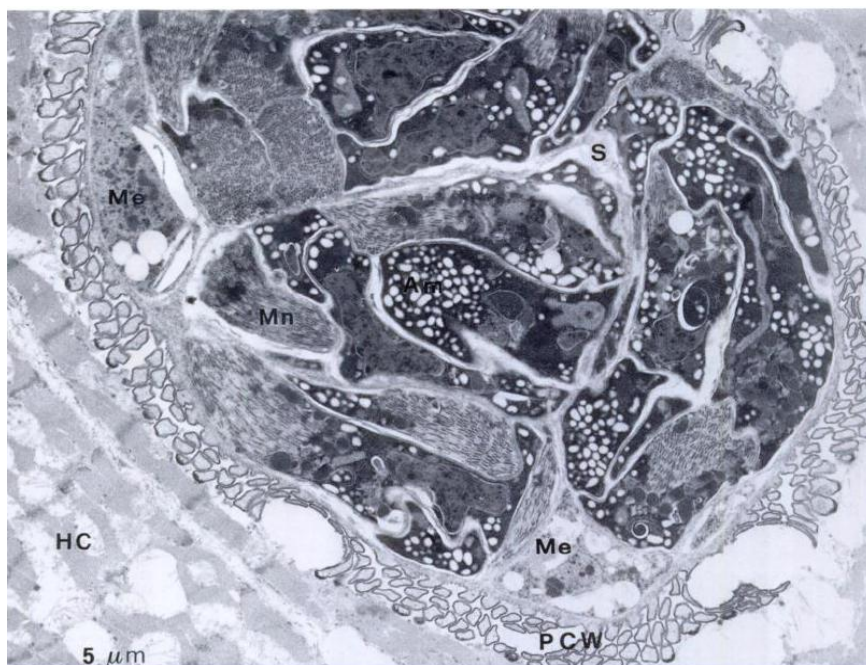


Fig 2.2: Transmission electron micrograph of a transversally sectioned sarcocyst from *Ovis musimon* showing groups of bradyzoites separated by thin septa (S) of ground substance and the palisade-like projections of the primary cyst wall (PCW). Hc, host cell; Me, Merozoite; Mn, Micronemes; A, Amylopectin granules. From Nigro et al. 1991.

The wall may be relatively simple, consisting of only minor modifications of the parasitophorous vacuole (PV) membrane to form the primary cyst wall (PCW). However, in some species the PCW is highly complex and contains branches, folding and villar protrusions that result from microtubules, microfilaments and electron-dense bodies/granules that may modify with the age of the cyst. The PCW is immediately under-layed by electron dense ground substance arranged in septa that usually divide groups of bradyzoites in different compartments. A secondary cyst wall is rarely present (i.e. *S. gigantea* in sheep) and is composed of fibrillar material of host cell origin that encloses the parasitized myocytes (Lindsay 1995).

Relatively little is known of the immunity induced by infection with *Sarcocystis* spp. but research indicates that protective immunity does develop and that cell-mediated mechanisms are probably important. It seems likely that *Sarcocystis* spp. stimulate immune mechanisms similar to those induced by *T. gondii* and *N. caninum*. Immunity to one species does not appear to trigger protective immunity to another species (Fayer and Dubey 1984).

The consequences of sarcocysts' infection are extremely different depending on the host (definitive, intermediate or accidental) and on the stage of disease.

In intermediate hosts, like sheep, the infection is mostly asymptomatic, and the presence of muscular cysts is considered an incidental finding occurring in virtually all (close to 100%) production ruminants.

However, even in sheep some species of *Sarcocystis*, particularly those with a canine definitive host, may cause clinical symptoms including fever, inappetence and reduced productivity (Uggla and Buxton, 1990).

Fayer and Elsasser (1991) explained those symptoms with the release of interleukin-1 (IL-1), prostaglandin E2 (causing fever) and tumor necrosis factor-alpha (TNF- α), which is released by macrophages infected by *Sarcocystis* species and causes inappetence, anemia and suppression of the release of pituitary growth hormone (GH), with resultant weight loss. Less frequently, abortion and stillbirths (Uggla and Buxton, 1990) or central nervous signs, including acute myopathy, ataxia, paresis and death (Jeffrey et al., 1988; Dubey et al., 1989; O'Toole et al., 1993) have been associated with sarcocystosis. Acute syndrome (named Dalmeny disease) is associated with the 2 phases of schizogony within endothelial cells of small blood vessels (Buxton et al., 1998). Apparently, the severity of clinical symptoms is dose dependant in experimental disease (Rommel, 1985) and pregnant sheep infected with high doses of *S. tenella* gave birth early to small, weak lambs and developed myositis, myocarditis and encephalitis after parturition (Munday, 1981).

In general, in muscular sarcocystosis, most available literature reports only little lymphocytic endomysial infiltrate accompanied by mild degenerative muscle fiber changes (hyaline or floccular degeneration) in appropriate intermediate hosts. On pathology textbooks is reported that the extent of muscle change bears little relationship to the numbers of developing cysts, but generally, very low numbers of *Sarcocystis* produce no reaction. As cysts mature, and the contained bradyzoites become more

distinct, the cyst capsule within the enlarged muscle fiber becomes thicker and more clearly differentiated from the muscle sarcoplasm. In some parasitic species, the outer capsular zone develops distinct radial striations, which, on electron microscopy, prove to be complex convolutions of the cyst wall. Hence, histologically, *Sarcocystis* are usually distinguished in thin-walled and thick walled species. Small pores allow communication between cyst contents and muscle cell content, but apart from the obvious nutritional dependence of the parasite on muscle fiber, little is known of the biochemical interplay which must take place (Jubb, Kennedy and Palmer's VI edition).

The most known muscle pathology associated with *Sarcocystis spp.* infection in intermediate hosts, especially cattle, is eosinophilic myositis (EM). EM is a subacute to chronic inflammatory myopathy affecting skeletal and cardiac muscle, characterized grossly by the presence of multifocal greenish to yellowish nodules within affected muscles (Barnes et al., 1968, Jensen et al., 1986). These lesions are found at slaughter or during meat cutting and result in considerable economic losses. Granstrom et al. (1989) speculated that cattle with EM lesions are genetically predisposed to produce IgE in response to *Sarcocystis* bradyzoite antigen, and that EM represents an abnormal response to sarcocyst degeneration, including a host-dependent, *Sarcocystis*-specific, type-I hypersensitivity (Wouda et al., 2006, Gajadhar et al., 1987). In 2012 Vangeel and colleagues were able to sperimentally induce EM intramuscularly injecting adjuvanted *Sarcocystis* antigen in 2 calves (Vangeel et al., 2012).

Gabor et al. in 2010 reported a severe necrotizing and histiocytic myositis and cellulitis with central caseation associated with multiple sarcocysts (*S.aucheniae* and *S. lamacanis*) in a Llama. A granulomatous myositis associated with *Sarcocystis* spp. infection has been documented in wild ducks and attributed to the initial penetration of muscle fibers or to cyst rupture and degeneration (Wobeser et al. 1982). Since the inflammatory response was very similar to that in tuberculosis, the authors suggested a cell-mediated reaction. Sarcocystis-associated encephalitis and myositis characterized by lymphohistiocytic, granulomatous and, occasionally, eosinophilic myositis was also described in pigeons and associated with a Th1 response (Olias et al., 2009, 2013). Severe chronic muscle inflammation is very rarely reported in appropriate intermediate hosts and clinically relevant cases are sporadic in horses (Traub-Dargatz et al., 1994).

Sarcocystis-related muscle pathology is much more severe and histologically different in accidental intermediate hosts. Recurrent outbreaks of muscular sarcocystosis among tourists visiting islands in Malaysia have focused international attention on sarcocystosis (Fayer et al., 2015); indeed, humans may become accidental intermediate hosts after ingesting sporocysts can develop symptomatic disease including fever, myalgia, headache, arthralgia, vomiting and chronic, mainly lymphoplasmacytic polymyositis (Greve 1985, Lau et al., 2014, Claire et al., Italiano et al., 2012, Esposito et al., 2012, Tappe et al., 2013, Abubakar et al., 2013). Less frequently *Sarcocystis* infection has been associated with eosinophilic myositis in humans as well (Arnes et al., 1999). Sporadic

reports of aberrant muscular sarcocystosis characterized by severe chronic symptomatic myositis has also been reported in dogs (Shasrabudhe et al., 1966, Blagburn et al., 1989, Sykes et al., 2012, Chapman et al., 2005, Sykes et al., 2011), cats (Kirkpatrick et al., 1986) and nonhuman primates (Gozalo et al., 2007).

Taking into account the striking variation in sarcocystis-related muscle disease, in addition with the anecdotal observation from our group of chronic muscle inflammation in affected ruminants, the aim of this study was to investigate if, even in sheep, parasitized muscle fibers could play a role in immune-stimulation, as sporadically described in accidental muscular sarcocystosis in accidental hosts.

2.2 Materials and methods

2.2.1 Animals:

The study included skeletal muscle biopsies (*semimembranosus* or *semitendinosus muscles*) from 78 sheep coming from different areas of Basilicata Region, that were regularly slaughtered and sampled in the context another large epidemiological study (see Alessandro Costagliola's doctoral thesis, Department of Veterinary Medicine and Animal Production, University Federico II of Naples. "New Prospective on Sentinel Animal Systems: Experiences in Southern Italy Polluted Areas" 2017, XXIX cycle). All muscles were immediately transported under

refrigeration temperatures at the Laboratory of Comparative Neuromuscular disorders of the Department of Veterinary Medicine of Naples and snap frozen in isopentane pre-cooled in liquid nitrogen within 2 hours after sampling.

2.2.2 Sarcocyst species identification:

DNA was extracted from 20 frozen muscle samples by using the DNeasy Blood and Tissue Kit (QIAGEN, Valencia, CA). Broad spectrum *Sarcocystis* spp. PCR for partial 18S rRNA gene sequence was performed. The 18S rDNA gene was amplified by nested polymerase chain reaction (PCR) and primer 1L (5'-CCATGCATGTCTAAGTATAAGC-3') and primer 1H (5'-TATCCCCATCACGATGCATAC-3') in the primary reaction, followed by primer 3L (5'-CTAGTGATTGGAATGATGGG-3') and primer 2H (5'-ACCTGTTATTGCCTCAAACCTTC-3') in the secondary reaction. Four microliters of DNA template was used in a 25- μ L PCR sample and the following reaction conditions: 35 mM Tris-HCl, pH 9.0, 25 mM KCl, 3.5 mM MgCl₂, 5 pmoles of each primer, 1 mM dNTPs, and 1 unit of polymerase. The PCR was performed as follows: 95°C for 2 minutes; followed by 35 cycles at 94°C for 40 seconds, 50°C for 30 seconds, and 72°C for 1.5 minutes; followed by 72°C for 6 minutes. The product was separated by agarose gel electrophoresis and Sanger's sequencing performed. Finally BLAST annealing analysis was done to identify the species.

2.2.3 Histology and immunohistochemistry

Frozen sections (10 μm thick) were subjected to a standard panel of histochemical stains (Paciello, 2009) including hematoxylin and eosin (HE), Engel's trichrome (ET), NADH-tetrazolium reductase (NADH-TR), succinate dehydrogenase (SDH), Cytochrome oxidase (COX), ATPase at pH 9.4 and 4.3, and periodic acid–Schiff (PAS) reaction. A scoring system was designed to assess the degree of fiber atrophy as follows based on assessment of 100 fibers at 200X magnification: mild (score 1), <10% atrophic fibers; moderate (score 2), 10% to 50% atrophic fibers; and severe (score 3), >50% of atrophic fibers. A scoring system was also defined for lymphocytic inflammation based on light microscopy: no inflammation (score 0); mild inflammation (score 1), 5 to 25 lymphocytes/plasma cells per high-power field (HPF) (400X); and moderate inflammation (score 2), 26 to 50 lymphocytes/ plasma cells per HPF. At least 10 fields at 400X magnification were evaluated for each section by 2 independent pathologists (T.B.P. and O.P.) under an optical microscope (Nikon E600; Nikon, Tokyo, Japan), with a concordance rate of 95%. For immunohistochemistry (IHC), frozen sections (8 μm thick) were processed with the MACH1 Universal HRP Polymer Detection Kit (Biocare Medical LLC, Concord, CA). Briefly, the sections were dried for 1 hour at room temperature and fixed in acetone at 4C for 3 minutes; peroxide block was applied for 15 minutes at room temperature, and then the sections were incubated for 30 minutes with background sniper (Biocare Medical LLC). The primary antibodies were diluted in phosphate-

buffered saline (PBS) and incubated overnight at 4°C. MACH1 mouse probe was applied for 20 minutes at room temperature. Horseradish peroxidase (HRP)–polymer was added for 30 minutes at room temperature. After every step of the procedure, the sections were washed in 0.01 M PBS (pH 7.2–7.4). The reaction was revealed by using 3,3'-diaminobenzidine (DAB) chromogen diluted in DAB substrate buffer. Finally, sections were counterstained in Carazzi's hematoxylin. Primary antibodies were directed against major histocompatibility complex I (H58A, mouse monoclonal antibody, dilution 1:200; VMRD, Pullman, WA), major histocompatibility complex II (H42A, mouse monoclonal antibody, 1:200; VMRD), CD3 (IS503, rabbit polyclonal antibody, 1:50; Dako, Milan, Italy), CD79a (HM57, mouse monoclonal antibody, 1:50; Dako), CD4 (17D1, mouse monoclonal, VMRD, 1:50), CD8 (PT36B, mouse monoclonal, VMRD, 1:50) and Dystrophin ROD domain (DYS 1, clone Dy4/6D3, Novocastra Laboratories Ltd UK, dilution 1:50). The percentage of muscle fibers with sarcolemmal positivity to major histocompatibility complex I and II (MHC I and II) was scored as follows: absent/none (score 0), 0%; mild (score 1), 1% to 25%; and moderate (score 2), 26% to 50%. For evaluation of MHC I and II, fibers directly adjacent to the inflammatory infiltrate were avoided, since positive endomysial inflammatory cells can make evaluation of sarcolemmal positivity difficult. The positive staining for MHC I and II varied from a continuous staining throughout the sarcolemma to a discontinuous sarcolemmal pattern. Endomysial blood vessels, which are normally positive for MHC I and II, were used as positive internal controls for immunohistochemistry with anti-MHC I and MHC II antibodies.

Frozen section of normal sheep lymph nodes was used as positive controls for immunohistochemistry with anti-CD3, CD79a, CD4, and CD8. The total inflammation score (IS) was obtained by summing the scores for lymphoplasmacytic inflammation, MHC I, and MHC II.

2.2.4 Immunofluorescence

To determine if there is a co-localization between Dystrophin and Major Histocompatibility Complex I on muscle fibers and on parasitophorous vacuole, immunofluorescence was carried out on selected cases (n. 10) as follows. Cryosections were dried at room temperature for 1 hour, preincubated with normal mouse serum diluted 1:10, and overlaid overnight in a humid chamber at 4°C with primary antibody directed against Dystrophic ROD domain (DYS 1, clone Dy4/6D3, Novocastra Laboratories Ltd UK, dilution 1: 10). A FITC fluorochrome-labeled rabbit anti mouse secondary antibody was applied (1:50; Jackson Laboratories, Bar Harbor, ME, USA) on sections for 2 hours at room temperature. Slides were rinsed with PBS and a second primary antibody directed against MHC I (H58A, mouse monoclonal antibody, dilution 1:10; VMRD, Pullman, WA) was applied overnight at 4°C. A TRITC fluorochrome-labeled rabbit anti mouse secondary antibody was applied (1:50; Jackson Laboratories, Bar Harbor, ME, USA) on sections for 2 hours at room temperature. Slides were rinsed with PBS and mounted with a solution of 1 part glycerol/ 1 part PBS. For scanning and photography, a laser scanning microscope (LSM 510; Zeiss, Goettingen, Germany) was used with illumination at 488 nm and read using a 505- to 560- nm band pass filter.

As a negative control, serial sections of muscle were incubated with PBS omitting the primary antibody.

2.2.5 Statistical analysis.

For measuring the association between

- 1) number of cysts and: inflammation, number of cysts and MHC I and II score, and inflammation score (IS)
- 2) atrophy score and: inflammation, number of cysts and MHC I and II score, and inflammation score (IS)
- 3) inflammation, MHC I, MHC II, inflammation score and number of MHC I and DYS1 positive cysts.

Statistical analysis was performed using SSPS software with a level of significance of 0.005. The correlations were performed using the Pearson correlation test.

2.3 Results:

2.3.1 *Sarcocystis* species identification:

All samples tested revealed 100% identity to *Sarcocystis tenella* by BLAST alignment (Fig 2.1).

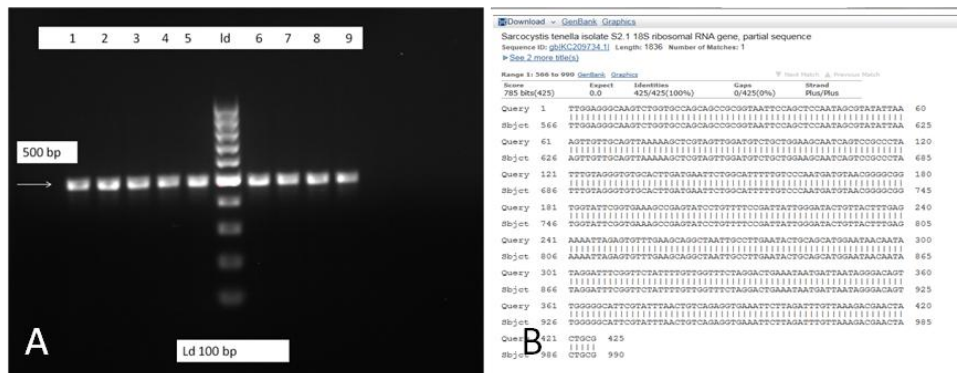


Fig. 2.3: *Sarcocystis* species identification. A distinct 500bp band at PCR was found (consisting with *Sarcocystis* 18S rRNA gene sequence). Then, sequence alignment by BLAST database revealed 100% of identity to *S. tenella*.

2.3.2 Histology and Immunohistochemistry

Detailed results of histopathology and immunohistochemistry are presented in Table 2.2.

case number	cysts number	atrophy	inflammation	MHC I	MHC II	CD4	CD8	CD79	MHC I positive Cysts	Dys 1 positive cysts	infl. score (inflammation+MHC I+MHC II)
1	9	1	0	2	2	0	0	0	0	0	4
2	7	2	0	1	1	0	0	0	0	0	2
3	3	1	0	0	0	0	0	0	0	0	0
4	11	0	0	2	1	0	0	0	0	0	3
5	15	1	0	2	2	0	0	0	5	0	4
6	9	0	0	1	1	0	0	0	0	0	2
7	10	1	0	1	1	0	0	0	4	0	2
8	1	1	0	2	2	0	0	0	0	0	4
9	13	1	0	3	2	0	0	0	0	0	5
10	0	1	0	0	0	0	0	0	0	0	0
11	4	0	0	1	1	0	0	0	0	0	2
12	10	1	0	1	1	0	0	0	5	0	2
13	7	1	0	1	1	0	0	0	0	0	2
14	60	2	0	2	1	0	0	0	1	1	3
15	17	0	0	2	2	0	0	0	2	2	4
16	2	2	0	1	1	0	0	0	0	0	2
17	8	0	0	1	1	0	0	0	3	0	2
18	3	0	0	1	1	0	0	0	1	0	2

Lymphoplasmacytic myositis and expression of MHC I in ovine muscular sarcocystosis

case number	cysts number	atrophy	inflammation	MHC I	MHC II	CD4	CD8	CD79	MHC I positive Cysts	Dys 1 positive cysts	infl. score (inflammation+MHC I+MHC II)
19	5	1	0	2	2	0	0	0	2	0	4
20	32	2	0	2	2	0	0	0	12	1	4
21	3	1	0	1	1	0	0	0	2	0	2
22	8	2	0	1	1	0	0	0	3	0	2
23	6	0	0	1	1	0	0	0	3	0	2
24	20	1	1	3	1	1	2	0	13	2	5
25	23	1	1	2	3	1	2	1	10	2	6
26	4	2	1	2	2	0	2	0	0	0	5
27	16	1	1	2	1	1	2	1	5	0	4
28	9	1	1	2	1	1	2	0	5	0	4
29	4	1	1	1	1	1	1	1	2	0	3
30	10	1	1	3	3	1	3	0	4	0	7
31	18	2	1	3	3	2	2	1	12	3	7
32	8	1	1	2	2	1	2	0	3	0	5
33	10	1	1	2	2	0	1	0	4	0	5
34	13	1	1	2	2	1	2	0	4	0	5
35	7	1	1	2	2	1	1	0	4	0	5
36	8	0	1	2	2	1	1	0	5	0	5
37	26	1	1	2	3	1	2	0	11	0	6
38	23	2	1	1	1	0	1	0	14	0	3
39	2	1	1	1	1	0	1	1	0	0	3
40	19	2	1	2	2	0	1	0	15	2	5
41	26	2	1	1	0	0	1	0	2	0	2
42	4	2	1	1	1	1	0	1	1	0	3
43	8	2	1	1	1	1	2	1	12	0	3
44	28	2	1	3	3	1	2	0	15	0	7
45	4	2	1	2	2	1	2	0	0	0	5
46	15	2	1	2	2	1	3	0	4	0	5
47	21	2	1	1	1	0	1	0	10	0	3
48	2	1	1	2	2	1	1	0	0	0	5
49	2	0	1	1	1	0	2	1	0	0	3
50	7	1	1	1	1	1	2	1	0	0	3
51	1	1	1	2	3	2	2	0	0	0	6
52	4	1	1	2	2	1	3	0	0	0	5
53	17	1	1	3	3	1	1	0	10	4	7
54	10	1	1	3	2	2	3	0	4	0	6
55	2	2	1	2	1	1	2	0	0	0	4
56	10	1	2	3	2	2	3	0	3	0	7
57	0	0	2	1	1	2	3	0	0	0	4
58	4	2	2	1	1	2	2	0	0	1	4
59	1	1	2	3	3	+	2	0	0	0	8
60	22	1	2	3	2	1	2	1	9	3	7
61	20	1	2	1	1	1	2	0	8	3	4
62	9	1	2	2	1	2	3	0	8	0	5
63	35	1	2	1	2	1	2	0	13	3	5
64	22	0	2	1	+	2	3	0	15	2	3
65	2	2	2	2	1	1	3	1	2	0	5
66	7	2	2	2	1	2	3	0	2	0	5
67	70	1	2	3	2	1	3	0	30	10	7
68	6	3	2	3	2	1	2	0	3	0	7

case number	cysts number	atrophy	inflammation	MHC I	MHC II	CD4	CD8	CD79	MHC I positive Cysts	Dys 1 positive cysts	infl. score (inflammation+MHC I+MHC II)
69	25	3	2	3	2	2	2	1	12	0	7
70	11	0	2	2	2	0	1	0	4	0	6
71	9	2	2	2	1	1	2	0	7	4	5
72	30	1	2	2	1	1	2	0	13	4	5
73	8	1	2	3	3	1	3	1	7	0	8
74	15	1	2	3	1	0	2	1	10	0	6
75	9	2	2	1	1	1	2	0	6	0	4
76	18	2	3	3	3	2	3	1	17	1	9
77	58	1	3	3	3	1	3	0	32	11	9
78	6	1	3	2	1	2	2	0	6	0	6

Table 2.2 Summary of histopathological findings.

As expected, intra-sarcoplasmic round to oval, septate sarcocysts (ranging from 3 to 60 cysts/cm²) with thin wall (<1 μm), containing myriads of crescent-shaped bradyzoites (Fig. 2.4, A) were detected in the vast majority of muscle biopsies (97,2 % -76 out of 78) of cases.

72% (55 out 76) of cases showed inflammatory changes scored as mild (58,1% - 32 out of 55), moderate (72% -30 out of 55) or severe (5,4% - 3 out of 55). Inflammation consisted of multifocal endomysial foci of lymphoplasmacytic inflammation (Fig. 4, C), occasionally centered around parasitized cysts (Fig. 2.4, B) or arranged in perivascular cuffs. Multifocally, in about 30% of cases. lymphocytes and plasmacells were admixed with esterase positive macrophages (Fig. 2.4, D) or invaded necrotic muscle fibers (sarcoclastosis). Notably, eosinophils were constantly absent.

Increased variability in fiber size was a prominent finding in almost all cases (85,8% -67 out of 78) and was classified as mild in 61% of cases (41 out of 67), moderate in 34% of cases (23 out of 67) and severe in 2,9% of cases (2 out of 67).

In more inflamed cases (30%) mitochondrial abnormalities such as central palor and presence of “moth eaten” fibers were observed at histoenzimatic stains COX (Fig. 2.4 E), NADH and SDH.

Sarcolemmal overexpression of MHC I (Fig. 2.3 A) was detected in 76 out of 78 cases (97,4%), that is both in biopsies with evident inflammatory infiltrate and in cases without visible inflammation. It was score as mild in 26 cases out of 76 (34%), moderate in 32 cases (42,7%) and severe in 17 cases (24,3%). Similarly, MHC II (Fig. 2.3 B) was positive in 96% of cases (3 animals) and classified as mild in 36 cases (48%), moderate in 26 cases (34,6%) and severe in 11 cases (14,6%).

The predominant lymphocytic populations were CD3+, CD8+ with lesser numbers of CD4+ (Fig. 2.5). CD79+ cells were present in 15/55 (27%) of cases showing inflammatory infiltrate at hematoxylin and eosin stain. T lymphocytes were predominantly CD8+ in 63% of cases (35/55) and purely CD8 + in 18% of cases (10/55) (Fig. 2.5). In 8 cases (14%) CD4+ and CD8+ lymphocytes were in an equal proportion. Only in 1 case CD4 positive lymphocytes were more represented than CD8 positive lymphocytes.

In 56 cases (73%) MHC I labeled also the wall of the cysts in a scattered, inconstant fashion (Fig. 2.6 A, C, F); three different staining pattern of MHC I immunopositivity were observed: in most cases only the cysts wall was immunopositive (Fig. 2.6 C- about 70%). Parasitized muscle fibers displayed occasional immunopositivity to MHC I without positivity on the sarcolemma (Fig. 2.6 D- about 5%). In few cases (about 5%), and especially when accompanied by prominent inflammatory

infiltrate, both the sarcolemma and the cyst wall resulted MHC I positive (Fig. 2.6 E). In remaining 20% of parasitized muscle fibers both the sarcolemma and the cyst wall were negative to MHC I.

2.3.3 Immunofluorescence

To explore a possible co-localization between the sarcolemmal protein Dystrophin and Major histocompatibility complex I, immunofluorescence was performed on cases displaying Dystrophin positivity on the cyst wall at immunohistochemistry (n. 19 cases-20%).

The cyst wall immunopositivity to Dystrophin was confirmed only in 9 cases and in a small percentages of cases (less than 10% of the cysts in the section), but, when positive a granular, multifocal co-localization between MHC I and Dys I was observed (Fig. 2.7 E-F). No positivity was detected in sections incubated with PBS rather than primary antibodies.

2.3.4 Statistical analysis

The number of cysts was positively correlated with inflammation degree ($P < 0,05 = 0,04$), inflammation score ($P < 0,05 = 0,04$), MHC I and MHC II score ($P < 0,05 = 0,004$) and number of MHC I positive cyst wall ($P < 0,05 = 0,00001$).

The atrophy score was not correlated with inflammation degree ($P = 0,07$) and inflammation score ($P = 0,09$).

MHC I, MHC II and inflammation score were positively correlated with the number of MHC I and DYS1 positive cysts ($P = 0,001$, $0,0001$, respectively).

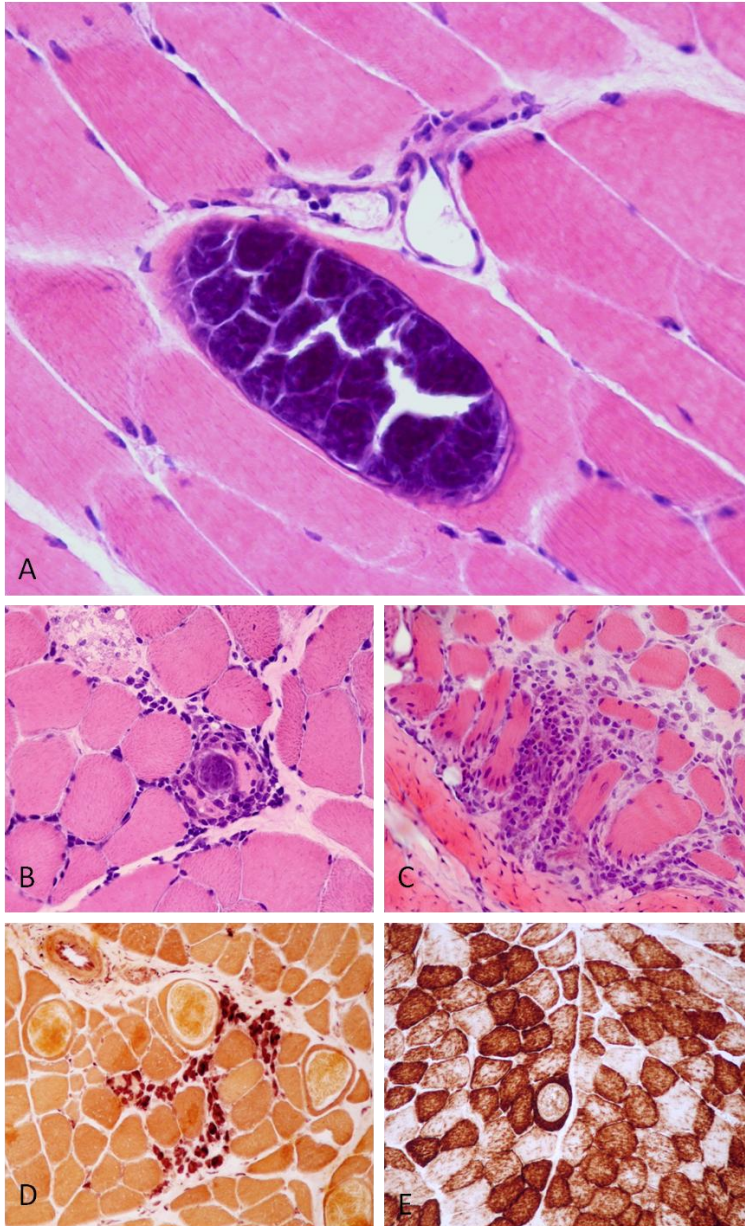


Fig. 2.4 Histopathology. Hematoxylin and eosin (A-C), nonspecific esterase (D) and COX stain (E). A) Thin walled, septate sarcocyst containing myriad of banana shaped bradizoytes. B) lymphocytic infiltrate surrounding a parasitized muscle fiber. C) endomyxial chronic infiltrate. E) esterase positive inflammatory infiltrate consisting with macrophages. F) fibers with abnormal COX staining: “moth eaten” aspect and central pallor.

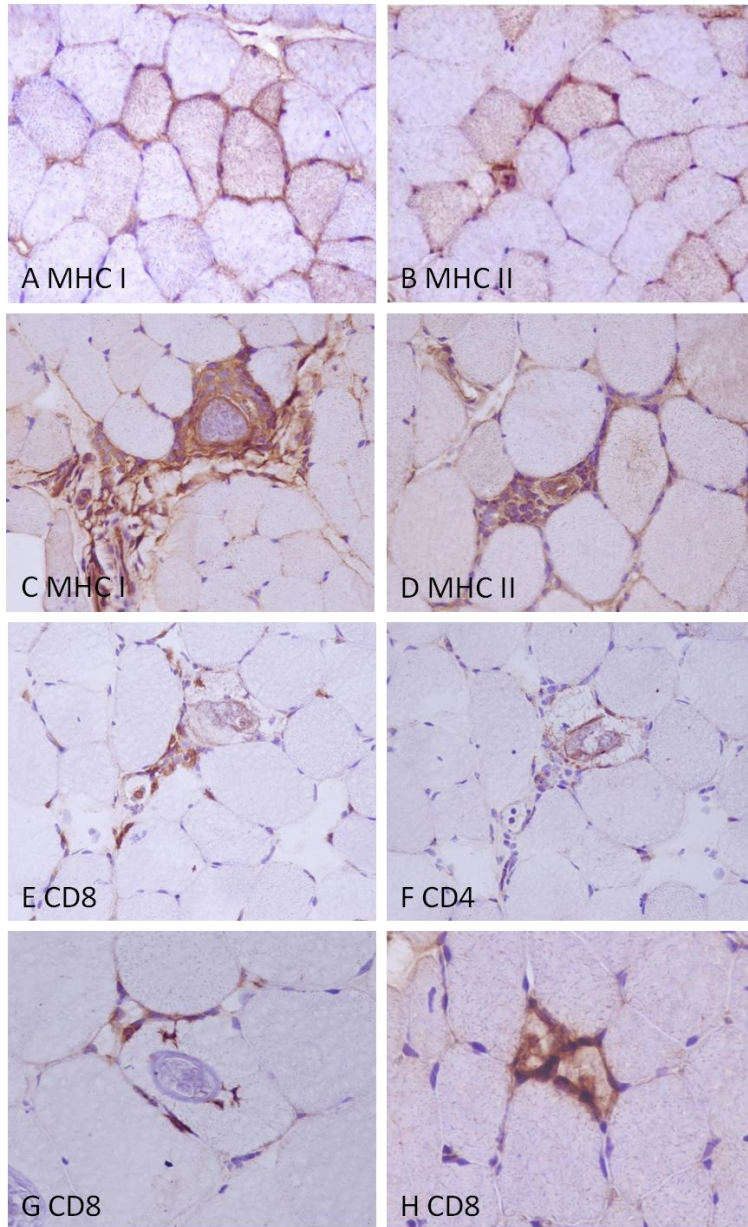


Fig. 2.5: immunohistochemistry. HRP method, hematoxylin counterstain. A and B: MHC I and II were overexpressed on the sarcolemma of muscle fibers. Inflammatory cells associated with parasitized cysts (C) or arranged perivascularly (D) are MHC I and II positive, respectively. The inflammatory infiltrate is predominantly CD8 positive (E, F). CD8 positive lymphocytes invade a parasitized (G) or not parasitized (H) fiber.

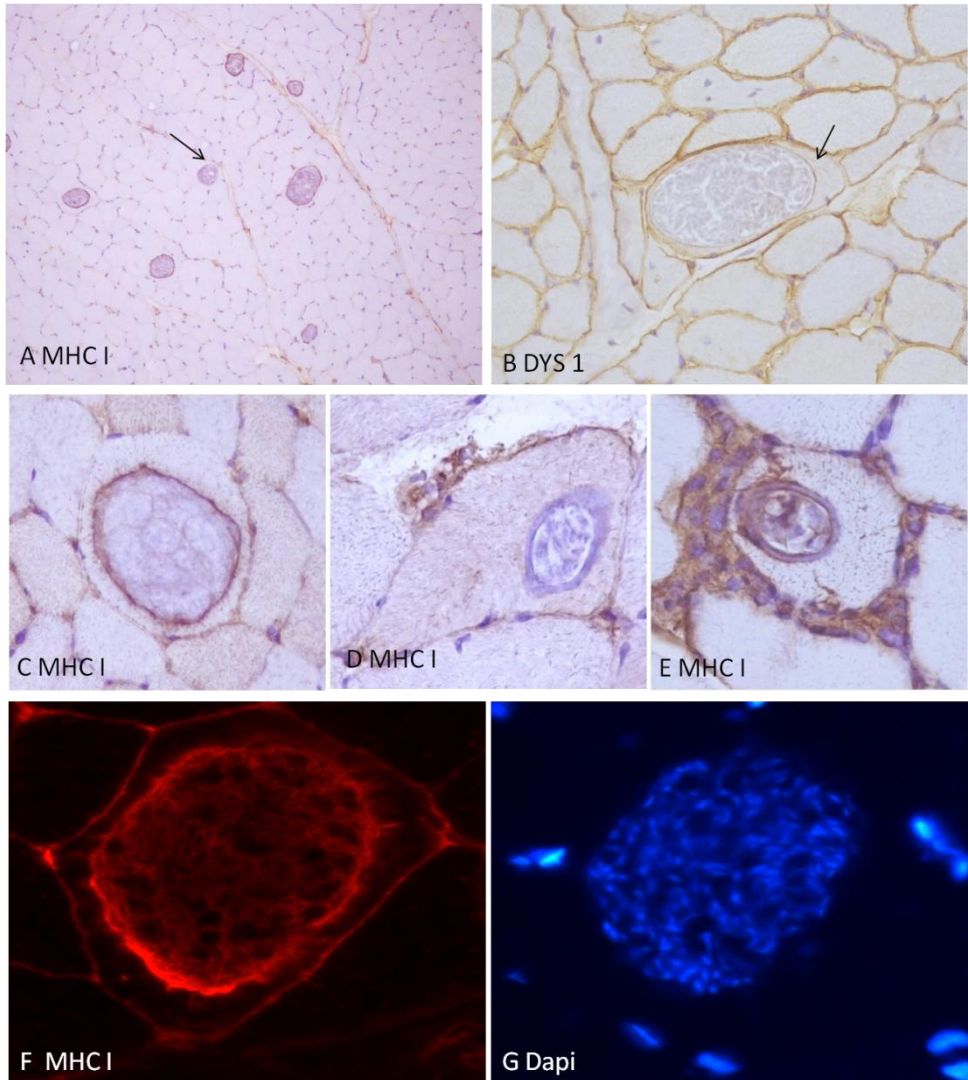


Fig. 2.6 Immunohistochemistry and Immunofluorescence. (A) MHC I labels the wall of the cysts in a scattered fashion, with sparse negative cysts (arrow). (B) In a small percentage of cases DYS 1 labeled the wall of the cysts (arrow). (C-E) Three different combinations of staining patterns of MHC I: cyst wall positive, sarcolemma negative (A), sarcolemma positive, cyst wall negative (B), both sarcolemma and cyst wall positive (D). (E) The MHC I labeled the cyst wall and the sarcolemma also in immunofluorescence. (F). Dapi nuclear stain shows myriads of bradyzoite nuclei within the cyst.

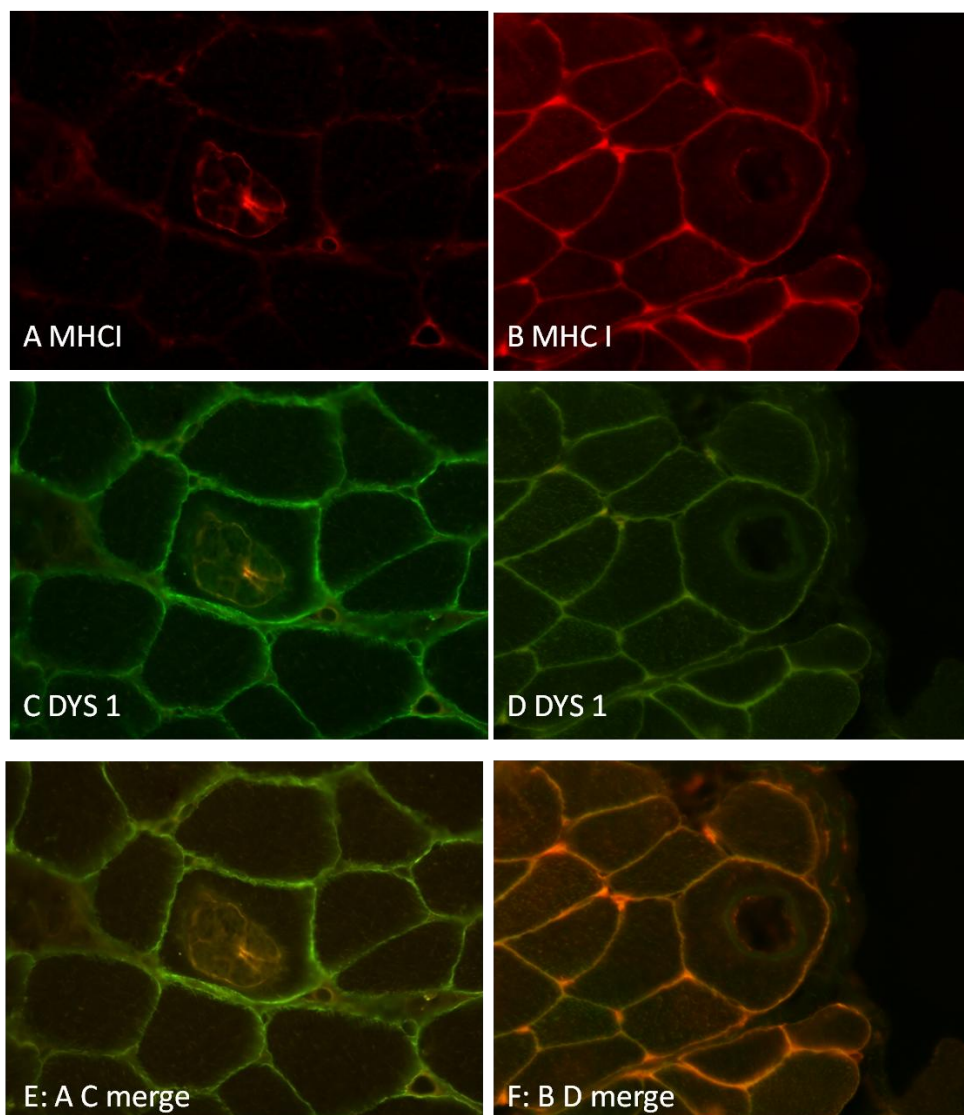


Fig. 2.7: Immunofluorescence. MHC I (red, TRIC) labeling of parasitophorous vacuole and cyst septa (A) or membrane of parasitized fiber with partial labeling of the internal portion of the cyst (B). Anti-Dystrophin antibody (DYS 1, green FITC) distinctly labels the sarcolemma (C, D) and partially the cysts (C,D). MHC I and DYS 1 colocalize on the sarcolemma of a parasitized fiber (F) and focally the internal portion of the cyst (E,F merge, orange color).

2.4 Discussion

As shown in the introduction, despite *Sarcocystis* is widely regarded as a “silent” muscle pathogen, it is associated with a wide range of disease manifestation, ranging from localized forms (eosinophilic myositis), to acute and peracute systemic febrile disease and abortion during endothelial schizogony phase (Dalmey disease) as well as clinically relevant polymyositis in accidental intermediate hosts. These different clinical manifestations are partly imputable to different phases of the lifecycle of the parasite and partly to the degree of adaptation of the host’s immunitary system.

Lymphoplasmacytic infiltrate associated with muscular sarcocystosis in appropriate intermediate host is occasionally mentioned in the literature (Jeffrey et al., 1989, Buxton et al., 1989, Jubb Kennedy and Palmers 2017); however, an accurate incidence analysis and histopathological characterization of this inflammatory change has not been documented so far.

We reported a variable degree of chronic lymphoplasmacytic infiltrate in 72% of muscle biopsies of sheep naturally infected with *Sarcocystis tenella*, and the percentage of inflammation positive cases becomes even higher considering the sarcoplasmic expression of MHC I and II (97%) as a more sensitive indicator of muscle inflammation.

Statistical analysis revealed that the degree of muscle inflammation, either in terms of inflammatory infiltrate either of MHC I sarcolemmal expression, is positively correlated with the number of cysts, confirming a

strong relationship between the etiological agent and histological markers of inflammation.

However, since the distribution of cysts is not always homogeneous within a muscle group, when parasites are not visible in histopathological sections, the presence of *Sarcocystis* can not be immediately ruled out in case of muscle inflammation.

Complexively, our results indicate that chronic inflammation in ovine muscular sarcocystosis is likely underestimated. The presence of inflammatory infiltrate, mainly consisting of CD3/CD8 positive T lymphocytes, together with the strong sarcolemmal immunopositivity to MHC I suggest that parasitized muscle fibers are not merely inert “victims” of intracellular parasitism, but, as in other myopathies, may play an active role in antigen presentation and in maintaining pathological events (Englund, 2001; Paciello, 2007, Paciello 2009). If so, this common protozoal disease should be included in the differential diagnosis of polymyositis in many species of animals, including humans; furthermore it should be excluded before considering idiopathic and immune-mediated myopathy as underlying condition of muscle inflammation.

Expression of MHC class I and II antigens on the surface of muscle fibers has already been described in other infectious (i.e. *Toxoplasma* and *Leishmania* related myositis- Matsubar. 1990, Paciello, 2009) and immune-mediated myositis of humans and dogs (Dalakas, 2011, Vatteemi, 2014). Indeed, increasing evidences suggest that myositis formerly considered “idiopathic” are in fact related to underlying systemic parasitic and viral diseases triggering immune-mediate muscle damage in both

humans and dogs (Paciello, 2009, Evans, 2004, Dalakas, 2010). For those reasons it is possible that in a close future these two entities (infective and immune-mediated myositis) would be considered partially overlapping.

Differently from the previous chapter, in which we described a presumptive immune-mediated myositis in horses affected by chronic piroplasmosis, in sarcosystis-related myositis the etiological agent is clearly detectable within muscle tissue; this means that the parasite can induce muscle damage and trigger muscle inflammation in at least two different ways: I) by a direct damage to the cell or, less likely, II) stimulating an immune-mediated by a possible molecular mimicry between self and parasite's antigens (see chapter 1).

The direct role of *Sarcocystis* in inducing a cell damage possibly stimulating the MHC I overexpression may be related to the perturbation of endoplasmic reticulum (ER) homeostasis (ER stress). ER stress (Rayavarapu, 2012) is reported in response to intracellular parasitism (Galluzzi et al. 2017) and in human inflammatory myopathies (Vattemi, 2004, Nagaraju 2005). In mammalian cells ER stress activates the unfolded protein response (UPR), that is an elaborate signaling cascade activated to restore ER homeostasis and ensure cell survival mediated by three transmembrane proteins: IRE1, that stimulates the production of proinflammatory cytokines and stimulates autophagy, PERK, that activates an antioxidant response, and ATG6, that is involved in the regulation of protein folding and lipid synthesis.

In our samples, prominent mitochondrial abnormalities were detected in more severely inflamed cases (30%). Mitochondrial abnormalities are

frequently associated with muscle inflammation, as reported in several human inflammatory myopathies where they are generally associated with damage to the mitochondrial DNA (Oldfors, 2006; Varadhachari, 2010). Mitochondrial damage can activate ER stress since the endoplasmic reticulum has an intimate contact with mitochondria in specialized areas called mitochondria-associated ER membranes (MAM). It is thus conceivable that ER stress pathways and mitochondria work together to cause myofiber damage also in Sarcocystis related myositis. ER stress itself has been associated with the activation of inflammatory responses in skeletal muscle: NF- κ B, JNK, interleukin-6, and TNF- α have been shown to be activated by ER stress mechanisms (Nagaraju, 2005).

A novel and interesting finding of our work, is the expression of MHC I and II on the parasitophorous vacuole of Sarcocystis. To the author's knowledge, the same finding was described only once in the literature, in a severe case of myositis in a dog being an accidental intermediate host of *Sarcocystis* spp (Sykes, 2011), and interpreted as an active involvement of this parasite's structure in the pathogenesis of muscle inflammation.

In apicomplexan parasites, the parasitophorous vacuole membrane (PVM) derives from the host cell plasmalemma, whose biochemical composition undergoes significant changes as the intravacuolar parasite grows. In particular, the host cell proteins are progressively and selectively excluded from the parasitophorous vacuole membrane, while those of the parasite are incorporated. As the result, the changed PVM becomes not fusigenic for host cell lysosomes (Beier, 2003) and is protected from the immunity

system of the host. In our study, in approximately 20% of cases, scattered cysts expressed the sarcolemmal protein Dystrophin and co-localized with MHC I in 10% of cases. This finding could be explained with an incomplete exclusion of host cell protein from the parasitophorous cell membrane; how this finding could influence the inflammatory machinery is unknown.

The immunostaining pattern to MHC I on parasitized fibers displayed at least four three different combinations: cyst-only immunopositivity (70%) sarcolemma-only positivity (5%), both sarcolemma and cyst wall positivity (5%), no staining of both structures (20%). The percentage of MHC I positive parasitized fibers was statistically correlated to the overall MHC I positivity score, to the inflammation score and to the number of cysts present into the sections. If the positivity of the cyst wall appears before or after the sarcolemmal one is not known but can be an interesting issue for further research about the pathogenesis of muscular sarcocystosis.

The reasons underlying the different combination staining patterns are unknown but may reflect different stages of immunitary activation of the parasitized muscle fibers or be the consequence of cysts' degeneration, that is considered the most relevant factor triggering inflammation in muscular sarcocystosis. Further research is needed to explore this hypothesis.

In conclusion, we systematically described and characterized an inflammatory myopathy concomitant with muscle sarcocystosis in sheep. This condition is characterized by infiltration of mainly CD8+ T

lymphocytes and expression of MHC I and II on the fiber surface and, by a still poorly understood mechanism, on the parasitic cyst wall.

Our data suggest also that the sheep may represent a good animal model for the study of immunopathogenesis of chronic muscle inflammation in muscular sarcocystosis possibly associated with clinical syndromes in humans.

References:

- Abubakar S. et al. Outbreak of human infection with *Sarcocystis nesbitti*, Malaysia, 2012. *Emerg Infect Dis.* 2013 Dec;19(12):1989-91.
- Al-Hyali e al- Effect of lysate of *Sarcocystis gigantea* in rats- Iraqi. *J of Vet Sci*, Vol. 25, No. 2, 2011 (81-85)
- Arness et al. An Outbreak Of Acute Eosinophilic Myositis Attributed To Human *Sarcocystis* Parasitism- *Am. J. Trop. Med. Hyg.*, 61(4), 1999, pp. 548–553
- Bahari et al- Molecular Identification of Macroscopic And Microscopic Cysts of *Sarcocystis* in Sheep in North Khorasan Province, Iran- *IJMCM Original Article Winter 2014*, Vol 3, No 1
- Barnes RW, McIlwain PK: 1968, Bovine eosinophilic myositis. *Proc 10th Annu Midwest Interprofessional Seminar on Diseases Common to Animals and Man*, pp. 22-22a.
- Beĭer TV et al. [Formation and diversity of parasitophorous vacuoles in parasitic protozoa. The *Coccidia* (Sporozoa, Apicomplexa)]. *Tsitologĭia.* 2003;45(4):339-56.
- Blagburn BL, Braund KG, Amling KA, et al. Muscular *Sarcocystis* in a dog. *Proc Helminthological Soc Washington* 1989;56:207–210.
- Buxton D, Protozoan infections (*Toxoplasma gondii*, *Neospora caninum* and *Sarcocystis* spp.) in sheep and goats: recent advances. *Vet Res* 1998 29:289–310.
- Buxton D Protozoan infections (*Toxoplasma gondii*, *Neospora caninum* and *Sarcocystis* spp.) in sheep and goats: recent advances. *Veterinary Research, BioMed Central*, 1998, 29 (3-4), pp.289-310.
- Cawthorn et al- Histological and ultrastructural appearance of severe *Sarcocystis fayeri* infection in a malnourished horse- *J Vet Diagn Invest* 2:342-345
- Chapman J, et al. Clinical muscular sarcocystosis in a dog. *J Parasitol* 2005;91:187–190.
- Chiesa F et al. A new molecular approach to assess the occurrence of *Sarcocystis* spp. in cattle and products thereof: preliminary data. 2013. *Ital J Food Safety* 2:e41.

Dalakas M. C. Review: an update on inflammatory and autoimmune myopathies. *Neuropathology and Applied Neurobiology*. 2011;37(3):226–242.

Del Cacho et al- IL-17A regulates *Eimeria tenella* schizont maturation and migration in avian coccidiosis- *Veterinary Research* 2014, 45:25

Dubey JP, Speer CA, Fayer R, 1989. *Sarcocystosis of Animals and Man*. Boca Raton, FL: CRC Press, 1–91, 143–144.

El Morsei et al. Morphologic identification of a new *Sarcocystis* sp. in the common moorhen (*Gallinula chloropus*) (Aves: Gruiformes: Rallidae) from Brolos Lake, Egypt-*Parasitol Res*. 2014 Jan;113(1):391-7.

Ely et al. Elevated antibody to *Sarcocystis* associated with eosinophilic myositis in cattle-*J Vet Diagn Invest* 1:53-56 (1989)

Englund P, et al. Skeletal muscle fibers express major histocompatibility complex class II antigens independently of inflammatory infiltrates in inflammatory myopathies. *Am J Pathol*. 2001;159(4): 1263–1273. 22.

Esposito et al- Ongoing outbreak of an acute muscular *Sarcocystis*-like illness among travellers returning from Tioman Island, Malaysia, 2011-2012 *Euro Surveill*. 2012;17(45).

Evans J, et al. Canine inflammatory myopathies: a clinicopathologic review of 200 cases. *J Vet Intern Med*. 2004;18(5):679–691. 23.

Fayer R., Dubey J.P., Protective immunity against sarcocystosis in cattle, *Vet. Parasitol*. 15 (1984) 187-201I.

Fayer R., Elsasser T.H., Bovine sarcocystosis: how parasites negatively affect growth, *Parasitol. Today* 7. 1991, 2S(1-255).

Fayer et al. Human Infections with *Sarcocystis* Species. *Clin Microbiol Rev*. 2015 Apr;28(2):295-311.

Fayer et al. *Sarcocystis* spp. in Human Infections- *Clinical Microbiology Reviews*, Oct. 2004, p. 894–902

Frelief PF, et al. Bovine sarcocystosis. pathologic features of naturally occurring infection with *Sarcocystis cruzi*. *Am. J. Vet. Res*. 40:651-657. 1979.

Galluzzi L, et al. Endoplasmic reticulum stress and unfolded protein response in infection by intracellular parasites. *Future Sci OA*. 2017 May 12;3(3).

Gabor M, et al. Chronic myositis in an Australian alpaca (*Llama pacos*) associated with *Sarcocystis* spp. *J Vet Diagn Invest* 22:966–969 (2010)

Giannetti et al- *Sarcocystis gracilis*-like sarcocysts in a sheep- *Veterinary Record* (2005) 156, 322-323

Gozalo et al. Chronic Polymyositis Associated with Disseminated Sarcocystosis in a Captive-born Rhesus Macaque- *Vet Pathol* 44:695–699 (2007)

Granstrom D, et al. Type-II hypersensitivity as a component of eosinophilic myositis (muscular sarcocystosis) in cattle, *Am. J. Vet. Res.* 50 (1989) 571-574.

Granstrom et al. Type-I hypersensitivity as a component of eosinophilic myositis (muscular sarcocystosis) in cattle. *m J Vet Res.* 1989 Apr;50(4):571-4.

Greve. Sarcosporidiosis--an overlooked zoonosis. Man as intermediate and final host. *Dan Med Bull.* 1985 Aug;32(4):228-30.

Italiano et al., *Sarcocystis nesbitti* Causes Acute, Relapsing Febrile Myositis with a High Attack Rate: Description of a Large Outbreak of Muscular Sarcocystosis in Pangkor Island, Malaysia, 2012- *PLoS Negl Trop Dis* 8(5): e2876

Jeffrey M, et al. Immunocytochemistry of ovine sporozoan encephalitis and encephalomyelitis, *J. Comp. Pathol.* 98 (1988) 213-224.

Jeffrey et al. A myopathy of sheep associated with sarcocystis infection and monensin administration. *Vet Rec.* 1989 Apr 22;124(16):422-6.

Jensen, et al. Eosinophilic myositis and muscular sarcocystosis in the carcasses of slaughtered cattle and lambs. *American Journal of Veterinary Research*, 1986 47, 587-593.

Jubb. Kennedy and Palmers, Elsevier, VI edition, Vol. 1 pp 234

Kim et al. Downregulation of Chicken Interleukin-17 Receptor A during *Eimeria* Infection- *Infection and Immunity* p. 3845–3854 2014

Kirkpatrick CE, et al. *Sarcocystis* sp. in muscles of domestic cats. *Vet Pathol.* 1986 Jan;23(1):88-90

Lau YL, et al. Sarcocystis nesbitti infection in human skeletal muscle: possible transmission from snakes. *Am J Trop Med Hyg.* 2014 Feb;90(2):361-4.

Landsverk et al. A Sarcocystis-like Protozoon in a Sheep with Lymphadenopathy and Myocarditis- *Vet. Pathol.* 15: 186-1 95 (1978).

Lechner et al. Parasite-Specific IL-17-Type Cytokine Responses and Soluble IL-17 Receptor Levels in Alveolar Echinococcosis Patients- *Clinical and Developmental Immunology* Volume 2012, Article ID 735342.

Levine ND. The taxonomy of Sarcocystis (Protozoa, Apicomplexa) species. *J Parasitol.* 1986 Jun;72(3):372-82.

Lindsay et al. Sarcocystis and Sarcocystosis. 1995, *BAM* 5 3 249-254

Mandour et al. On the presence of Sarcocystis miescheri sp. nov. in camels of Qena Governorate-Egypt. *Acad. J. biolog. Sci.*, 3 (1): 1- 7 (2011)

Matsubara S. et al. Acute toxoplasma myositis: an immunohistochemical and ultrastructural study *Acta Neuropathol* (1990) 81:223-227

Meistro S et al. Sarcocystis Spp. Prevalence in Bovine Minced Meat: A Histological and Molecular Study. *Ital J Food Saf.* 2015 Jun 9;4(2):4626. eCollection 2015 May 28.

Nagaraju K, et al. Activation of the endoplasmic reticulum stress response in autoimmune myositis: potential role in muscle fiber damage and dysfunction. *Arthritis Rheum.* 2005;52:1824–1835.

Munday BL., Premature parturition in ewes inoculated with *Sarcocystis ovicanis*, *Vet. Parasitol.* 9 (1981) 17-26.

Nagaraju K, et al. Activation of the endoplasmic reticulum stress response in autoimmune myositis: potential role in muscle fiber damage and dysfunction. *Arthritis Rheum.* 2005;52:1824–1835.

Nigro et al. Ultrastructure Of The Cyst And Life Cycle Of Sarcocystis Sp. From Wild Sheep (*Ovis musimon*) –*journal of wildlife diseases* 27, 2, 1991, 217-224

O'Donoghue et al., The prevalence and intensity of Sarcocystis spp infections in sheep. *Aust Vet J* 1986 63:273–278

Oldfors A, et al. Mitochondrial abnormalities in inclusion-body myositis. *Neurology*. 2006;66(2)(suppl 1):S49–S55. 53.

O'toole et al. Experimental ovine sarcocystosis: sequential ultrastructural pathology in skeletal muscle. *J Comp Pathol*. 1987 Jan;97(1):51-60.

O'Toole D., et al. Ovine myeloencephalitis/leukomalacia associated with a Sarcocystis-like protozoan. *J. Vet. Diagn*. 5 (1993) 212-225.

Olias et al. Modulation of the host Th1 immune response in pigeon protozoal encephalitis caused by *Sarcocystis calchasi*- *Veterinary Research* 2013, 44:10

Olias et al. A novel *Sarcocystis*-associated encephalitis and myositis in racing pigeons- *Avian Pathology*, 2009 38:2, 121-128

Paciello O., et al. Canine inflammatory myopathy associated with *Leishmania infantum* infection. *Neuromuscular Disorders*. 2009;19(2):124–130.

Rayavarapu S, et al. Endoplasmic reticulum stress in skeletal muscle homeostasis and disease. *Curr Rheumatol Rep*. 2012 Jun;14(3):238-43

Rommel M et al. Die Sarkosporidiose der Haustiere und des Menschen, Berl. Muench. Tier5rzt]. *Wochenschr*. 92 (1979) 457-464.

Rommel M., *Sarcocystosis of domestic animals and humans*, In *Practice* 7 (1985) 158-160.

Sahasrabudhe VK, Shah HL. The occurrence of *Sarcocystis* sp. in the dog. *J Protozool* 1966;13:531.

Saito, et al. *Sarcocystis mihoensis* from sheep in Japan-*J Vet Med Sci* 59(2), 103-106-1997

Senaud, J. Contribution a l'étude des sarcosporidies et des toxoplasmes *Toxoplasma*. 1967. *Protistologica* 3:169–232

Sibley-*Invasion and Intracellular Survival by Protozoan Parasites-Immunol Rev*. 2011 March ; 240(1): 72–91.

Sykes et al. Severe Myositis Associated with *Sarcocystis* spp. Infection in 2 Dogs- *Vet Intern Med* 2011;25:1277–1283

Tappe D, et al.. Human and animal invasive muscular sarcocystosis in Malaysia--recent cases, review and hypotheses. *Trop Biomed.* 2013 Sep;30(3):355-66.

Terreel et al. Chronic Eosinophilic Myositis in a Rhesus Monkey Infected with *Sarcosporidiosis*-*Vet. Path.* 9: 266-271 (1972)

Traub-Dargatz et al. Multifocal myositis associated with *Sarcocystis* sp in a horse. *J Am Vet Med Assoc.* 1994 Dec 1;205(11):1574-6.

Uggla et al. Immune responses against *Toxoplasma* and *Sarcocystis* infections in ruminants: diagnosis and prospects for vaccination-*Rev. sci. tech. Off. int. Epiz.*, 1990, 9 (2), 441-462

Vangeel et al. Intramuscular inoculation of cattle with *Sarcocystis* antigen results in focal eosinophilic myositis. *Vet Parasitol.* 2012 Feb 10;183(3-4):224-30.

Vangeel L, et al. Molecularbased identification of *Sarcocystis hominis* in Belgian minced beef. 2007 *J Food Protect* 70:1523-6

Varadhachary AS, et al. Mitochondrial pathology in immune and inflammatory myopathies. *Curr Opin Rheumatol.* 2010;22(6):651–657. 68.

Vattemi G, et al. Endoplasmic reticulum stress and unfolded protein response in inclusion body myositis muscle. *Am J Pathol.* 2004;164:1–7.

Vattemi G., et al. Muscle biopsy features of idiopathic inflammatory myopathies and differential diagnosis. *Autoimmunity Highlights.* 2014;5(3):77–85.

Wobster et al. Myositis in Association with *Sarcocystis* sp. *Infection in Wild Ducks- Avian Diseases*, Vol. 26, No. 2 (Apr. - Jun., 1982), pp. 412-418

Wouda et al. Eosinophilic Myositis due to *Sarcocystis hominis* in a Beef Cow- *J. Comp. Path.* 2006, Vol.135, 249^253

Wu et al. Cardiac fibroblasts mediate IL-17A–driven inflammatory dilated cardiomyopathy- *J. Exp. Med.* 2014 Vol. 211 No. 7 1449-1464

Yoshida et al. Interleukin-17 plays a role in successful resolution of *Trypanosoma cruzi* infection- *The Journal of Immunology*, 2007, 178, 43.17

Chapter 3: Age related skeletal muscle atrophy and upregulation of autophagy in dogs

Published as: Pagano TB, Wojcik S, Costagliola A, De Biase D, Iovino S, Iovane V, Russo V, Papparella S, Paciello O. Age related skeletal muscle atrophy and upregulation of autophagy in dogs. Vet J. 2015 Oct;206(1):54-60.

3.1 Introduction

Sarcopenia, the age related loss of muscle mass and strength, is a multifactorial condition that occurs in a variety of species and represents a major healthcare concern for older adults in human medicine (Evans, 1995; Doherty, 2003; Buford et al., 2010). A decline in muscle mass generally indicates a degradation in muscle protein content and several studies have demonstrated an age-related reduction in the synthesis of specific muscle proteins (Proctor et al., 1998; Nair, 2005; Augustin and Partridge, 2009) with a concurrent increase in proteolysis. Skeletal muscle has four main proteolytic systems, namely, lysosomal, caspase, calpain and ubiquitin– proteasome, all of which could potentially contribute to age related muscular atrophy.

Autophagy is a ubiquitous and highly conserved catabolic process, which involves intracellular degradation of cytoplasmic components through a lysosomal pathway. The process is involved in a variety of mechanisms related to ageing, including mitochondrial turnover, removal of misfolded protein aggregates and apoptosis. It has been proposed that age-related alterations in autophagy might play a major role in sarcopenia (Tukaj, 2013).

Three main types of autophagy have been described: (1) microautophagy, in which lysosomes directly take up portions of cytoplasm for degradation; (2) chaperone-mediated autophagy, in which chaperone proteins recognize and transport cytoplasmic proteins to the lysosome; and (3)

macroautophagy, where there is non selective sequestration of cytoplasmic material for lysosomal degradation. The latter process has been the focus of a large body of research and represents the most important type of autophagy (Tukaj, 2013; Wojcik, 2013); it consists of several steps, specifically induction or initiation and cargo selection, vesicle nucleation and expansion, lysosomal targeting, lysosome docking and autophagosome–lysosome fusion, vesicle breakdown and recycling (Klionsky and Emr, 2000; Tooze and Schiavo, 2008). Nucleation is considered to be a crucial event that generates an active phagophore (or isolation membrane), which is the foundation kinases required for autophagy (Ulk1/2) function together with the Class III phosphatidylinositol 3-kinase (PI3K) VPS34 complex, which contains Beclin 1 (Tukaj, 2013). For phagophore expansion, elongation and sequestration into double-membrane vesicles (autophagosomes), recruitment of microtubule-associated protein light chain 3 (LC3)-II is required (Longatti and Tooze, 2009).

Sequestration of ubiquitinated cargo within the phagophore is greatly aided by p62/SQSTM-1 (Pankiv et al., 2007). The nascent autophagosomes subsequently fuse with lysosomes to form an autophagolysosome, in which the cytoplasmic cargo is degraded by lysosomal acid hydrolases and where the degradation products are recycled (Tukaj, 2013).

The aims of the present study were to investigate whether autophagy was up-regulated in skeletal muscle from older dogs affected by sarcopenia, compared with similar tissues from younger healthy dogs, and to determine whether the size of the dog influenced this process.

3.2: Materials and methods

3.2.1 Animals and tissue samples

Twenty-five dogs (10 male, 15 female) of various breeds, aged between 15 and 22 years of age, were recruited into the study (Table 3.1). The dogs had died of natural causes or had been euthanized with informed owner consent by means of intravenous injection of 10 mg/kg Pentothal (Abbott Laboratories) and 70 mg/kg Tanax (MSD Animal Health). None of the study dogs showed any clinical evidence of neuromuscular disease or metabolic diseases including hypothyroidism, hyperadrenocorticism, renal disease, diabetes mellitus or neoplasia. None of the study dogs had a history of inappetence prior to entry into the study or had recently received glucocorticoid therapy, or any other drugs known to have an effect on muscle tissue. Each owner consented to necropsy and use of tissues for research purposes, according to the ethical guidelines of the Diagnostic Service of the Department of Pathology and Animal Health of the University of Naples Federico II. Immediately post-mortem, muscle biopsies of approximately 1–2 cm diameter were obtained from the biceps femoris muscle. All samples were frozen in isopentane pre-cooled in liquid nitrogen, and stored at -80°C until further processed. Biopsies of biceps femoris muscle, obtained from five healthy young dogs, aged between 2 and 5 years (Table 3.1), euthanized for reasons unrelated to the study, were used as control tissue for histological, immunohistochemical and Western blotting analyses, again with owner consent.

Age related skeletal muscle atrophy and upregulation of autophagy in dogs

Case #	Breed	Sex	Weight	Age (years)	Muscle atrophy
1	Rottweiler	F	> 10 kg	15	yes
2	Mix breed	M	< 10 kg	17	yes
3	Pitt Bull	F	< 10 kg	16	yes
4	Mix breed	M	< 10 kg	16	yes
5	Spitz	FS	< 10 kg	18	yes
6	Mix breed	FS	< 10 kg	16	yes
7	German shepherd	M	> 10 kg	15	yes
8	Labrador	M	> 10 kg	19	yes
9	Mix breed	M	> 10 kg	16	yes
10	Poodle	FS	< 10 kg	18	yes
11	Mix breed	M	> 10 kg	16	yes
12	Mix breed	F	< 10 kg	18	yes
13	German shepherd	F	> 10 kg	16	yes
14	Mix breed	F	< 10 kg	19	yes
15	Mix breed	FS	< 10 kg	21	yes
16	German shepherd	FS	> 10 kg	17	yes
17	Boxer	M	> 10 kg	16	yes
18	Yorkshire	FS	< 10 kg	17	yes
19	Yorkshire	F	< 10 kg	18	yes
20	Setter	F	> 10 kg	17	yes
21	Mix breed	M	<10 kg	19	yes
22	Mix breed	FS	>10 kg	18	yes
23	Doberman	M	> 10 kg	15	yes

24	Labrador	M	> 10 kg	16	yes
Case #	Breed	Sex	Weight	Age (years)	Muscle atrophy
25	Yorkshire	F	< 10 kg	20	yes
26	Mix breed	M	<10 kg	3	no
27	German shepherd	F	>10 kg	5	no
28	Mix breed	FS	<10 kg	4	no
29	Labrador	M	>10 kg	2	no
30	Yorkshire	M	<10 kg	3	no

Table 3.1 Study population. M, male; F, female; FN, female neutered.

3.2.2 Histological examination

Tissue sections of 10 µm were cut in a transverse plane with a cryostat (-20 °C) and were stained according to the methods detailed previously (Paciello and Papparella, 2009). Briefly, haematoxylin and eosin (H&E) and Engel trichrome were used for a basic morphological examination of muscle fibers; NADH-tetrazolium reductase (NADH-TR), succinic dehydrogenase (SDH) and cytochrome oxidase (CYOX) were used to indicate activity and distribution of mitochondria; ATPase at pH 9.4 and pH 4.3 was employed for histochemical fiber subtyping; and esterase staining was used to evaluate lipofuscine aggregates inside muscle fibers.

Scoring of the major morphological alterations, observed in the biopsies, was performed by light microscopy at 20× magnification. The proportions of atrophic fibers, necrotic fibers, ragged and pre-ragged red fibers, rimmed vacuoles, CYOX negative fibers and accumulation of lipofuscines

were scored as follows: 0 (none); 1–25% of affected fibers (classified as mild); 26–50% of affected fibers (classified as moderate); >50% of affected fibers (classified as severe). Approximately 20 fields at 20× magnification were evaluated for each section by two independent pathologists (TBP, OP) with a concordance rate of 95%.

3.2.3 Immunohistochemical examination

Immunohistochemical analysis was performed according to the method previously described (Paciello and Papparella, 2009). Briefly, 10 µm sections of muscle tissue were obtained using a cryostat. Slides were air dried for 1 h at room temperature, washed in phosphate-buffered saline (0.01 M PBS, pH 7.2) and fixed in acetone at 4 °C for 3 min. Endogenous peroxide activity was blocked using 0.3% hydrogen peroxide in methanol (Sigma–Aldrich), applied for 15 min at room temperature.

After two washes in PBS, sections were incubated for 30 min at room temperature with Background Sniper (BiocareMedical). Sections were incubated overnight at 4 °C with the primary antibodies against Beclin-1 (Santa Cruz Biotechnology) diluted 1:300; LC3 (Abcam), diluted 1:3000; and p62 (Santa Cruz Biotechnology), diluted 1:200 in PBS. The immunoblot confirmed the specificity of these antibodies in canine tissues in accordance with guidelines published by Kurien et al. (2011). After two washes with PBS, the MACH 1 Universal HPR-Polymer Detection Kit (Biocare Medical) was used according to the manufacturer's instructions. The sections were subsequently counterstained in haematoxylin, dehydrated in alcohol, clarified in xylene and mounted in aqueous

mounting medium. In the corresponding negative control sections, the primary antibody was either omitted or replaced with a 1:20 dilution of mouse serum (for p62 antibody) or rabbit serum (for Beclin-1 and LC3) (Jackson ImmunoResearch). The degree of immunoreactivity was categorized as follows: 0, negative staining observed in muscle fibers; 1–25% positively stained fibers; 26–50% positively stained fibers; > 50% positively stained fibers.

3.2.4 Western blotting

Muscle tissues from geriatric dogs and young control dogs were sectioned at 20 μm by cryostat and lysed at 4 $^{\circ}\text{C}$ in 200 μL of lysis buffer (TBS, 20 mM Tris-HCl pH 7.6, 140 mM NaCl, 30 mM sodium pyrophosphate, 5 mM EDTA, 0.55% Nonident P40, 1% Triton X-100, 50mM NaF, 0.1mM Na_3VO_4 , 1mM PMSF, 1mM benzamidine, 1 mM iodoacetamide, 1 mM phenantroline). Protein concentrations were determined by BCA protein assay (Pierce), and lysates were adjusted to equivalent concentrations with lysis buffer. Aliquots of muscle lysate (30 μg protein per lane) were then separated by SDS-PAGE. Proteins were transferred to PVDF membranes and blocked overnight at 4 $^{\circ}\text{C}$ with 5% non-fat dried skimmed milk (Marvel, Premier Beverages) in Tris-buffered saline, supplemented with 0.05% Tween 20 (TTBS). Membranes were incubated with primary antibodies against Beclin-1 (Santa Cruz Biotechnology) at 1:500 dilution, LC3 (Abcam) at 1:3000 dilution or p62 (Santa Cruz Biotechnology) at 1:500 dilution. Horseradish peroxidase-conjugated secondary antibodies

were applied in blocking solution for 1 h at room temperature. Immunoreactive bands were visualized by autoradiography using Super Signal West Pico Chemiluminescent Substrate Kit (Pierce). Membranes were subsequently stripped and re-probed using anti- β -actin monoclonal antibody (Sigma-Aldrich) to confirm equal loading of proteins in all lanes. Band intensities were determined on scanned images using Image J software¹ to determine average pixel intensity.

3.2.5 Statistical methods

Data obtained from Western blotting were analyzed with Stat view software (Abacus Concepts) by one-factor analysis of variance (single-factor ANOVA). Data comparing aged vs. young dogs from assessment of immunohistochemistry and morphology, including comparisons of Beclin-1 and LC3 immunoreactive fiber distribution in the groups of dogs lighter than 10 kg and heavier than 10 kg, were compared using Fisher's exact test. Differences in the gender distribution were assessed using Chi-squared tests of homogeneity and independence. P values <0.05 were considered statistically significant.

3.3 Results

3.3.1 Histochemical analysis

In the muscle biopsies from the geriatric dogs, fiber atrophy was observed significantly more frequently compared with the control biopsies (P < 0.001; Table 3.2). H&E staining of muscle tissues from the geriatric dogs

showed variability in the fiber diameter sizes and mild, moderate or severe fiber atrophy (Fig. 3.1a). Staining for ATPase performed at pH 4.3 and 9.4 showed that atrophy involved mainly type II fibers (Fig. 3.1b). In the majority of the older animals, the number of atrophic fibers varied from 1% to 25%, but more pronounced atrophy (>25% of fibers) was observed in several of the older dogs (Table 3. 2).

The frequency of necrotic fibers within muscle biopsies was significantly greater ($P < 0.05$) in the geriatric dogs compared with similar samples from the young dogs. In most cases, fiber necrosis was categorized as mild (Table 3.2) and sometimes sarcoclastosis was also observed. Rimmed vacuoles were observed within some muscle fibers (Fig. 3.1c) that were classified as mild in most cases, although these were moderate in other dogs (Table 3.2). However, the prevalence of rimmed vacuoles was not significantly different comparing geriatric and young dogs ($P = 0.1$).

A few angulated atrophic fibers and rare pyknotic nuclear clumps were also observed. Engel trichrome staining revealed the presence of pre-ragged and ragged red fibers (Fig. 3.1d) indicating mitochondrial proliferation. This phenomenon was more prevalent in the muscle biopsies from the geriatric dogs (graded mild to moderate; Table 3.2) compared with those from the young dogs ($P < 0.05$).

In the muscle biopsies from the geriatric dogs, alterations in CYOX activity were observed. Moth-eaten fibers, sub-sarcolemmal mitochondrial collection and partially or totally negative fibers were observed (Fig. 3.1e), indicating mitochondrial dysfunction. The prevalence of biopsies with CYOX negative fibers was significantly greater in the muscle biopsies

from the geriatric dogs (graded mild to moderate; Table 3.2) compared with those from the young dogs ($P < 0.05$). Esterase staining revealed intracytoplasmic material, consistent with accumulation of lipofuscines (Fig. 3.1f). This accumulation of lipofuscine within muscle fibers was significantly more prevalent in the muscle biopsies from the geriatric dogs compared with those from the young dogs ($P < 0.05$; Table 3.2). NADH-TR and SDH stains showed dysfunctional mitochondria distribution, associated with the presence of moth-eaten fibers (data not shown). There were no significant differences in any of the histochemical parameters comparing muscle biopsies from male and female dogs within the geriatric dog group or between bodyweight categories.

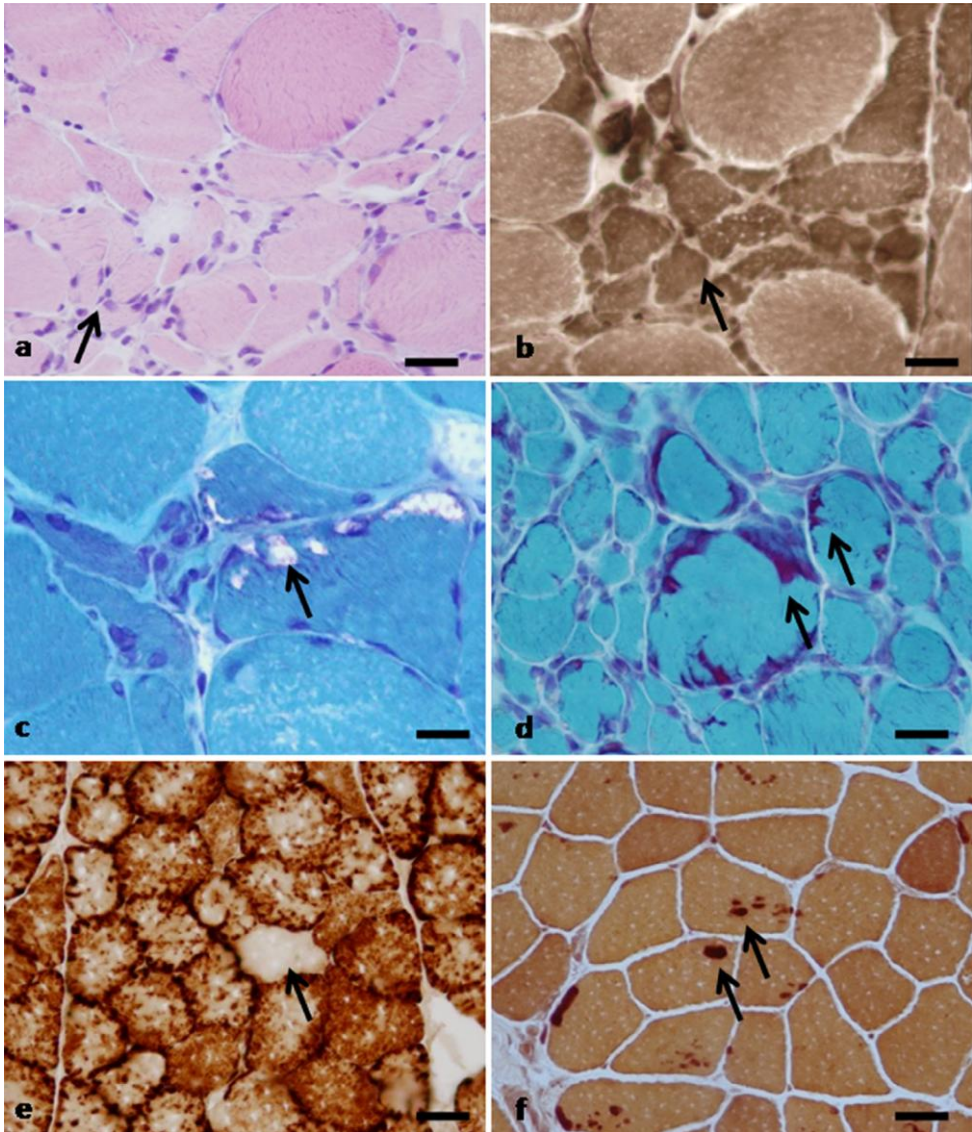


Fig. 3.1: Representative histological sections of biceps femoris muscle from geriatric dogs. (a) H&E staining showing atrophic muscle fibres (arrow). Bar = 40 μm . (b) ATPase staining showing that atrophy involves mainly type II fibres (arrow). Bar = 35 μm . (c) Engel trichrome staining showing fibers with subsarcolemmatic rimmed-vacuoles (arrow). Bar = 30 μm . (d) Engel trichrome staining showing muscle fibers with mitochondrial proliferation in subsarcolemmatic zone (arrows). Bar = 30 μm . (e) CYOX staining showing several moth-eaten fibers, and a CYOX negative fiber (arrow). Bar = 50 μm . (f) Non-specific esterase staining showing intracytoplasmic material, compatible with accumulation of lipofuscines (arrows). Bar = 50 μm .

3.3.2 Immunohistochemistry

Muscle biopsies from the healthy dogs were negative on immunohistochemistry for Beclin-1, LC3 and p62 (data not shown). In muscle biopsies from the geriatric dogs, Beclin-1 and LC3 immunoreactivity was observed in 21/25 samples (Table 3.2). Interestingly, the majority of tissue samples demonstrating >25% Beclin-1 positive fibers also contained fibers with rimmed vacuoles. Beclin-1 expression was observed as spots within individual muscle fibers, or as whole fibers with moderate to strong intensity of immunoreactivity (Fig. 3.2a). Some muscle biopsies showed subsarcolemmal Beclin-1 immunoreactivity in almost 10% of fibers. LC3 immunoreactivity (Fig. 3.3a) was more variable in terms of the proportion of positive fibers (Table 3.2).

In contrast to Beclin-1 and LC3, p62 immunoreactivity was observed in only 3/25 muscle biopsies, with few fibers showing small spots of immunoreactivity (Fig. 4a). In the p62 positive cases, biopsies demonstrated LC3 immunoreactivity in >25% of muscle fibers (Table 3.2).

3.3.3 Western blotting analysis

Expression of Beclin-1, LC3 and p62 was investigated in muscle tissue lysates by Western blotting. Immunoreactivity for Beclin-1 (60 kDa band; Fig. 3.2b) and for the two isoforms of LC3 (18 kDa band for LC3 I and 16 kDa band for LC3 II; Fig. 3.3b) and p62 (62 kDa band; Fig. 3.4b) was identified. Densitometry results, normalised for β -actin expression, showed

a significant difference in expression of Beclin-1 ($P < 0.01$; Fig. 3.2c), total LC3 ($P < 0.01$; Fig. 3.3c) and increased LC3 II/ LC3 I ratios, comparing samples from geriatric vs. young dogs. In contrast, there was lower p62 expression in muscle tissue samples from geriatric dogs compared with those from the young dogs (Fig. 3.4c).

Cas e #	Fiber Atrophy	necrotic fibers	Ragged and Pre-ragged Red Fibers	Rimmed Vacuoles	COX Negative Fibers	Accumulation of Lipofuscins	Beclin-1 Positivity	LC3 Positivity	P62 Positivity
1	10 to 50%	0	0	0	< 10%	10 to 50%	26–50 %	26–50 %	0
2	> 50%	< 10%	10 to 50%	0	0	0	0	0	0
3	< 10%	10 to 50%	< 10%	10 to 50%	< 10%	> 50%	> 50 %	> 50 %	0
4	10 to 50%	< 10%	> 50%	0	10 to 50%	10 to 50%	> 50 %	> 50 %	0
5	10 to 50%	0	0	< 10%	0	0	26–50 %	26–50 %	0
6	10 to 50%	< 10%	0	0	< 10%	0	0	0	0
7	> 50%	< 10%	0	0	0	< 10%	1–25 %	26–50 %	1–25 %
8	< 10%	0	0	0	0	0	0	0	0
9	> 50%	< 10%	10 to 50%	< 10%	< 10%	10 to 50%	1–25 %	1–25 %	0
10	10 to 50%	0	0	0	> 50%	0	1–25 %	1–25 %	0
11	< 10%	< 10%	10 to 50%	< 10%	0	< 10%	26–50 %	26–50 %	1–25 %
12	10 to 50%	0	0	0	0	> 50%	1–25 %	1–25 %	0
13	> 50%	< 10%	> 50%	0	< 10%	10 to 50%	26–50 %	1–25 %	0
14	< 10%	< 10%	10 to 50%	10 to 50%	0	0	> 50 %	> 50 %	0
15	>	0	0	0	10 to	0	1–25	1–25	0

Age related skeletal muscle atrophy and upregulation of autophagy in dogs

	50%				50%		%	%	
Case #	Fiber Atrophy	necrotic fibers	Ragged and Pre-ragged Red Fibers	Rimmed Vacuoles	COX Negative Fibers	Accumulation of Lipofuscines	Beclin-1 Positivity	LC3 Positivity	P62 Positivity
16	< 10%	< 10%	< 10%	> 50%	0	0	> 50 %	> 50 %	0
17	< 10%	0	0	0	< 10%	< 10%	0	0	0
18	10 to 50%	0	< 10%	< 10%	10 to 50%	0	> 50 %	> 50 %	0
19	10 to 50%	0	0	0	< 10%	< 10%	1-25 %	1-25 %	0
20	< 10%	< 10%	10 to 50%	10 to 50%	0	< 10%	26-50 %	26-50 %	1-25 %
21	10 to 50%	0	0	0	0	> 50%	1-25 %	1-25 %	0
22	> 50%	< 10%	> 50%	0	< 10%	10 to 50%	26-50 %	1-25 %	0
23	< 10%	< 10%	10 to 50%	< 10%	0	0	> 50 %	> 50 %	0
24	> 50%	0	0	0	10 to 50%	0	1-25 %	1-25 %	0
25	10 to 50%	0	< 10%	< 10%	10 to 50%	0	> 50 %	> 50 %	0
C1	0	0	0	0	0	0	0	0	0
C2	0	0	0	0	0	0	0	0	0
C3	0	0	0	0	0	0	0	0	0
C4	0	0	0	0	0	0	0	0	0
C5	0	0	0	0	0	0	0	0	0

Table 3.2 Summary of histopathology and immunohistochemistry results.

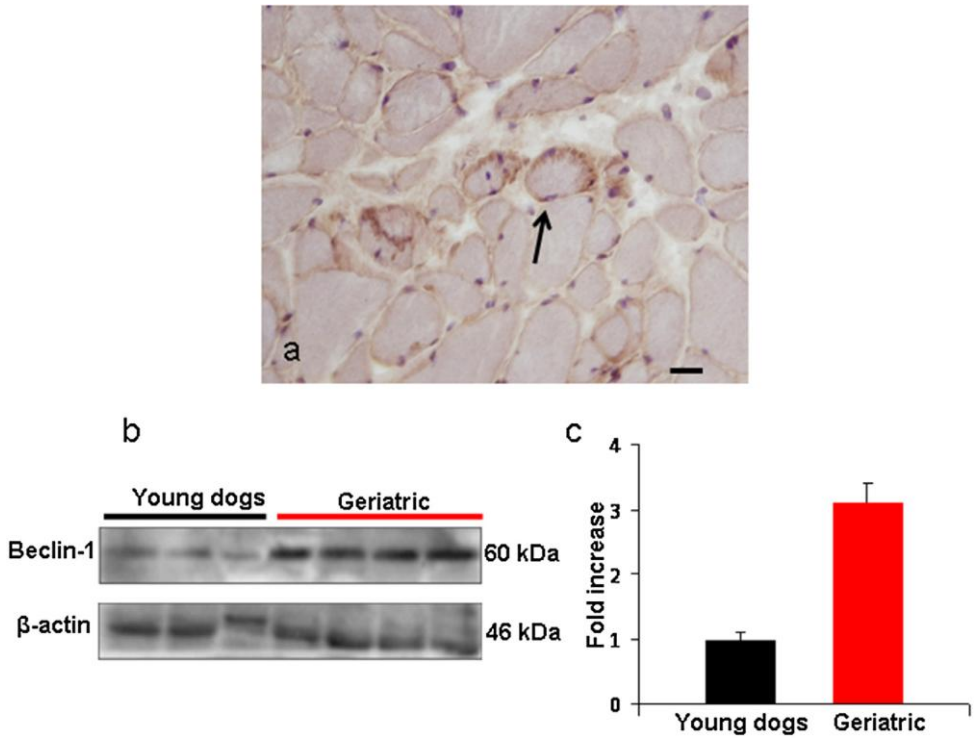


Fig. 3.2: Immunohistochemical staining for Beclin-1 in biceps femoris muscle. (a) Muscle tissue section showing strong expression of Beclin-1 in sarcoplasm and on sarcolemma (arrow). HRP method with Mayer's haematoxylin counterstain. Bar = 50 μ m. (b) Representative Western blot evaluating Beclin-1 expression in muscle tissue lysates from young and geriatric dogs. β -actin immunoreactivity shown as a loading control. (c) Results of densitometric analysis of immunoblots. Data shown represent the mean and SE of the fold increase in Beclin-1 expression, normalised against β -actin. Three independent immunoblots were assessed.

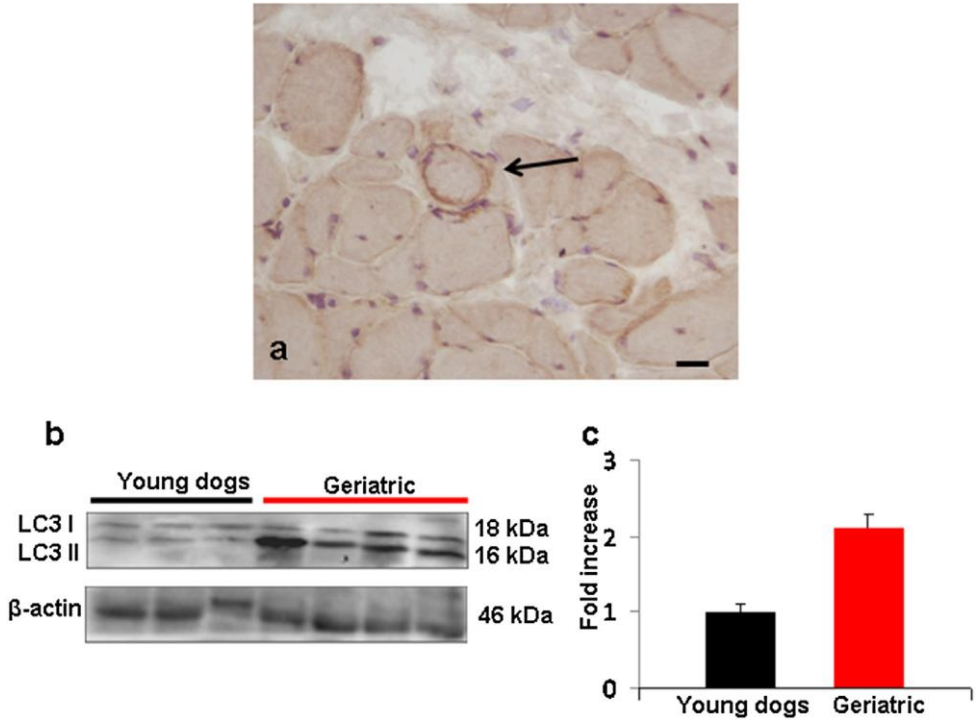


Fig. 3.3: Immunohistochemical staining for LC3 in biceps femoris muscle. (a) Muscle tissue section showing strong expression of LC3 in sarcoplasm (arrow). HRP method with Mayer's haematoxylin counterstain. Bar = 50 μ m. (b) Representative Western blot evaluating LC3 expression in muscle tissue lysates from young and geriatric dogs. β -actin immunoreactivity shown as a loading control. (c) Results of densitometric analysis of immunoblots. Data shown represent the mean and SE of the fold increase in LC3 expression, normalised against β -actin. Three independent immunoblots were assessed.

3. 4 Discussion

The effect of aging on skeletal muscles in dogs has been investigated previously (Braund et al., 1982; Hutchinson et al., 2012), although there are substantial gaps in our understanding of this process. In geriatric humans and animal models of ageing, several alterations in muscle structure and function have been reported in association with an altered rate of autophagy. Increased levels of autophagy can exacerbate muscle wasting (Mammucari et al., 2007; Zhao et al., 2007; Iovino et al., 2012) and accumulation of autophagic vacuoles has been associated with various myopathies, such as Danon disease and Pompe disease (Sugie et al., 2005; Raben et al., 2007). Furthermore, in murine models of progeria, there is enhanced autophagy in various tissues, when compared with wild type mice (Mariño and López-Otín, 2008). In the present study, we describe the presence of autophagic markers such as Beclin-1 and LC3 in skeletal muscles of geriatric dogs, associated with several histochemical features of myopathy. The most prominent histopathological findings included fiber atrophy, mitochondrial abnormalities in terms of functionality and/ or distribution within the cytoplasm, and the presence of esterase positive material, consistent with the presence of lipofuscines inside the muscle fibers.

Loss of muscle mass can occur during many catabolic physiological and pathophysiological processes, including physical inactivity and starvation or anorexia, associated with systemic disease. In our study, we excluded dogs demonstrating such conditions in order to evaluate the consequences

of the normal ageing process on skeletal muscles. It has been established that oxidative stress, occurring with ageing, can contribute to muscle atrophy via upregulation of autophagy (Calvani et al., 2013). The markers of autophagy that we observed seemed to correlate with the features of muscle atrophy. Selective atrophy of the type II fibers can be interpreted as an age-related finding, as described in humans (Nilwik et al., 2013), since we excluded dogs that might have other reasons for type II atrophy (e.g. due to the presence of an endocrinopathy or following steroid therapy).

The presence of esterase-positive lipofuscines and mitochondrial dysfunction and accumulation inside muscle fibers were other prominent histological findings. Lipofuscin formation is a manifestation of reactive oxygen species (ROS)-induced damage, and their relationship with the lysosomal compartment is also confirmed by the presence of esterase-positive vacuoles in several autophagic vacuolar myopathies, such as Danon disease and X-linked myopathy with excessive autophagy (Nishino, 2007).

Ageing also leads to increased accumulation of dysfunctional mitochondria, associated with mutations in mitochondrial DNA (mtDNA), which is particularly vulnerable to ROS-mediated mutagenesis (Terman et al., 2010). Since removal of damaged mitochondria occurs via an autophagy-mediated process (termed mitophagy), the mitochondrial-lysosomal theory of ageing has been proposed (Terman et al., 2010). We suggest that the progressive accumulation of lipofuscines inside the lysosomes can impair mitophagy, resulting in accumulation of dysfunctional mitochondria, which contribute to further generation of

ROS, increased formation of lipofuscines and, finally, lysosomal labilisation with activation of the apoptotic or necrotic pathway. This process could potentially explain our research findings in terms of the mitochondrial dysfunction and accumulation and presence of lipofuscines in skeletal muscle from geriatric dogs.

Muscle fibers from geriatric dogs often contained rimmed vacuoles and, in contrast to samples from young dogs, demonstrated immunoreactivity for LC3 and Beclin-1, but not p62. Beclin-1 and LC3 expression indicate activation of early and late phases of autophagy, respectively (Tukaj, 2013). The stress-inducible intracellular protein p62 is involved in many signaling responses to growth factors and stress (Tooze and Schiavo, 2008) and has the capacity to interact indirectly or directly with both components of autophagic machinery and ubiquitin. p62 accumulates due to the autophagy blockade, binds to ubiquitinated proteins and prevents their delivery and degradation by the proteasome, resulting in a toxic effect (Korolchuk et al., 2010). Inefficient fusion between autophagosomes and lysosome can lead to accumulation of proteinaceous material, containing p62, in the cytoplasm, with decreased levels of 'free' p62, associated with a high ratio of LC3-II to LC3-I, which is considered to be a further indicator of activation of the autophagy pathway (Komatsu et al., 2007).

It is possible that, with increasing age, formation of dysfunctional mitochondria induces muscle cells to enhance mitophagy. However, lipofuscine-filled lysosomes might not efficiently degrade this material, leading to accumulation of autophagosomes inside the cell, with accumulation of damaged mitochondria. Thus, enhanced levels of

autophagy in skeletal muscle might represent a prosurvival strategy of muscle cells to contrast the progressive accumulation of damaged constituents, but finally fail in its original purpose, contributing to muscle damage. The cytoprotective function of autophagy is mediated in many circumstances by negative modulation of apoptosis (Gordy and He, 2013). Thus, evaluation of markers of apoptosis, such as caspase 3, would be an interesting avenue of research into canine sarcopenia. Furthermore, autophagy dynamics in skeletal muscle appear to be unusual, when compared with other tissues. For example, during the fasting state, most tissues show a transient activation of autophagy, which only lasts a few hours, whereas skeletal muscle shows a more persistent generation of autophagosomes that can continue for several days (Mizushima et al., 2004). Since autophagy is responsible for degradation of several longlived proteins as well, this chronic mechanism might contribute to the degenerative changes observed in muscle tissue.

3.5 Conclusions

The present study provides some insight into the mechanisms associated with sarcopenia in dogs as they age. Studying the histological features and cellular mechanisms underlying muscle senescence in dogs can potentially contribute to our understanding of sarcopenia in humans. Comparative ageing research in companion animals that share the same environment, diet and exposure to pollutants, etc., makes the canine a more realistic model than laboratory rodents. Greater knowledge of the changes

that occur in canine skeletal muscle with ageing is also of value to veterinary pathologists when undertaking histopathological examination of muscle biopsies, allowing them to distinguish changes due to ageing from those resulting from disease.

References

Augustin, H., Partridge, L., 2009. Invertebrate models of age-related muscle degeneration. *Biochimica et Biophysica Acta* 1790, 1084–1094.

Braund, K.G., McGuire, J.A., Lincoln, C.E., 1982. Observations on normal skeletal muscle of mature dogs: A cytochemical, histochemical, and morphometric study. *Veterinary Pathology* 19, 577–595.

Buford, T.W., Anton, S.D., Judge, A.R., Marzetti, E., Wohlgemuth, S.E., Carter, C.S., Leeuwenburgh, C., Pahor, M., Manini, T.M., 2010. Models of accelerated sarcopenia: Critical pieces for solving the puzzle of age-related muscle atrophy. *Ageing Research Reviews* 9, 369–383.

Calvani, R., Joseph, A.M., Adhietty, P.J., Miccheli, A., Bossola, M., Leeuwenburgh, C., Bernabei, R., Marzetti, E., 2013. Mitochondrial pathways in sarcopenia of aging and disuse muscle atrophy. *Biological Chemistry* 394, 393–414.

Doherty, T.J., 2003. Aging and sarcopenia. *Journal of Applied Physiology* 95, 1717–1727.

Evans, W.J., 1995. What is sarcopenia? *Journal of Gerontology: Medical Sciences* 50A, 5–8.

Gordy, C., He, Y.W., 2013. The crosstalk between autophagy and apoptosis: Where does this lead? *Protein and Cell* 3, 17–27.

Hutchinson, D., Sutherland-Smith, J., Watson, A.L., Freeman, L.M., 2012. Assessment of methods of evaluating sarcopenia in old dogs. *American Journal Veterinary Research* 73, 1794–1800.

Iovino, S., Oriente, F., Botta, G., Cabaro, S., Iovane, V., Paciello, O., Viggiano, D., Perruolo, G., Formisano, P., Beguinot, F., 2012. PED/PEA-15 induces autophagy and mediates TGF- β 1 effect on muscle cell differentiation. *Cell Death and Differentiation* 19, 1127–1138.

Klionsky, D.J., Emr, S.D., 2000. Autophagy as a regulated pathway of cellular degradation. *Science* 290, 1717–1721.

Komatsu, M., Wang, Q.J., Holstein, G.R., Friedrich, V.L., Jr., Iwata, J., Kominami, E., Chait, B.T., Tanaka, K., Yue, Z., 2007. Essential role for autophagy protein Atg7 in the maintenance of axonal homeostasis and the prevention of axonal degeneration. *Proceedings of the National Academy of Sciences of the United States of America* 104, 14489–14494.

Korolchuk, V.I., Menzies, F.M., Rubinsztein, D.C., 2010. Mechanisms of cross-talk between the ubiquitin-proteasome and autophagy-lysosome systems. *Federation of European Biochemical Societies Letters* 584, 1393–1398.

Kurien, B.T., Dorri, Y., Dillon, S., Dsouza, A., Scofield, R.H., 2011. An overview of Western blotting for determining antibody specificities for immunohistochemistry. *Methods in Molecular Biology* 717, 55–67.

Longatti, A., Tooze, S.A., 2009. Vesicular trafficking and autophagosome formation. *Cell Death and Differentiation* 16, 956–965.

Mammucari, C., Milan, G., Romanello, V., Masiero, E., Rudolf, R., Del Piccolo, P., Burden, S.J., Di Lisi, R., Sandri, C., Zhao, J., et al., 2007. FoxO3 controls autophagy in skeletal muscle in vivo. *Cell Metabolism* 6, 458–471.

Mariño, G., López-Otín, C., 2008. Autophagy and aging: New lessons from progeroid mice. *Autophagy* 4, 807–809.

Mizushima, N., Yamamoto, A., Matsui, M., Andrade, F.H., Dupont-Versteegden, E.E., 2004. In vivo analysis of autophagy in response to nutrient starvation using transgenic mice expressing a fluorescent autophagosome marker. *Molecular Biology of the Cell* 15, 1101–1111.

Nair, K.S., 2005. Aging muscle. *The American Journal of Clinical Nutrition* 81, 953–963.

Nilwik, R., Snijders, T., Leenders, M., Groen, B.B., van Kranenburg, J., Verdijk, L.B., van Loon, L.J., 2013. The decline in skeletal muscle mass with aging is mainly attributed to a reduction in type II muscle fiber size. *Experimental Gerontology* 48, 492–498.

Nishino, I., 2007. Lysosomal myopathies. In: Aminoff, M.J., Boller, F., Swaab, D.F., Mastaglia, F.L., Hilton-Jones, D. (Eds.), *Handbook of Clinical Neurology*, vol. 86. pp. 205–214.

Paciello, O., Papparella, S., 2009. Histochemical and immunohistological approach to comparative neuromuscular diseases. *Folia Histochemica et Cytobiologica* 47, 143–152.

Pankiv, S., Clausen, T.H., Lamark, T., Brech, A., Bruun, J.A., Outzen, H., Øvervatn, A., Bjørkøy, G., Johansen, T., 2007. p62/SQSTM1 binds directly to Atg8/LC3 to facilitate degradation of ubiquitinated protein aggregates by autophagy. *Journal of Biological Chemistry* 282, 24131–24145.

Proctor, D.N., Balagopal, P., Nair, K.S., 1998. Age-related sarcopenia in humans is associated with reduced synthetic rates of specific muscle proteins. *Journal of Nutrition* 128, 351S–355S.

Raben, N., Roberts, A., Plotz, P.H., 2007. Role of autophagy in the pathogenesis of Pompe disease. *Acta Myologica* 26, 45–48.

Sugie, K., Noguchi, S., Kozuka, Y., Arikawa-Hirasawa, E., Tanaka, M., Yan, C., Saftig, P., von Figura, K., Hirano, M., Ueno, S., et al., 2005. Autophagic vacuoles with sarcolemmal features delineate Danon disease and related myopathies. *Journal of Neuropathology and Experimental Neurology* 64, 513–522.

Terman, A., Kurz, T., Navratil, M., Arriaga, E.A., Brunk, U.T., 2010. Mitochondrial turnover and aging of long-lived postmitotic cells: The mitochondrial-lysosomal axis theory of aging. *Antioxidants and Redox Signaling* 12, 503–535.

Tooze, S.A., Schiavo, G., 2008. Liaisons dangereuses: Autophagy, neuronal survival and neurodegeneration. *Current Opinion in Neurobiology* 18, 504–515.

Tukaj, C., 2013. The significance of macroautophagy in health and disease. *Folia Morphologica* 72, 87–93.

Wojcik, S., 2013. Crosstalk between autophagy and proteasome protein degradation systems: Possible implications for cancer therapy. *Folia Histochemica et Cytobiologica* 51, 249–264.

Zhao, J., Brault, J.J., Schild, A., Cao, P., Sandri, M., Schiaffino, S., Lecker, S.H., Goldberg, A.L., 2007. FoxO3 coordinately activates protein degradation by the

Age related skeletal muscle atrophy and upregulation of autophagy in dogs

autophagic/ lysosomal and proteasomal pathways in atrophying muscle cells. *Cell Metabolism* 6, 472–483.

Chapter 4

Expression and biochemical properties of cellular Prion protein in skeletal muscle of aged cows

Based on: Teresa Bruna Pagano, Fabienne Serra, Davide De Biase, Torsten Seuberlich, Anna Oevermann, Serenella Papparella and Orlando Paciello. Expression and biochemical properties of cellular Prion protein in skeletal muscle of cows are not age dependent. 71° Congresso SISVET, XIV Convegno AIPVET. Napoli , 28 Giugno -1 Luglio 2017

4.1 Introduction

The cellular prion protein (PrP^C) is 250-amino acid sialoglycoprotein that is attached to the lipid raft of the plasmamembrane via a C-terminalglycosylphosphatidylinositol (GPI) anchor (Stahl et al., 1990). In the cell PrPC may be expressed in different glycosylated forms, corresponding to the variable occupancy of the residues Asn180 and Asn196 (Haraguchi et al.,1989). The C-terminal domain has a rigid and distinctive secondary structure, while the N-terminal portion is more flexible, unstructured and contains a unique octapeptide repeat (OR) region (Zahn et al., 2000). The OR confers PrPC one of its most salient features, i.e., the ability to bind divalent cations, prominently copper and to a lesser extent zinc, nickel, iron, and manganese (Stocheletal.,1998; Arena et al., 2012). The OR structure is highly conserved among different species (Hornshaw et al, 1995) thus highlighting its important function in defense against oxidative stress via reduction of Cu²⁺ to Cu⁺ (Liu et al., 2011).

PrPC is essential for prion propagation in human and animal prion diseases (Transmissible Spongiform Encephalopathies-TSE), characterized by accumulation of an aberrant, proteinase resistant, isoform of PrP (called PrP^{Sc}). TSE are a group of neurodegenerative and infectious diseases that affects several mammalian species including sheep (scrapie, the prototypical prion disease), humans (CJD and Kuru), deer (chronic wasting disease; CWD) and cattle (BSE). (Prusiner, 1981,1982, 1998; Collinge et al., 2001). TSE can have a genetic, infectious, or sporadic origin and are typically

marked by neuronal death and astroglial proliferation. In human inherited forms of TSE, the formation of PrP^{Sc} is secondary to the structural instability of mutated prion protein whereas in sporadic and infectious forms PrP^{Sc} is derived by a post-translational conformational switch of the normal prion protein (PrP^C) to a betasheet enriched disease-associated isoform (PrP^{Sc}). PrP^{Sc} is able to accumulate within the CNS owing to newly acquired biological and physico-chemical properties such as insolubility in nondenaturing detergents, propensity to aggregate and relative resistance to protease digestion. Routine diagnostic tests rely on these properties for identification of PrP^{Sc} in the form of the PK resistant core fragment (PrP^{res}) (Silva et al. 2015).

The requisite role of PrP^C in TSE (Transmissible Spongiform Encephalopathies) has been unequivocally demonstrated in experiments using PrP^C knockout mice, since PrP null mice (Prnp0/0) are completely resistant to experimental TSE infection (Sailer et al., 1994).

4.1.1 Cellular prion protein in somatic tissues:

Quantitative analyses of PrP^C distribution in the body have been reported in several species, revealing that PrP^C is expressed in a wide range of tissues. However, the amount of PrP^C varies significantly between different tissues, with highest levels in nervous and lymphoid systems (Ford et al., 2002; Horiuki 1995).

Peralta and colleagues in 2009 analyzed fifteen bovine somatic tissues for PrP^C expression by quantitative western blot and confirmed

highest expression of PrP^C in cerebellum, obex and spinal cord. Intermediate levels were detected in thymus, intestine, nerve, heart and spleen, and lower levels in lung, muscle, kidney, lymph node, skin, pancreas and liver (Peralta et al, 2009). Their data showed low (4.2% relative to levels in the cerebellum, $p < 0.05$) levels of PrP^C in bovine skeletal muscle. This reduced level suggests a low propensity for PrP^C to PrP^{Sc} conversion in skeletal muscle and PrP^{Sc} accumulation even in BSE-infected animals.

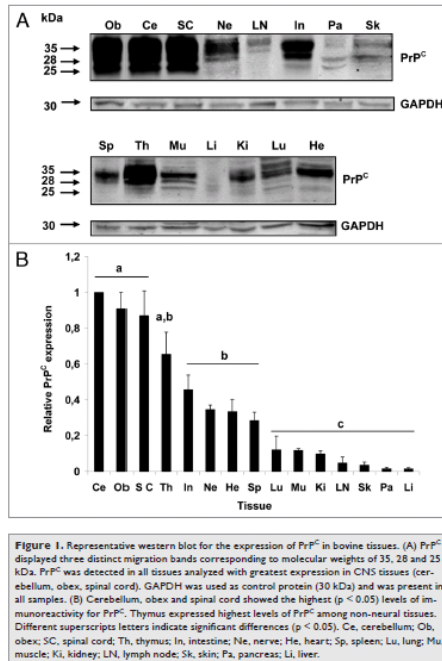


Fig. 4.1 expression of PrP^C in bovine tissues. From Peralta et al. 2009.

4.1.2: Functions of Cellular Prion Protein in nervous system

The cellular prion protein is known to have a role in neuron protection from oxidative stress through antioxidant activity, by sensing copper and/or free radical stimuli (Vassallo and Herms, 2003), in modulation of calcium entry through NMDA receptor pore by inhibition of the channel activity (Cowan et al., 2001; Lo et al., 2007). It has also an anti-apoptotic effect on Bax-mediated cell death (Bounhar et al., 2006; Lo et al., 2007). PrP^c is involved in myelin sheath formation and structural preservation through its modulation of β -secretase1 (BACE1) (Parkin et al., 2007).

4.1.3: Function and localization of Cellular Prion Protein in skeletal muscle

Most of available information about the function of cellular prion protein in skeletal muscle is based on experiments on laboratory animals. Prion protein is essential for maintaining normal redox homeostasis, muscle size, and contractile function in adult animals (Smith et al., 2011). In particular, PrP deficient mice have an age-dependent impairment of aerobic performance (Massimino et al., 2016), decreased CuZn-superoxide dismutase (SOD1) and catalase (Klamt et al.) and impaired muscle regeneration (Stella et al., 2010). Moreover an upregulation of cellular prion protein is observed when myotubes differentiate from myoblasts (Brown et al., 1998).

Although literature data are sparse, it seems that PrP^c expression varies among species, among muscles, and with age. In general, a detailed characterization of PrP^c metabolism in skeletal muscles is still lacking;

According to Smith and colleagues cellular prion protein content varies among murine skeletal muscles PrP content differs among mouse muscles (gastrocnemius > extensor digitorum longus, > tibialis anterior; soleus > diaphragm) as does glycosylation levels (di-, mono-, nonglycosylated; gastrocnemius, extensor digitorum longus, tibialis anterior = 60%, 30%, 10%; soleus, 30%, 40%, 30%; diaphragm, 30%, 30%, 40%) (Smith et al., 2011). The same authors found that PrP is predominantly di-glycosylated in human diaphragm.

The expression and cellular processing of PrP^c change during myogenesis, and in muscle fibers with different contractile properties (Massimino et al., 2006). These authors reported a significantly higher amount of PrP^c at western blot in tibialis anterior muscle than in soleus, with prevalent di-glycosylated and unglycosylated form in tibialis anterior and in soleus, respectively.

It's likely that the PrP^c content in different muscle groups reflects the relative amount in "fast" (or type 2), and "slow" (or type 1) fibers; indeed co-localizing PrP^c and fast and low myosin a detectable amount of PrP^c was evident only on fast fibers sarcolemma at immunofluorescence (Massimino et al., 2006).

By immunohistochemistry, PrP^c is reported to be normally expressed, at low levels, on the sarcolemma and muscle spindles (Zanusso et al., 2001).

Moreover, studies using transmission electron microscopy (TEM) and immunofluorescence demonstrated PrP^c at the level of neuromuscular junctions (NMJ) in humans (Gohel et al., 1999).

4.1.4 The cellular prion protein in muscle diseases

To the author's knowledge, only few papers focused on the cellular prion protein in muscle diseases, and only data restricted to the human species are available.

Increased expression of the cellular prion protein has been reported in muscles of human patients with sporadic inclusion-body myositis (s-IBM) and hereditary inclusion-body myopathy (h-IBM) (Askanas et al., 1993; Sarkozi et al., 1994). These disorders are characterized by an accumulation of paired-helical filaments (PHF), amyloid fibrils, hyperphosphorylated tau and other pathological proteins within muscle fibers associated with chronic inflammation only in the sporadic form (Askanas et al., 1998).

Muscle inflammation has been reported to facilitate the accumulation of PrP^{sc} in muscle in 2 different mouse models of immune-mediated inflammatory myopathy (Neumann et al., 2013).

In 2001 Zanusso et al. described an increased expression of PrP^c also in human polymyositis, dermatomyositis and neurogenic muscle atrophy. The same authors revealed that only PrP^c, and not PrP^{sc}, accumulates in s-IBM (Zanusso et al., 2001).

4.1.5 The pathological prion protein (PrP^{sc}) in muscle tissue

It has been shown that prions can also replicate and accumulate in skeletal muscles (Bosque et al., 2002; Casalone et al., 2005) raising concern about prion transmissibility following ingestion of TSE-tainted meat. Sarcoplasmic deposits of PrP^{sc} have been described in the skeletal muscle of terminally diseased cows and sheep with infectivity of skeletal muscles from affected cattle to transgenic mice (Peden et al. 2006, Suardi et al. 2012). PrP^{sc} deposition has been observed inside the cytoplasm of isolated fibers with scattered distribution, mainly as small amorphous aggregates and, less frequently, in the form of granular deposits (Suardi et al., 2012).

Pathological prion protein has been demonstrated also in semitendinosus/membranosus and gluteal muscles of White-Tailed Deer Infected with Chronic Wasting Disease (CWD) in a concentration 2000-10000 -fold lower than in brain tissue (Daus et al. 2010).

Low levels of PrP^{sc} were detected in the muscle spindles of the masseter, intercostal, triceps brachii, psoas major, quadriceps femoris and semitendinosus muscles from 3 field and 6 experimental cases of classical bovine spongiform encephalopathy (Okada 2013).

Joshi-Barr and co-workers in 2014 observed an age-dependent degenerative myopathy characterized by ubiquitinated, intracellular prion inclusions detectable at immunohistochemistry in transgenic expressing a “rigidloop” structural variant of PrP (RL-PrP) (Joshi-Barr et al., 2014).

4.1.6: Prion protein and aging. (from Gasperini 2014)

It is well established that the incidence of prion disease is higher with age; this consideration raised the possibility that aging process can alter PrP^c function influencing its propensity to convert in PrP^{Sc}.

Brain aging is related to neuron loss, deterioration of dendrite branches, Ca homeostasis changes and increased oxidative stress; all these functions are achieved also by prion protein. PrP^c is important in memory function and is more expressed in the hippocampus. In humans, but not in mice, brain PrP content increases with age (Williams et al., 2004), and mice over-expressing PrP^c are protected against some age-related brain changes.

Biochemical properties that may change with aging thus influencing the PrP^c propensity to turn in a PrP^{Sc} form are:

- 1) expression levels: there are conflicting results in different species and experiments. Indeed, only in some species PrP^c increases with age.
- 2) post translational modification (i.e. glycosylation and phosphorylation levels). Loss of glycosylation of prion protein has been shown to promote acquisition of scrapie-like properties in cultured cells (Lehmann et al, 2013). Mice studies on aging revealed that there is an increase in unglycosylated, truncated form (Xi Hue et al. 2007). Unglycosylated forms are more prone to bind cations such as copper, improving its antioxidant functions. This also improves prion protein mobility, facilitating PrP^{Sc} propagation in prion disease.
- 3) localization in the cell (i.e. inside-outside the lipid raft): a group discovered that with aging PrP^c moves from the detergent soluble

membrane fraction to the lipid raft in aged mice but no amount difference (Agostini et al., 2013).

4.2 Aim of the project:

In the south of Italy the extensive breeding of the autochthonous cow breed Podolica is common and many animals are slaughtered in old age (>20 years). Those animals commonly show muscle impairment such as moderate to severe muscle atrophy, weakness and difficulty walking in the absence of any chronic disease. Thus, they are likely to be considered a spontaneous model of muscle aging.

The aim of the present project is to evaluate, by immunohistochemical and immunoblot analysis, the presence and the distribution of PrP^c in skeletal muscle from aged cows compared to muscles from younger animals.

The possible influence of age related muscle inflammation (“inflammaging”- Franceschi et al., 2007) on prion protein expression will be considered as well.

To the best of our knowledge, an attempt to quantify possible age-related differences in PrP^c content in bovine species has been made only on brain samples (Yoshioka et al 2011). In their work, PrPC content does not varies between aged (10 years old) and young cows but the amount in the detergent-insoluble fraction in the aged cattle was significantly higher than that of young cattle.

Thus, regarding muscle tissue, the two main topics of interest are:

a) PrPC physiological localization and characteristics in muscle tissue and their putative modification in aging compared to young animals

2) possible age-related changes in PrPC biochemical properties. The latter may be triggered by the cellular aging process and may promote prion aggregate formation.

Muscle cryosections were examined by a standard panel of histological and histoenzymatic stains as well as immunohistochemistry for:

- PrP, to detect its localization in muscle tissue
- Major Histocompatibility Complex class I, to demonstrate the inflammatory activation of muscle fibers even in absence of inflammatory infiltrate
- Desmin, to discriminate degenerated muscle fibers that have a reduced signal for desmin

Immunoblot was performed on muscle and brain homogenates in order to analyze the amount of PrPC, its glycosylation profile, proteinase resistance, solubility levels after high speed centrifugation and tendency to aggregate by sucrose gradient assay.

4.3 Materials and Methods

4.3.1: Animals:

Skeletal muscle and brain samples of 12 aged (7-22 years old) and 8 young (1 year old) (table 4.1, figure 4.1) cross-breed Podolica cows were collected at the slaughterhouse and immediately (<3 h from collection) snap frozen in liquid nitrogen as previously described (Dubowitz and Sewry, 2003).

All the brains were tested BSE negative using mandatory tests for BSE at the NeuroCenter (Division of Neurological Sciences, Vetsuisse Faculty, University of Bern, Bern, Switzerland).

Case number	age (years)	Ear brand
1	12	IT065990027459
2	1	IT065990382360
3	1	IT065990423063
4	11	IT076990040755
5	1	IT065990426498
6	1	IT06599039952
7	16	IT065800846982
8	19	IT065800830637
9	15	IT065800858207
10	12	IT06599007723
11	8	IT065990171082
12	22	IT065990029472
13	7	IT065990171094
14	1	IT065990029876
15	1	IT065990040496
16	12	IT065990027720

Case number	age (years)	Ear brand
17	7	IT065990217149
18	13	IT065800905251
19	1	IT065990425745
20	1	IT065990425746

Table 4.1: samples collected, signalment and ear brand of the animals



Fig. 4.2: macroscopical pictures of aged cows at the slaughter house. Case number 10 (22 years): the very consumed inferior incisors and the yellow subcutaneous fat of the carcass testimonies the old age of the animal.

4.3.2: Histology and histochemistry

For histological and histochemical examination, sections were cut in a transverse plane at 10 mm with a cryostat (-20°C) and stained according to our routinely performed extensive laboratory stains (Paciello and Papparella, 2009).

Specifically, the following stains were performed: hematoxylin and eosin (HE) and Engel trichrome (ET) for a basic morphologic evaluation of muscle fibers and intramuscular nerve branches; reduced nicotinamide adenine dinucleotide tetrazolium reductase (NADH-TR) to observe distribution of mitochondria and the myofibrillar network; succinate dehydrogenase (SDH) and cytochrome oxidase (COX) to evaluate activity and distribution of mitochondria; nonspecific esterase for the evaluation of the neuromuscular junctions and lipofuscins; ATPase at pH 9.4 and 4.3 for histochemical fiber type I and II subtyping, respectively;

Approximately 20 fields at 20x magnification were evaluated for each section by 2 independent pathologists (Dr. Teresa Bruna Pagano, Prof. Serenella Papparella) with a concordance rate of 95%.

4.3.3: Immunohistochemistry and immunofluorescence:

Immunohistochemistry: 8 μm muscle cryosections were air dried for 1h (or with an air dryer, 20 min at cold temperature) and post fixed for 3 minutes at 4°C . After washing in tap water for 15 min, the endogen peroxidase block: (3% H_2O_2 in Methanol) was applied for 15 min. Then the sections were washed in running tap water for 5 min and in twice in PBS-T for 5 min. Protein block was performed using Normal Goat

Serum (NGS) 5% in PBS for 20 min. Primary antibody (F99: 1:400 (Neurocenter), L42: 1: 500 (Neurocenter); 1: 300 and 6H4: 1: 500; 1:800 (Neurocenter) was applied for 1 h at room temperature. After 2 washes in PBS-T 2 for 5 min, the secondary antibody (Bottle A -DAKO Kit K5003) was applied for 10 min.

After 2 washes in PBS-T 2 for 5 min, the Secondary antibody (Bottle B - DAKO Kit K5003) was used for 10 min. Detection was get using bottle ABC (DAKO Kit K5003) for 5- 10 min based on the stain intensity. Then the sections were washed in running tap water for 5 min and counterstain with hematoxylin. For Desmin, Major Histocompatibility complex Class I, CD4, CD8 and MAC 387 antibodies the MACH1 (Biocare Medical, LLC, Concord, CA, USA) was used. In brief, the cryosections were incubated with primary antibodies (diluted in phosphate-buffered saline) overnight at 4°C. After 2 washes in phosphate-buffered saline, MACH 1 mouse probe (Biocare Medical, LLC, and Concord, CA, USA) was applied for 20 minutes at room temperature. After, MACH-1 Universal HPR-Polymer (Biocare Medical) was added for 30 minutes at room temperature. The reaction was detected by DAB chromogen diluted in DAB substrate buffer. Finally, sections were counterstained in hematoxylin and mounted in aquatex.

The primary antibodies used are illustrated in table 4.2.

To confirm the non pathogenic nature of prion protein, selected sections were pre-treated with proteinase K.

Blood vessel endothelial cells within sections were used as internal control for MHC I expression. In the corresponding negative control sections, the

primary antibody was either omitted or replaced with normal serum from the same species of primary antibody (rabbit or mouse).

Immunofluorescence: this technique was used on selected cases in order to co-localize PrP and MHC I. 8 μm sections were cut from selected muscle specimens on a cryostat and dried at room temperature for 45 minutes. Sections were fixed in acetone for 10 minutes at 4 °C and after were washed three times for 5 minutes with PBS at room temperature. Sections were incubated with 10% normal rabbit sera in PBS for 30 minutes at room temperature and after were washed three times for 5 minutes with PBS at room temperature. First primary antibody MHC I (diluted 1:50 in PBS with 20% normal rabbit serum) was diluted in PBS and 70 μl were added to each section for incubation overnight at 4 °C. On control section was added serum diluted in PBS 1:100. After washing three times with PBS for 5 minutes at room temperature, in the dark, FITC-conjugated rabbit anti-mouse IgG (H+L) (1:300; Jackson Laboratories, West Grove, PA, USA) was added to each section, except on control section where was added only PBS, and incubated for 40 minutes at room temperature. The sections were rinsed again in PBS and incubated with the second primary antibody against 6H4 (diluted 1:50 in PBS with 20% normal rabbit serum) for 24 h at 4 °C. After rinsing in PBS, the sections were treated with affinity-purified rabbit anti-mouse IgG-Fab conjugated to FITC fluorochrome (1:50; Jackson Laboratories), for 1 h at room temperature.

For double immunofluorescence staining, fluorochrome conjugated Fab fragments were used (Jackson Laboratories) to avoid antibody cross-reaction using two primary mouse antibodies, according to the method previously described (Paciello, 2007). Sections were washed three times again with PBS for 5 minutes and mounted under coverslips in VECTASHIELD® H-1200 (Vector, Burlingame, CA, USA) to prevent fading of fluorescence.

Specimens were examined and photographed with a laser-scanning confocal microscope (LSM-510; Zeiss, Oberkochen, Germany). FITC was irradiated at 488 nm and detected via a 505-560 nm band pass filter.

4.3.4 Statistical analysis of histological data:

To quantify the histological and immunohistochemical findings and facilitate statistical analysis, the following three tier score systems were applied for each parameter (Table 4.3):

Finally, an Overall PrP positivity score was obtained by summing PrP+ score and PrP+ sarcoplasmic inclusion score.

All data were imported into a program for statistical analysis (GraphPad Prism-GraphPad Software, San Diego, CA). Statistical significance was set at $P < .05$. For each animal, an overall positivity score to PrP was obtained by summing the sarcolemmal positivity score and the sarcoplasmic positivity score to PrP. All histological scores (lymphoplasmacytic inflammation score, fiber degeneration score, angular atrophy score, PrP sarcolemmal positivity score, PrP sarcoplasmic

positivity score) of young and old animals were compared using the Mann Whitney test. Data were checked for normality of distribution with a Shapiro-Wilk's W test. The relationship between IS, histological score, and fiber atrophy was evaluated by a Spearman rank correlation test (rs).

score	0: none	1: mild	2: moderate	3: severe
Lymphoplasmacytic inflammation score	no inflammation	5-25 inflammatory cells x HPF (400X) in 10 fields	26 to 50 inflammatory cells x HPF (400X) in 10 fields	>50 inflammatory cells x HPF (400X) in 10 fields
Degeneration score	no degenerated fibers/100 fibers at 200X	1-10 degenerated fibers/100 fibers at 200X	11-25 degenerated fibers/100 fibers at 200X	>25 degenerated fibers/100 fibers at 200X
Angular atrophy score	no angular fibers/100 fibers at 200X	1-10 angular fibers/100 fibers at 200X	1-10 angular fibers/100 fibers at 200X	1-10 angular fibers/100 fibers at 200X
Sarcolemmal PrP+ score	absent	Mild intensity*	Moderate intensity*	Strong intensity*
Sarcoplasmic PrP+ score	absent	1-5 positive fibers/100 fibers at 200X	6-10 positive fibers/100 fibers at 200X	>10 positive fibers/100 fibers at 200X
MHC I score	absent	1-25 positive	26-50 positive fibers/100 fibers at 200X	>50 positive fibers/100 fibers at 200X

Table 4.2. histological scoring. *=3 the scoring was made by two independent pathologists (OP, TBP) with a minimum concordance rate of 95%. In case of discrepancies, the opinion of another pathologist (SP) was requested.

4.3.5 Sample preparation and western blotting:

Muscle frozen samples were homogenized at 10% (w/v) in RIPA buffer (100 mM NaCl, 10 mM EDTA, 0.5% NP40, 0.5% sodium deoxycholate, 10 mM Tris, pH 7.4) in a BIO-RAD 2 ml tube (without buffer but with iron beads) and spun several times in the BIO-RAD machine. Brain frozen samples were homogenized at 10% (w/v) in Prionics homogenization buffer with a FASTH device (Consul). All samples were analyzed with and without PK digestion and/or deglycosylation using standard methods. The PK digestion was done with the reagents of the Prionics Check Western kit, according to the manufacturer's instructions and at a final PK concentration of 100 μ g/ml. For PK titration experiments, the PK stock solution was diluted from 1:1 to 1:1000 in 1x homogenization buffer. Deglycosylation was performed for 90 min at 37 °C with PNGaseF (New England Biolabs) under denaturing conditions according to the manufacturer's instructions. Samples were denatured by boiling in SDS sample buffer and resolved on either 4–20% Tris-Glycine gradient gels (Life technologies) for epitope mapping, or on 12% Bis-Tris precast gels (Life technologies) for all the other experiments. Proteins were then transferred to PVDF membranes (Immobilon-P Millipore) for 1hr at 150V. PrP probing was done by incubating the membrane with Sha31 antibody (0.1 μ g/ml, overnight at 4° C) as the primary antibody and a horseradish-peroxidase rabbit anti-mouse conjugate (Dako) as a secondary antibody, unless otherwise mentioned. Antibody binding was visualized with the ECL prime reagent kit (GE healthcare) and the LAS3000 chemiluminescence camera (Fuji). For epitope mapping, we used bovine

PrP specific antibodies recognizing epitopes that span from the N-terminal to the C-terminal regions, namely SAF32, 9A2, Sha31, and ROS-JB10.

All the western-blot related experiments were performed according to Serra et al, 2016 and performed at the NeuroCenter, Division of Neurological sciences, University of Bern, Vetsuisse Faculty, Switzerland.

Antibody	Company & dilution	Technique
Sha 31 (core-binding)	Bio-Rad, 1: 10 000	WB (for all techniques)
6H4 (core-binding)	R-Pharma, 1: 800	IHC, IF
SAF 32 (N-terminal)	SpiBio, 1: 800	WB, epitope mapping
9A2(N-terminal)	₁₀₂ Wnk ₁₀₄ , 1: 250	WB, epitope mapping
94B4 (C-terminal)	1: 250	WB, epitope mapping
JB10 (C-terminal)	McCutcheon et al, 2014 1: 1000	WB, epitope mapping
Aspecific mouse IgG	DAKO X0931, concentration 0,1 mg/ml	Negative ctr in IHC and WB
Desmin	DAKO, 1:100	IHC
Major Histocompatibility complex I	VMRD, 1:200	IHC, IF

Table 4.3: antibodies and relative techniques used in the study.

Data obtained from quantitative Western blots were analyzed with Image J software by Student's t test. β -actin and tubulin were used as a loading control for brain and muscle, respectively). The autoradiographs shown are representative of 4 independent experiments. Bars represent the mean \pm SD of 4 independent experiments. P values $<.05$ were considered statistically significant.

4.3.6 Velocity sedimentation in sucrose step gradient

Brain and muscle homogenates (10% [w/v]) were prepared in PBS with 1% sarcosyl. The supernatant was recovered after pre-centrifugation at 1000g for 5 min and was loaded on top of a sucrose gradient, prepared by superimposing 350 μ l layers of 45%, 40%, 35%, 30%, 25%, 20%, 15%, and 10% sucrose solutions from bottom to top.

The gradients were centrifuged at 200,000g (46,000 rpm) for 65 min at 4°C using a P55ST2 rotor and a Hitachi CP100NX centrifuge. After centrifugation, the contents of the centrifuge tubes were sequentially removed from the bottom to the top to collect. 13 fractions of approximately 250 μ l each were collected and proteins were precipitated and recovered in chloroform and methanol after several spin rounds at 10,000 rpm for 5 min. The final pellet was resuspended in 50 μ l PBS + 0.5% sarkosyl or SDS page sample buffer and stored at -20°C until needed. The samples were subjected to Western blot analysis to detect PrPC in the individual fractions.

4.3.7 Separation of detergent-soluble and -insoluble PrP by one-step ultracentrifugation

Brain and homogenates and detergent-soluble and -insoluble fractions were prepared as previously described (Serra, 2016). Briefly, 10% (w/v) brain homogenates were suspended in 9 volumes of lysis buffer (10 mM Tris, 150 mM NaCl, 0.5% Nonidet P40, 0.5% deoxycholate, 5 mM EDTA, pH 7.4) on ice using a pestle. Five hundred μ l of brain homogenate was then centrifuged at 1000g for 10 min at 4 °C and the

supernatant was collected for ultracentrifugation at 115,000g (35,000 rpm) in a P55ST2 rotor and a Hitachi CP100NX centrifuge for 1 h at 4 ° C.

The supernatant S2 (detergent-soluble fraction) was transferred to a clean tube and the pellet P2 (detergent-insoluble fraction) was resuspended in 500 μ l lysis buffer. Half of the volume of S2 and P2 were subjected to PK digestion with a final concentration of 50 μ g PK/ml (Roche). The other half was left undigested. Each sample was boiled at 100 °C for 5 min with an equal amount of SDS sample buffer and analyzed by Western blot.

4.4 Results:

4.4.1 Histopathology:

Main histopathological findings are summarized in table 4.4.

As expected, muscle biopsies of aged cows showed myopathic features (Fig. 4.3 A, B, C) such as degenerated fibers (83%), angular atrophy (75%) and lymphocytic inflammation (41%). Those findings were similar to those reported in a recent paper from our group (Costagliola et al, 2016).

Vacuolated muscle fibers and less severe angular atrophy were found in a low number of young animals (25 and 12%, respectively).

Muscle samples from old cows showed also increased variability in diameter size of muscle fibers and mild to severe fiber atrophy, multifocal subsarcolemmal deposits of SDH (Succinate dehydrogenase) positive material, occasional sparse moth-eaten fibers at NADH (Nitroterazolium adenine dinucleotide) and reduced central positivity at cytochrome C oxidase (COX). ATP-ase stains at pH 4.3 and 9.4 on selected cases revealed a predominantly type II fiber in old animals. All those findings

were consistent with the typical age related muscular changes previously described (Costagliola et al., 2016).

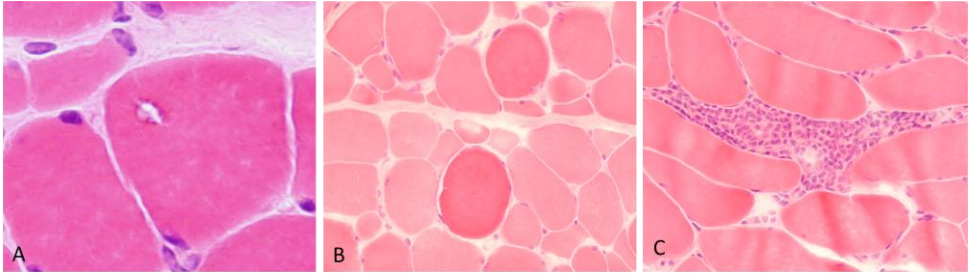


Fig. 4.3: Cryosections of skeletal muscle from old animals (A: case number 12, B. case number 18; C: case number 3). Hematoxylin and Eosin. Original magnification 400X (A) and 200X (B and C). Muscle fiber degeneration including sarcoplasmic rimmed vacuole (A) and presence of rigen/degen fibers (B). Endomyisial lymphoplasmacytic infiltrate (C).

4.4.2: Immunohistochemistry:

Immunohistochemistry for PrP^c revealed a distinct granular positivity in intramuscular nerve branches and muscle spindles in all cases (Fig. 4.4). As expected, the signal was completely digested after pre-treatment with Proteinase K, confirming the presence of only non-disease associated prion protein (Fig. 4.5). A faint membrane positivity was evident in 60% of cases (Fig. 4.4, B), consisting with a normal constitutive membrane expression of PrP.

The sarcolemma was positive in 37% of young animals and 75% of old animals. Sarcoplasmic PrP positive inclusions were detected in 25% of young and 75% of old animals. MHC I was overexpressed on the

membrane of muscle fibers in 12,5% of young animals and in 66,6% of old animals.

Case number	Age	Lymphoplasmocytic inflammation score	Fiber degeneration score	Angular atrophy score	Prp on nerves	Prp+ on sarcolemma	PrP+ sarcoplasmic inclusions	MH C I score	overall PrP positivity score
1	12	1	1	0	+	0	1	1	1
2	1	0	1	0	+	0	1	1	1
3	1	0	0	1	+	2	0	0	2
4	11	0	2	1	+	1	0	1	1
5	1	0	0	0	+	1	0	0	1
6	1	0	0	0	+	0	0	0	0
7	16	2	2	2	+	2	2	2	4
8	19	2	0	2	+	2	1	2	3
9	15	0	1	1	+	1	1	0	2
10	12	0	2	2	+	2	1	0	3
11	8	0	2	1	+	1	2	0	3
12	22	1	2	2	+	2	1	2	3
13	7	0	1	1	+	1	1	1	2
14	1	0	0	0	+	0	0	0	0
15	1	0	0	0	+	0	0	0	0
16	12	0	0	0	+	0	0	1	0
17	7	0	1	0	+	0	1	0	1
18	13	2	2	1	+	2	0	2	2
19	1	0	1	0	+	1	1	0	2
20	1	0	0	0	+	0	0	1	0

Table 4.4: Histopathology and immunohistochemistry results

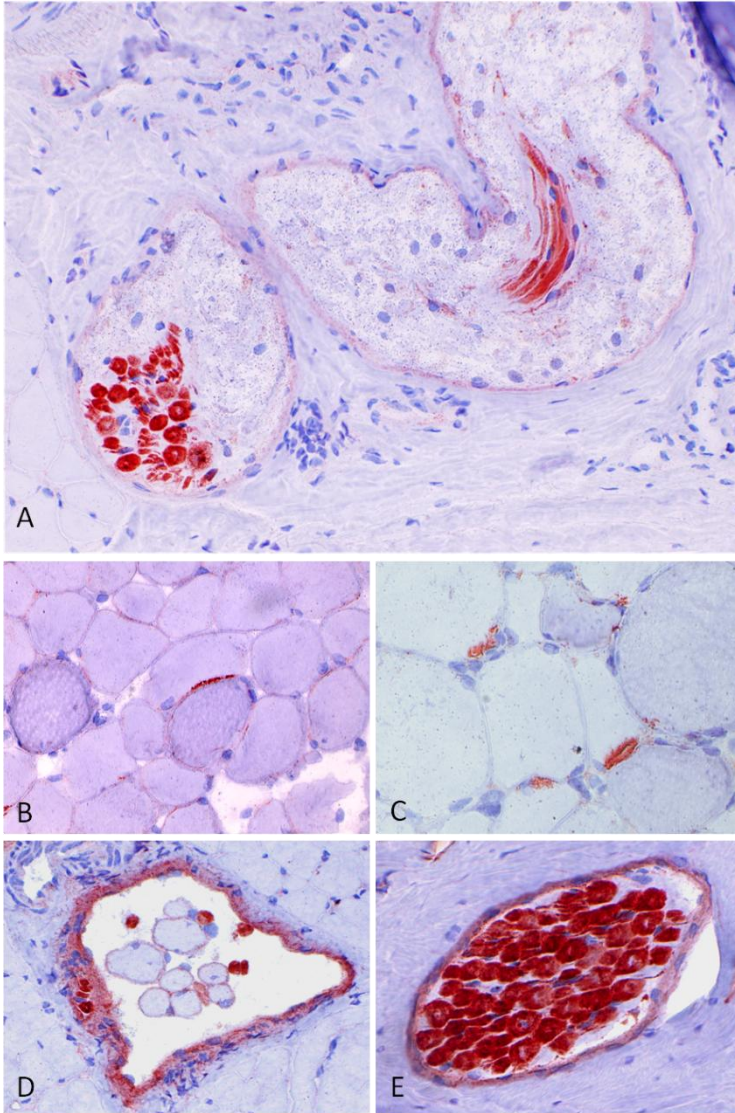


Fig. 4.4: Normal immunohistochemical findings. PrP (6H4) is expressed in myelin sheath of intramuscular nerve branches (A, E), on the sarcolemma (B), at neuromuscular junctions (C) and in muscle spindles (D).

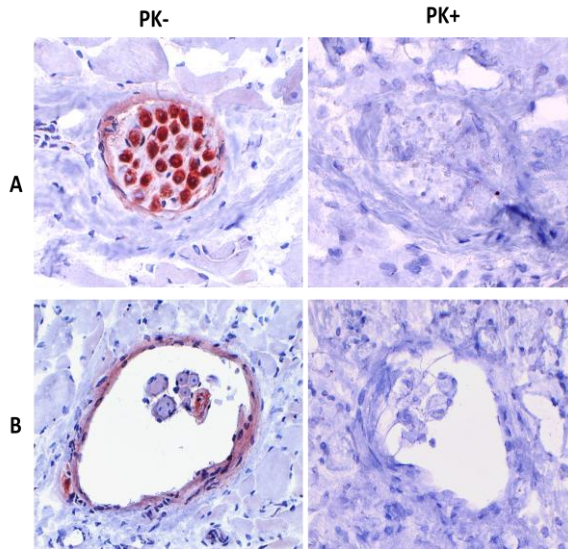


Fig. 4.5: Normal findings. In all animals, intramuscular nerve branches and muscle spindles stained positively to PrP antibody 6H4 (A, B, PK-) but the signal was completely digested after pre-treatment with proteinase K (A,B, PK+). Immunohistochemistry (HRP method), hematoxylin counterstain.

A focal subsarcolemmal granular positivity was found in degenerated fibers (desmin depleted) of both young (30%) and old (66%) animals with an increased immunolabeling of rimmed vacuoles (Fig. 4.7 E). Occasionally, mononuclear endomysial infiltrate was PrP positive as well.

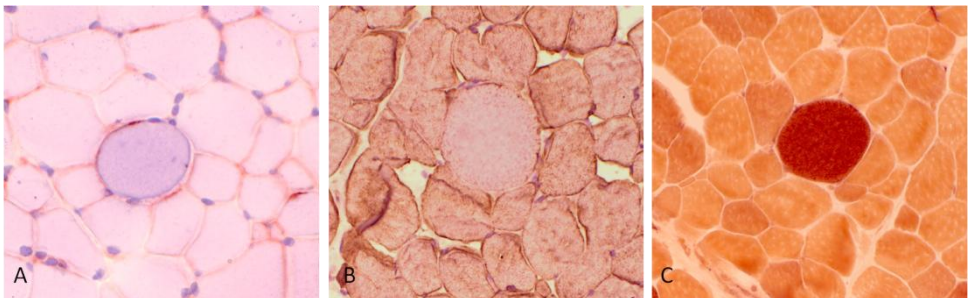


Fig. 4.6: Rigin/degen fibers show increased sarcolemmal positivity to PrP (A), decreased desmin signal (B) and stain positively to Esterase stain (C). Immunohistochemistry (HRP method) and histochemical stain non specific esterase. Original magnification 400X.

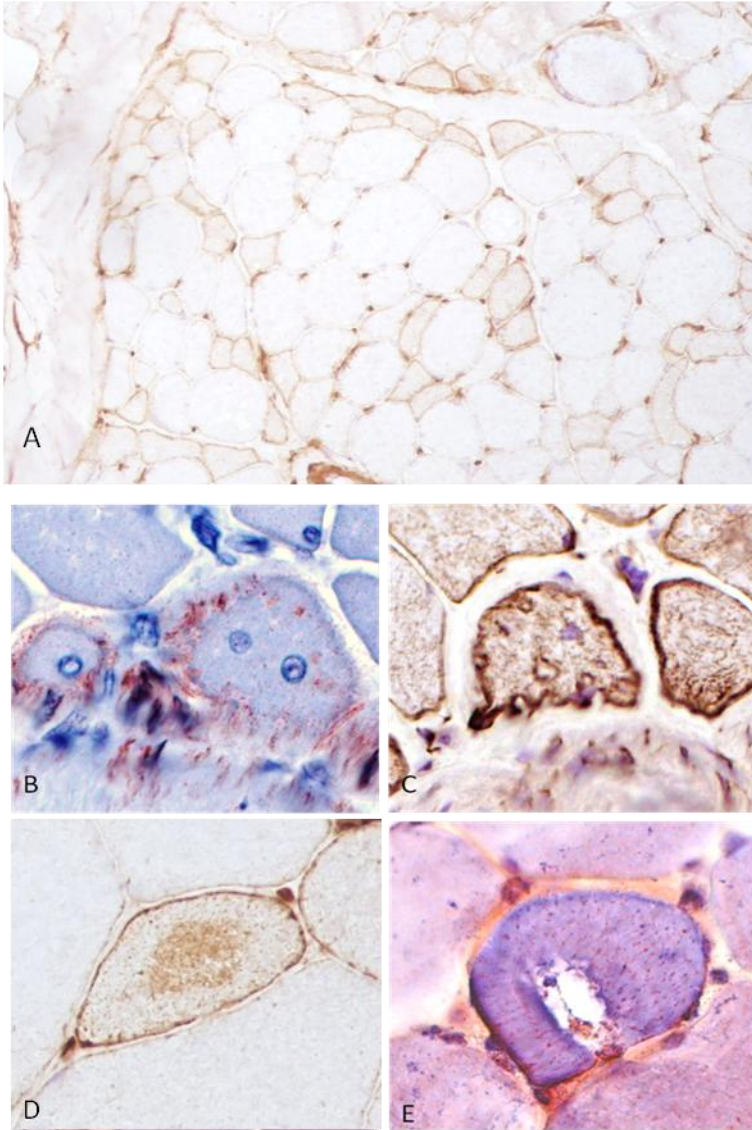


Fig. 4.7: Pathological findings. PrP is overexpressed in angular fibers (A), in regenerating fibers having multiple central nuclei (B) that stain positively to desmin (C), in sarcoplasmic inclusions (D) and rimmed vacuoles (E). Immunohistochemistry (HRP method), hematoxylin counterstain. Original magnification 200X (A) 400X (B).

4.4.3 Immunofluorescence:

On selected cases showing strongest positivity for MHC I at immunohistochemistry (n. 5 cases: 1, 7, 8, 12, 14) co-localization between PrP^c and MHC I on the plasmamembrane was observed (Fig. 4.8).

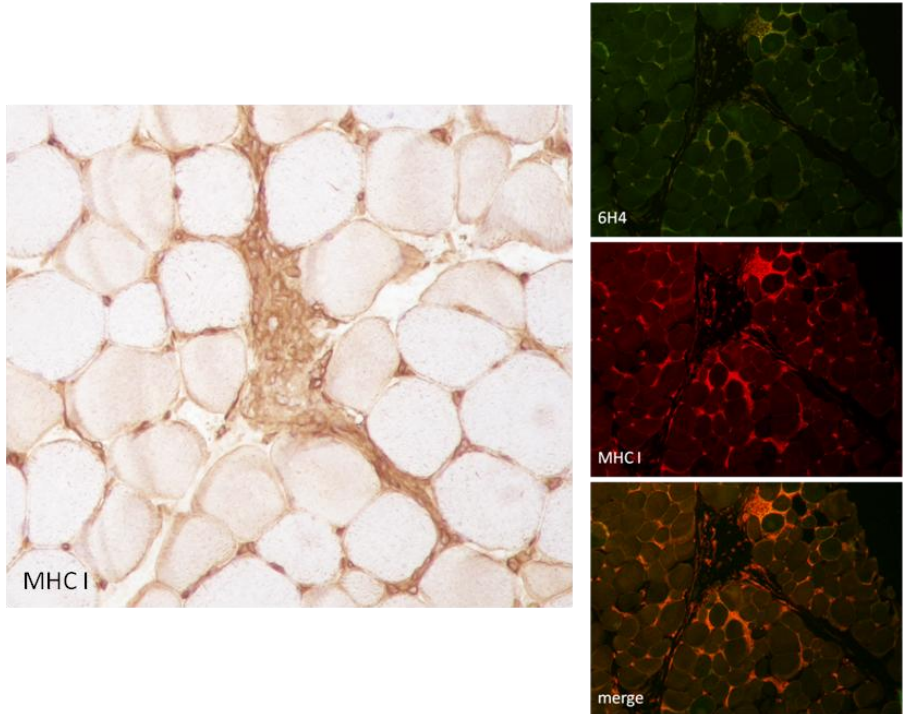


Fig. 4.8 Immunohistochemistry (left). MHC expression on the sarcolemma of muscle fiber adjacent to mononuclear, MHC I positive, inflammatory infiltrate. **Immunofluorescence, (right).** Cryosection of skeletal muscle with age related inflammation. Muscle fibers over expressing MHC I (TRIC- red color) are also more immuno-positive to PrP (6H4-green color). Multifocally MHC I and PrP colocalize on the sarcolemma of muscle fibers (merge, orange color).

4.4.4 Statistical analysis of histopathological findings

Lymphoplasmacytic inflammation score was basically higher in old compared to young animals, but this difference was not statistically significant ($P=0.2$). The lack of significance can be imputable to the presence of mild muscle inflammation of unknown origin in one young animal, and interpreted as non-meaningful.

Fiber degeneration score was significantly ($P=0.005$) higher in old animals compared to young ones (Fig. 4.9 A), as well as angular atrophy ($P=0.008$) (Fig. 4.9 B). PrP sarcolemmal positivity score did not significantly varied between young and aged animals ($P=0.1$) while PrP sarcoplasmic positivity score was significantly higher in old animals compared to young animals ($P=0.03$) (Fig. 4.9 B). MHC I score and overall PrP positivity score were both significantly higher in old animals compared to young ones ($P=0.04$ and $P=0.02$, respectively. Fig 4.9 C, D). Spearman correlation test revealed a positive correlation between fiber degeneration score and PrP sarcoplasmic inclusion score ($r_s=0.5$, $P=0.07$); MHC I score and overall PrP score ($r_s=0.3$, $P=0.1$) were not statistically correlated. Notably, there was a positive correlation between age and overall PrP positivity score ($r_s=0.6$, $P=0.003$).

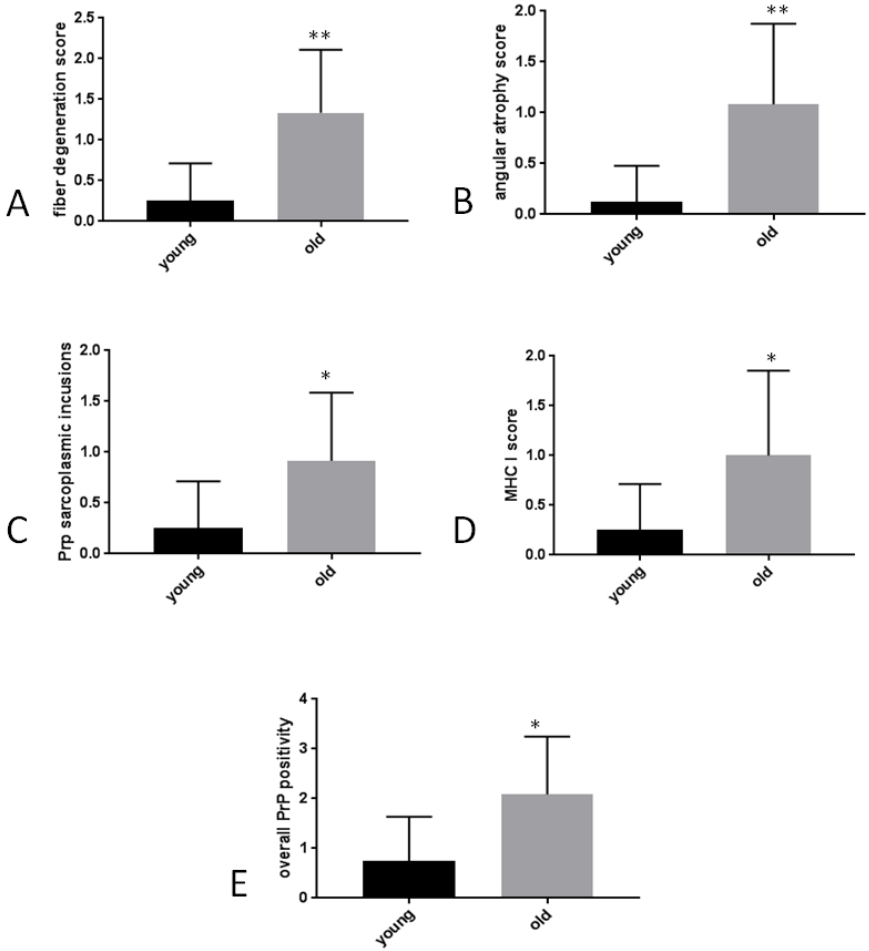


Fig. 4.9: Statistical comparison between histological score of young and old cows (only statistically significant data are shown).

4.4.5 Quantitative western blot

PrP^c showed three poorly distinct migration bands corresponding to molecular weights of approximately 35, 30 and 15-16 kDa which are likely associated with the di-, mono- and un-glycosylated forms of PrP^c, respectively. In all experiments, the more distinct band was those at 35KDa, indicating a possible predominant content of highly glycosylated PrP in this tissue.

The amount of prion protein detected using Sha31 antibody did not vary between old and young animals by statistical analysis; however a slightly higher content of PrP^c in muscles from young animals was noted (Fig. 4.9).

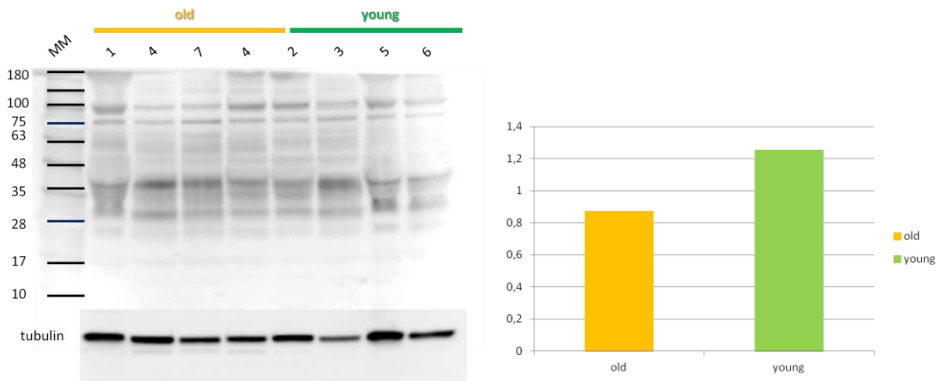


Fig. 4.9 Quantitative western blot. Representative results of semi quantitative western blotting comparing PrP signal in muscle homogenate from old (yellow) and young (green) animals. Tubulin was used as housekeeping protein for comparison. No significant differences were noted. Sha31 was used as primary antibody.

4.4.6 Glycoform profile and epitope mapping

The glycoform profile and the molecular mass of PrP^c in muscle samples appeared slightly different compared to the brain. In particular, compared to brain homogenate, the lower, unglycosylated band resulted having a higher molecular weight (approximately 2 KDa of difference) (Fig.4.10). Enzymatic deglycosylation reduced PrP^c species to a 30-kDa zone, and to a minor band at ~15 kDa, representing amino-truncated fragments (Figure 4.10 arrow).

Epitope mapping was performed using a panel of different antibodies directed against different regions of the prion protein. Constantly muscle homogenates showed a different profile compared to brain (Fig. 4.11).

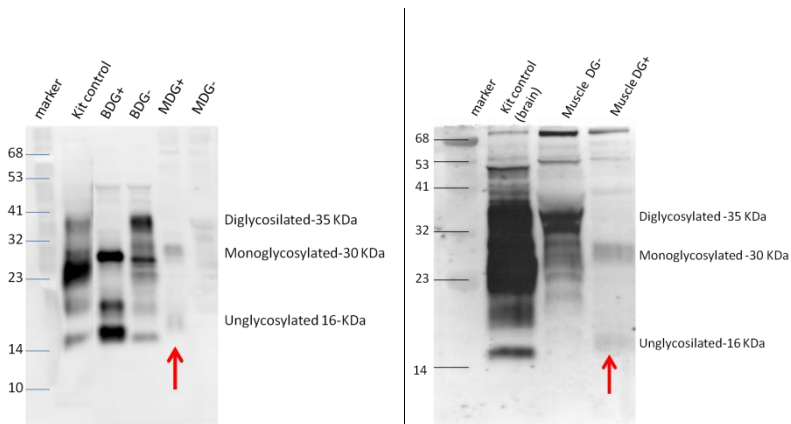


Fig. 4.10 Western blotting of non deglycosylated and deglycosylated muscle and brain. Representative results of brain and skeletal muscle homogenate blot after deglycosylation. The C1 unglycosylated band shows a higher molecular weight in muscle tissue after deglycosylation compared to brain. Sha31 was used as primary antibody (BDG+= brain deglycosylated, BDG-= brain not deglycosylated, MDG+=muscle deglycosylated, MDG-=muscle not deglycosylated).

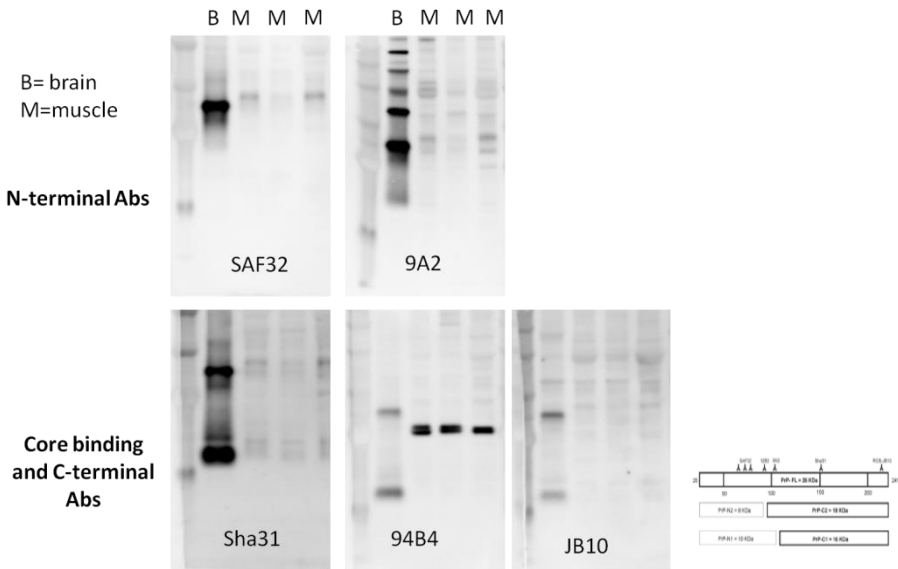


Fig. 4.11: Epitope mapping. Left: Representative results of epitope mapping using a panel of different antibodies directed against different regions of the prion protein. Constantly muscle homogenates (B) show a different profile compared to brain (B). Right: Schematic representation of PrP truncated fragments found in health and in disease... Epitopes of antibodies used in this study are indicated on the top (From Serra, 2016).

4.4.7 Proteinase K titration, sucrose gradient, soluble/insoluble fraction:

No significant differences between muscles and brains of young and old animals were detected by quantitative immunoblot and Proteinase K titration. The signal disappear approximately ad a concentration of 1/100 of the PK concentration used in Prionics® (Fig. 4.11).

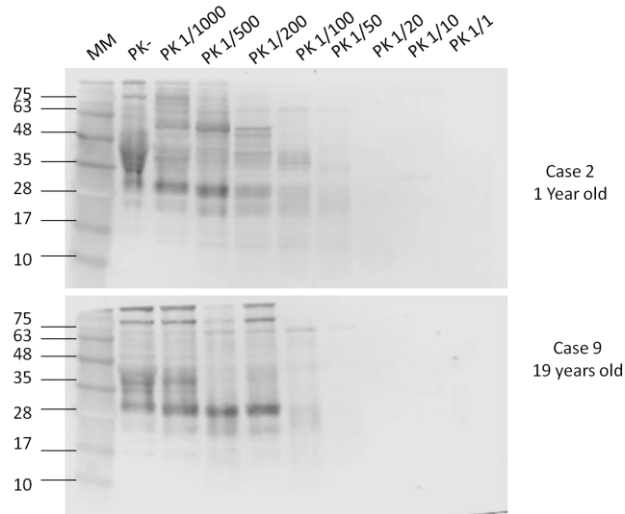


Fig. 4.11. PK titration. Representative results of PK titration on muscle homogenate from young (top) and old (bottom) animals. Sha31 was used as primary antibody.

Sucrose gradient velocity sedimentation gave variable results, with a generally lower amount of PrP in high density sucrose fractions in the muscle compared to the brain (Fig. 12, top). After high speed centrifugation the majority of muscle PrP^c was mainly found in the soluble fraction, without significant differences between young and old animals (Fig. 4.13). As expected both the soluble and the insoluble fractions were totally digested after treatment with Proteinase K (Fig. 4.13, bottom).

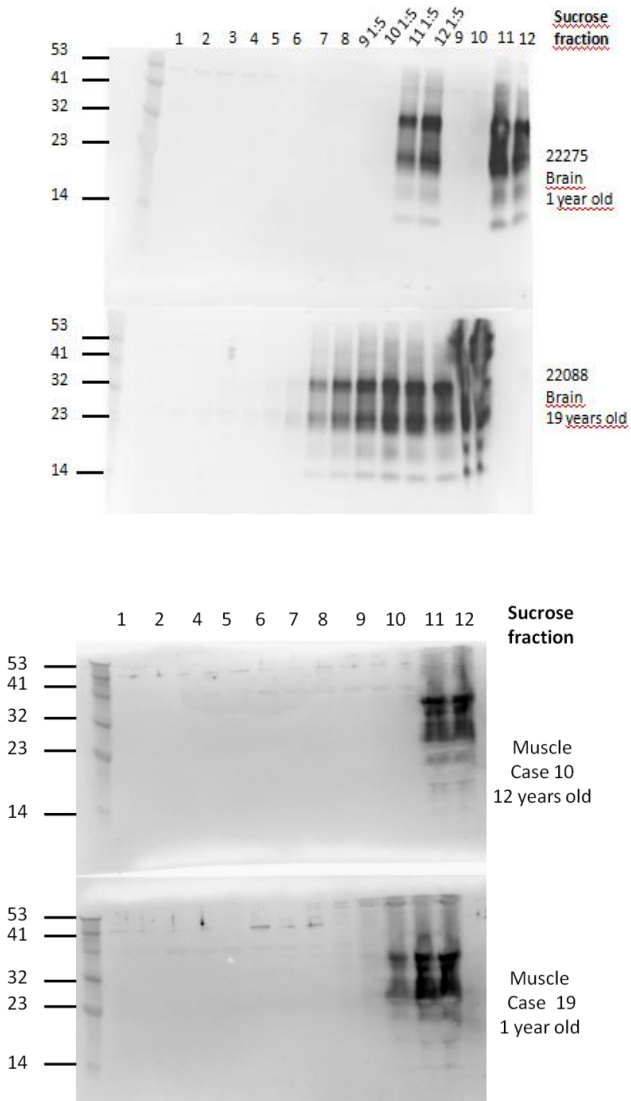


Fig. 4.12 Sucrose gradient. Representative results of sucrose gradient experiments comparing brain (top) and muscle (below) of old and young animals. In the brain PrP signal is still visible at fraction 7, indicating a greater tendency of Prion Protein to form aggregates in old animals compared to young. Such difference is not observed in the comparison between sucrose gradient of muscle tissue from old and young animals. Sha31 was used as primary antibody.

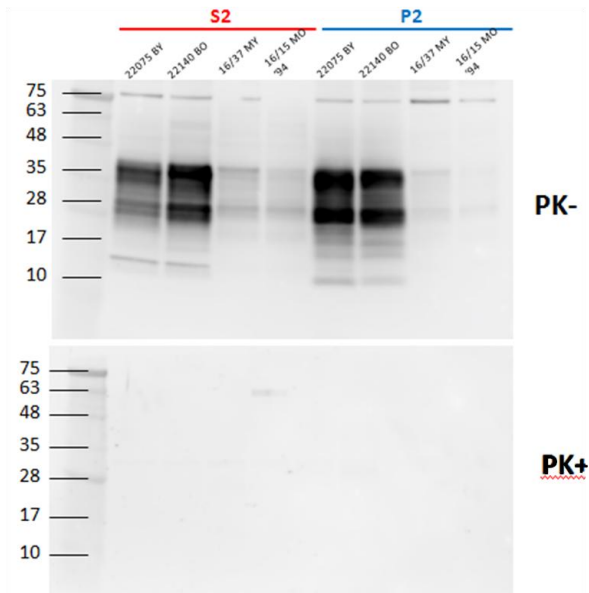


Fig. 4.13 Soluble-insoluble fractions Representative results of soluble/insoluble fraction experiments on muscle homogenates from young and old animals. After high speed centrifugation the majority of muscle PrPC was found in the soluble fraction, without significant differences between young and old animals. The signal is completely digested after treatment with PK (PK+).

4.5 Discussion:

The prion protein has become sadly popular after the outbreak of Prionic diseases (TSE) in human population. During recent years, however, increased scientific evidences suggested that its cellular variant (PrP^c) has several important physiological functions, being involved in protection against oxidative stress, in myelin sheath integrity maintenance, in calcium homeostasis and so on (Cowan et al., 2001; Lo et al., 2007, Vassallo and Herms, 2003 Gasperini et al., 2014). In the brain, PrP^c has also been shown to inhibit the production of amyloid- β , and an age-related impairment of brain PrP^c has been proposed as a factor involved in increased incidence of Alzheimer disease in older people (Whitehouse, 2011).

Nevertheless, information on cellular prion protein features, functions and metabolism in non neural tissues is still largely unavailable and most of research has been focused on PrP^{res} and nervous tissue.

Skeletal muscle is one of the most unexplored tissue in this field despite its potential key role in the transmission of prionic disease as a route for human disease. In experimental prion disease skeletal muscle has been proved to propagate prions and accumulate substantial titers of these pathogens (Bosque et al., 2001, Okada et al, 2013); infectivity in skeletal muscle of cattle with atypical bovine spongiform encephalopathy has been described as well (Suardi, 2012).

Here, we present preliminary results about PrP^c features in skeletal muscle. To the author's knowledge, this is the first report about PrP^c expression and biochemical properties in bovine muscle tissue. We tried to better

characterize the localization and the biochemical properties using innovative techniques that are commonly used to study PrP^{res} on the nervous tissue of diseased animals.

At first, much work was needed to adapt these techniques (i.e. sucrose gradient, soluble insoluble fractions, glycosylation profile etc.) on muscle tissue, in which the PrP^c is expressed in an extremely low amount compared to the brain (5%).

The main results of the present study suggest that:

- 1) PrP^c is normally detectable by immunohistochemistry in intramuscular nerve branches, muscle spindles and neuromuscular junctions in bovine frozen muscle tissue.
- 2) PrP^c is overexpressed in degenerated, vacuolated and angular atrophic muscle fibers as well as in muscle inflammation.
- 3) The glycoform profile of PrP^c differs between brain and muscle tissue.
- 4) The glycoform profile did not varied between young and old animals.
- 5) Detergent solubility, PK resistance and PrP^c tendency to aggregation in skeletal muscle do not vary with age.

The first finding is in accordance with human literature (Zanusso et al. 2014) but has been never reported before in bovine skeletal muscle.

Notably, previous papers reported a negative result at immunohistochemical detection of PrP^c in formalin fixed skeletal muscle tissue (Peralta, 2009), and only immunodetection of PrP in animal and

human individuals terminally affected by prion diseases has been described so far (Okada et al. 2013, Peden, 2006, Daus, 2011). In contrast, we found a distinct sarcolemmal and neural positivity to 6H4 antibody; it is likely that this result is imputable to the better antigenity quality that is typical of frozen tissues compared to formalin-fixed tissues. Moreover, we found that the antibody 6H4 works better on cryosections compared to F99, the most commonly used antibody to detect prion protein for diagnostic purpose on formalin fixed sections.

The second finding confirms the possible involvement of PrP^c in inflammatory and neurogenic muscle disorders also in bovine species. We found that muscle fibers in inflamed muscles displayed a higher positivity to PrP^c. This result is consistent with previously literature regarding the expression of prion protein in human inflammatory myopathies (Zanusso et al, 2014) and mouse models of inflammatory myopathies (Neuman, 2013). In particular, in the last paper, the authors observed, in early disease stages, that PrP^{sc} accumulation is driven by cells of hematopoietic origin, whereas at late disease stages, non-hematopoietic cells such as myocytes represent the main sites for PrP^{sc} accumulation. Since this accumulation is transient, the authors suggested that skeletal muscle has an intrinsically high ability to clear PrP^{sc} once myositis has ceased, possibly by means of autophagy (Neuman 2013). Joshi-Barr and colleagues in 2014 inhibited autophagy in vitro cultures of C2C12 myoblasts, and observed enhanced intracellular prion accumulations; thus, they proposed a role for autophagy in prion aggregate clearance. As further support of this hypothesis, Furukawa and colleagues in 2004 reproduced an experimental myopathy

implying a drug-induced blockage of autophagy in hamsters and found an anomalous accumulation of PrP in skeletal muscle (Furukawa, 2004). For future perspectives, it will be interesting to explore the association between prion expression and autophagy markers, possibly in old animals compared to young ones.

The reasons for the over-expression of prion protein in degenerated muscle fibers are unknown but, given the antioxidant properties of this protein, it may represent a cellular response to altered homeostasis typical of degenerative conditions.

The glycoform profile of prion protein has been largely studied in prion diseases. Atypical BSE (Casalone, 2004, Biacabe, 2004), indeed, differs from the classical form (C-BSE) based on a different glycoprofile of the PK resistant protein at western blot analysis. H-type is characterized by a higher molecular mass of the unglycosylated protein band, and L-type, or a bovine amyloidotic spongiform encephalopathy (BASE), is characterized by an unglycosylated protein band with a lower molecular mass. Sporadic reports of prion disease (H-type BSE) in cattle occurring after the ban of meat based food in 2001, has raised the hypothesis that the etiology of H-type BSE may be unrelated to the ingestion of prion-contaminated meat- and bone meal and the need for more knowledge about how the cellular prion protein may transform without being in contact with an exogenous source of PrP^{res} (Guldimann, 2012). Since most atypical BSE cases have occurred in cattle over 8 years of age, Yoshioka and coworkers in 2010 studied the biological properties of normal prion protein in the brain of young and aged cattle in order to clarify the existence of any relationship

between cattle age and occurrence of atypical BSE. They found that the amount of PrPC in the brain homogenates was not significantly different between young and aged cattle, but the amount in the detergent-insoluble fraction in the aged cattle was significantly higher than that of young cattle. In our work nor the total amount, nor the amount of detergent insoluble fraction nor the susceptibility to PK digestion varied between young and old animals, suggesting a different metabolism of prion protein in those two tissues. The different glycoprofile that we found between brain and tissue may be responsible for a different susceptibility of muscle tissue to propagate prions of atypical BSE, but this hypotheses needs to be further investigated. A similar finding was previously reported by Zanusso and colleagues in 2014.

In conclusion, in this final part of the thesis, we present preliminary results about cellular prion protein in muscle tissue. Although we didn't confirm the starting hypothesis of a possible age-related modification in the prion protein properties and expression, we described for the first time the overexpression of PrPC in muscle degeneration, inflammation and neurogenic atrophy in bovine species, opening new perspectives for the future study about the molecular bases of these findings.

References:

- Agostini F, Dotti C, G., Perez-Canamas A, Ledesma MD, Benetti F, Legname G. Prion protein accumulation in lipid rafts of mouse aging brain. 2013; PLoS ONE 8:e74244.
- Arena G, La Mendola D, Pappalard G, Sóvágód I and Rizzarelli E. Interactions of Cu²⁺ with prion family peptide fragments: considerations on affinity, speciation and coordination. 2012; *Coord. Chem. Rev.* 256, 2202–2218.
- Askanas V, Bilak M, Engel WK, Alvarez RB, Tomé F, Leclerc A. Prion protein is abnormally accumulated in inclusion-body myositis. 1993 *NeuroReport* 5: 25-28
- Askanas V, Engel WK. Newest approaches to diagnosis and pathogenesis of sporadic inclusion-body myositis and hereditary inclusion-body myopathies, including molecular-pathologic similarities to Alzheimer disease. In: *Inclusion-body myositis and myopathies*, Askanas V, Serratrice G, Engel WK (eds.), 1998, pp. 3-78, Cambridge University Press: Cambridge
- Biacabe, A. G., Laplanche, J. L., Ryder, S. and Baron, T. 2004. Distinct molecular phenotypes in bovine prion diseases. *EMBO Rep.* 5: 110–115.
- Borràs D, Ferrer I, Pumarola M. Age-related changes in the brain of the dog. *Vet Pathol.* 1999 May;36(3):202-11.
- Bosque PJ, Ryou C, Telling G, Peretz D, Legname G, DeArmond SJ, Prusiner SB Prions in skeletal muscle 3812–3817 *PNAS* March 19, 2002
- Bounhar Y, Mann KK, Roucou X, LeBlanc AC. Prion protein prevents Bax-mediated cell death in the absence of other Bcl-2 family members in *Saccharomyces cerevisiae*. *FEMS Yeast Res.* 2006 Dec;6(8):1204-12.
- Bueler H, Aguzzi A, Sailer A, Greiner RA, Autenried P, Aguet M, et al. Mice devoid of PrP are resistant to scrapie. *Cell* 1993; 73:1339-47.
- Burchell JT, Panegyres PK. Prion diseases: immunotargets and therapy. *Immunotargets Ther.* 2016 Jun 16;5:57-68. doi: 10.2147/ITT.S64795

Bibliography

- Casalone, C., Zanusso, G., Acutis, P., Ferrari, S., Capucci, L., Tagliavini, F., Monaco, S. and Caramelli, M. 2004. Identification of a second bovine amyloidotic spongiform encephalopathy: molecular similarities with sporadic Creutzfeldt-Jakob disease. *Proc. Natl. Acad. Sci. U.S.A.* 101: 3065–3070.
- Collinge J. Prion diseases of humans and animals: their causes and molecular basis. *Annu Rev Neurosci* 2001; 24:519-50.
- Cowan CM, Thai J, Krajewski S, Reed JC, Nicholson DW, Kaufmann SH, Roskams AJ. Caspases 3 and 9 send a pro-apoptotic signal from synapse to cell body in olfactory receptor neurons. *J Neurosci.* 2001 Sep 15;21(18):7099-109.
- Daus ML, Breyer J, Wagenfuehr K, Wemheuer WM, Thomzig A, Schulz-Schaeffer WJ, Beekes M. Presence and seeding activity of pathological prion protein (PrP(TSE)) in skeletal muscles of white-tailed deer infected with chronic wasting disease. *PLoS One.* 2011 Apr 1;6(4).
- Dubowitz V, Sewry CA. *Muscle Biopsy: A Practical Approach.* 3rd ed. London, UK: Saunders Elsevier; 2007.
- Ford MJ, Burton LJ, Morris RJ, Hall SM. Selective expression of prion protein in peripheral tissues of the adult mouse. *Neuroscience* 2002; 113:177-92.
- Franceschi C, Capri M, Monti D, Giunta S, Olivieri F, Sevini F, Panourgia MP, Invidia L, Celani L, Scurti M, Cevenini E, Castellani GC, Salvioli S. Inflammaging and anti-inflammaging: a systemic perspective on aging and longevity emerged from studies in humans. *Mech Ageing Dev.* 2007 Jan;128(1):92-105.
- Furukawa H1, Doh-ura K, Sasaki K, Iwaki T. Accumulation of prion protein in muscle fibers of experimental chloroquine myopathy: in vivo model for deposition of prion protein in non-neuronal tissues. *Lab Invest.* 2004 Jul;84(7):828-35.
- Gasperini L, Legname G Prion protein and aging. *Front Cell Dev Biol.* 2014; 2: 44.
- Goh AX, Li C, Sy MS, Wong BS. Altered prion protein glycosylation in the aging mouse brain. *J Neurochem.* 2007 Feb;100(3):841-54.
- Gohel C, Grigoriev V, Escaig-Haye F, Lasmézas CI, Deslys JP, Langeveld J, Akaaboune M, Hantäi D, Fournier JG. Ultrastructural localization of cellular prion protein (PrP_c) at the neuromuscular junction. *J Neurosci Res.* 1999 Jan 15;55(2):261-7.

Bibliography

- Guldimann C, Gsponer M, Drögemüller C, Oevermann A, Seuberlich T. Atypical H-type bovine spongiform encephalopathy in a cow born after the reinforced feed ban on meat-and-bone meal in Europe. *J Clin Microbiol.* 2012 Dec;50(12):4171-4.
- Haraguchi T, Fisher S, Olofsson S, Endo T, Groth D, Tarentino A, Borchelt DR, Teplow D, Hood L, Burlingame A, et al. Asparagine-linked glycosylation of the scrapie and cellular prion proteins. *Arch Biochem Biophys.* 1989 Oct;274(1):1-13.
- Horiuchi M, Yamazaki N, Ikeda T, Ishiguro N, Shinagawa M. A cellular form of prion protein (PrPC) exists in many non-neuronal tissues of sheep. *J Gen Virol* 1995; 76:2583-7.
- Hornshaw MP, McDermott JR, Candy JM. Copper binding to the N-terminal tandem repeat regions of mammalian and avian prion protein. *Biochem Biophys Res Commun.* 1995 Feb 15;207(2):621-9.
- Joshi-Barr S, Bett C, Chiang WC, Trejo M, Goebel HH, Sikorska B, Liberski P, Raeber A, Lin JH, Masliah E, Sigurdson CJ. De novo prion aggregates trigger autophagy in skeletal muscle. *J Virol.* 2014 Feb;88(4):2071-82.
- Klamt F, Dal-Pizzol F, Conte da Frota ML, Jr., Walz R, Andrades ME, da Silva EG, Brentani RR, Izquierdo I, and Fonseca Moreira JC. Imbalance of antioxidant defense in mice lacking cellular prion protein. *Free Radic Biol Med* 30: 1137–1144, 2001.
- Lehmann S, Harris DA. Blockade of glycosylation promotes acquisition of scrapie-like properties by the prion protein in cultured cells. 1997; *J. Biol. Chem.* 272, 21479–21487.
- Liu L, Jiang D, McDonald A, Hao Y, Millhauser GL, Zhou F. Copper redox cycling in the prion protein depends critically on binding mode. *J Am Chem Soc.* 2011 Aug 10;133(31):12229-37.
- Lo RY, Shyu WC, Lin SZ, Wang HJ, Chen SS, Li H. New molecular insights into cellular survival and stress responses: neuroprotective role of cellular prion protein (PrPC). *Mol Neurobiol.* 2007 Jun;35(3):236-44.
- Massimino ML, Ferrari J, Sorgato MC, Bertoli A Heterogeneous PrPC metabolism in skeletal muscle cells. *FEBS Lett.* 2006 Feb 6;580(3):878-84. Epub 2006 Jan 18.

Bibliography

- Massimino ML, Peggion C2, Loro F2, Stella R2, Megighian A2, Scorzeto M2, Blaauw B2, Toniolo L2, Sorgato MC1,2, Reggiani C1,2, Bertoli A2. Age-dependent neuromuscular impairment in prion protein knockout mice. *Muscle Nerve*. 2016 Feb;53(2):269-79. doi: 10.1002/mus.24708. Epub 2015 Nov 26.
- Neumann M, Krasemann S, Schröck K, Steinbach K, Glatzel M. Myositis facilitates preclinical accumulation of pathological prion protein in muscle. *Acta Neuropathol Commun*. 2013 Dec 3;1:78
- Okada H, Miyazawa K, Fukuda S, Iwamaru Y, Imamura M, Masujin K, Matsuura Y, Fujii T, Fujii K, Kageyama S, Yoshioka M, Murayama Y, Yokoyama T. The presence of disease-associated prion protein in skeletal muscle of cattle infected with classical bovine spongiform encephalopathy. *J Vet Med Sci*. 2014 Jan;76(1):103-7.
- Paciello O, Shelton GD, Papparella S. Expression of major histocompatibility complex class I and class II antigens in canine masticatory muscle myositis. *Neuromuscul Disord* 2007;17:313–20.
- Paciello O, Papparella S. Histochemical and immunohistological approach to comparative neuromuscular diseases. *Folia Histochem Cytobiol*. 2009; 47 (2): 143–152.
- Parkin ET, Watt NT, Hussain I, Eckman EA, Eckman CB, Manson JC, Baybutt HN, Turner AJ, Hooper NM. Cellular prion protein regulates beta-secretase cleavage of the Alzheimer's amyloid precursor protein. *Proc Natl Acad Sci U S A*. 2007 Jun 26;104(26):11062-7. Epub 2007 Jun 15.
- Peden AH, Ritchie DL, Head MW, and Ironside JW. Detection and Localization of PrPSc in the Skeletal Muscle of Patients with Variant, Iatrogenic, and Sporadic Forms of Creutzfeldt-Jakob Disease. *American Journal of Pathology*, Vol. 168, No. 3, March 2006
- Peralta o, Eyestone. Quantitative and qualitative analysis of cellular prion protein (PrPC) expression in bovine somatic tissues. *Prion*. 2009 Jul-Sep; 3(3): 161–170.
- Prusiner SB. Novel proteinaceous infectious particles cause scrapie. 1982, *Science* 216, 136–144.
- Prusiner SB. Prions. *Proc Natl Acad Sci USA* 1998; 95:13363-83.

Bibliography

- Prusiner, S.B., Groth, D.F., McKinley, M.P., Cochran, S.P., Bowman, K.A., Kasper, K.C. Thiocyanate and hydroxyl ions inactivate the scrapie agent. 1981. *Proc. Nat. Acad. Sci. U.S.A.* 78, 4606–4610.
- Sailer A, Büeler H, Fischer M, Aguzzi A, Weissmann C. No propagation of prions in mice devoid of PrP. *Cell.* 1994 Jul 1;77(7):967-8
- Sarkozi E, Askanas V, Engel WK. Abnormal accumulation of prion protein mRNA in muscle fibers of patients with sporadic inclusion-body myositis and hereditary inclusion-body myopathy. 1994 *Am J Pathol* 145: 1280-1284
- Serra F, Müller J, Gray J, Lüthi R, Dudas S, Czub S, Seuberlich T. PrP-C1 fragment in cattle brains reveals features of the transmissible spongiform encephalopathy associated PrP^{Sc}. *Brain Res.* 2017 Jan 21.
- Silva, C.J., Vazquez-Fernandez, E., Onisko, B., Requena, J.R., Proteinase K and the structure of PrP^{Sc}: The good, the bad and the ugly. 2015 *Virus Res.* 207, 120–126.
- Smith JD, Moylan JS, Hardin BJ, Chambers MA, Estus S, Telling GC, and Reid MB Prion Protein Expression and Functional Importance in Skeletal Muscle *Antioxid. Redox Signal.* 15, 2465—2475.2011
- Stahl N, Baldwin MA, Burlingame AL, and Prusiner SB. Identification of glycoinositol phospholipid linked and truncated forms of the scrapie prion protein. 1990 *Biochemistry* 29, 8879–8884.
- Stella R, Massimino ML, Sandri M, Sorgato MC, Bertoli A. Cellular prion protein promotes regeneration of adult muscle tissue. *Mol Cell Biol.* 2010 Oct;30(20):4864-76. doi: 10.1128/MCB.01040-09. Epub 2010 Aug 2.
- Stöckel J, Safar J, Wallace AC, Cohen FE, Prusiner SB. Prion protein selectively binds copper(II) ions. *Biochemistry.* 1998 May 19;37(20):7185-93.
- S, Vimercati C, Casalone C, Gelmetti D, Corona C, Iulini B, Mazza M, Lombardi G, Moda F, Ruggerone M, Campagnani I, Piccoli E, Catania M, Groschup MH, Balkema-Buschmann A, Caramelli M, Monaco S, Zanusso G, Tagliavini F. Infectivity in skeletal muscle of cattle with atypical bovine spongiform encephalopathy. *PLoS One.* 2012;7(2):e31449

Bibliography

- Vassallo N, Herms J. Cellular prion protein function in copper homeostasis and redox signalling at the synapse. *J Neurochem*. 2003 Aug;86(3):538-44. Review.
- Whitehouse IJ, Jackson C, Turner AJ, Hooper NM Prion protein is reduced in aging and in sporadic but not in familial Alzheimer's disease. *J Alzheimers Dis*. 2010;22(3):1023-31. doi: 10.3233/JAD-2010-101071.
- Williams WM, Stadtman E., Moskowitz J. Ageing and exposure to oxidative stress in vivo differentially affect cellular levels of PrP in mouse cerebral microvessels and brain parenchyma. 2004 *Neuropathol. Appl. Neurobiol.* 30, 161–168.
- Yoshioka Y1, Ishiguro N, Inoshima Y. Proteasome activity and biological properties of normal prion protein: a comparison between young and aged cattle. *J Vet Med Sci*. 2010 Dec;72(12):1583-7. Epub 2010 Aug 2.
- Zahn R, Liu A, Lührs T, Riek R, von Schroetter C, López García F, Billeter M, Calzolari L, Wider G, Wüthrich K. NMR solution structure of the human prion protein. *Proc Natl Acad Sci U S A*. 2000 Jan 4;97(1):145-50.

Conclusions:

The study of muscle pathology in veterinary medicine is a relatively young field of research which offers countless scientific insights about the pathogenesis of human and animal diseases, as well as about the validation of animal models in comparative medicine.

In these three years of scientific activities specific aspects about the etiopathogenesis of inflammatory myopathies and muscle aging have been investigated in four species of veterinary interest including horses, sheep, dogs and cows.

The main innovative aspects of this thesis are:

- 1) The first description in the literature of a likely immune-mediated myositis occurring in horses with chronic piroplasmosis
- 2) The demonstration of high prevalence of lymphoplasmacellular myositis in ovine muscular sarcocystosis characterized by the overexpression of MHC I and II on muscle fibers as well as on the cyst wall.
- 3) The report of enhanced autophagy in age-related muscle atrophy in dogs.
- 4) The first detailed description of cellular prion protein (PrPC) localization and biochemical properties in bovine muscle tissue and its possible involvement in neurogenic atrophy, muscle degeneration and chronic inflammation.

Our preliminary observations may open several new perspectives in the study of just listed subjects.

In particular, it would be of special interest to better characterize the possible autoantigens triggering muscle inflammation in equine piroplasmiasis, as already started by other researchers from our group in *Leishmania*-related myositis. The first step in this direction is to confirm the sarcolemmal location of these proteins using samples of sarcolemmal-pure homogenates by western blot by means of sera from affected animals as primary antibody. Then, further co-localization experiments between sera auto-antibodies and sarcolemmal protein would give useful information in validating selected sarcolemmal proteins as autoantigens.

The role of MHC I overexpression on the wall of sarcocysts has been of particular interest in this thesis. In a future perspective it would be interesting to study this phenomenon in experimental infections or in cell cultures of muscle fibers paying particular attention to the timing of onset of this feature. Indeed, it is still unknown whether the presence of this marker on the cyst wall may depend on a still incomplete extrusion of host cell protein from the parasitophorous vacuole or it is a consequence of a late activation of muscle fiber finalized to stimulate an inflammatory response against the parasite.

Information about the molecular mechanism underlying muscle aging in animals is still largely lacking in veterinary medicine. Here we focused on one of the mechanisms involved in muscle fiber proteostasis. In the future, it will be important to evaluate also other pathways possibly involved in muscle aging, such as the ubiquitin-proteasome system and oxidative stress.

Conclusions

The results of the project about prion protein in muscle tissue suggested a main link between the over-expression of this protein in a variety of pathological conditions of muscle fibers independently from the age. This concept may open new perspectives in the study of prion protein in muscle diseases, ranging from the inflammatory immune-mediated and infective myopathies to degenerative diseases in different species of veterinary interest.

In conclusion, we 1) added new scientific data to the veterinary literature in the field of muscle pathology that may serve as starting point for new research projects and 2) enhanced the pivotal role of histomorphological studies in the discovery of new pathogenetic aspects of muscle diseases in animals and possibly in humans.